

# 1   Marine biotoxin depuration rates: management 2   applications, research priorities, and predictions for 3   unstudied species

4   Christopher M. Free<sup>1,2\*</sup>, Yutian Fang<sup>2</sup>  
5

6   <sup>1</sup> Marine Science Institute, University of California, Santa Barbara, Santa Barbara, CA, 93106, USA

7   <sup>2</sup> Bren School of Environmental Science and Management, University of California, Santa Barbara, Santa  
8   Barbara, CA, 93106, USA

9

10   \* **Corresponding author:** Marine Science Institute, University of California, Santa Barbara, Santa  
11   Barbara, CA, 93106, USA; [cfree14@gmail.com](mailto:cfree14@gmail.com)

## 12   Abstract

13   Monitoring and managing the public health risk posed by marine biotoxins is a daunting  
14   challenge. With expansive coastlines, 1000s of seafood species, and dozens of biotoxins,  
15   monitoring cannot occur everywhere at once. Improving the cost-effectiveness of biotoxin  
16   monitoring is thus critical to expanding coverage to include more species, toxins, and locations.  
17   Notably, understanding the rate at which seafood species depurate biotoxins can be used to  
18   optimize the cadence of monitoring. We conducted a systematic review to collate marine  
19   biotoxin depuration rates and synthesize the factors that influence them; identify knowledge  
20   gaps, best practices, and research priorities; and generate predictions of depuration rates for  
21   unstudied species. We found that only 85 marine species have been studied for their biotoxin  
22   depuration rates. Depuration rates for non-bivalves and for toxins besides paralytic shellfish  
23   toxins (PSTs) are especially understudied. Depuration half-lives varied from 0.03 to 1269 days  
24   based on species, toxin, tissue, and environmental conditions. In general, depuration  
25   accelerates with increased temperature and food availability, with implications for aquaculture  
26   siting, depuration enhancement, and biotoxin monitoring. We identified unstudied bivalve and  
27   finfish species that are highly produced and vulnerable to HABs that are high priorities for future  
28   research. Finally, we used a Bayesian regression model to predict PST depuration rates for 102  
29   unstudied bivalve species, the only clade-syndrome with sufficient training data. These  
30   predictions can guide efficient monitoring and management until lab- or field-based depuration  
31   rates become available. We recommend that future studies directly estimate depuration rates to  
32   ensure their comparability across studies and utility to managers.

33

34   **Keywords:** harmful algal blooms, phycotoxin, toxin, elimination, detoxification, excretion,  
35   toxicokinetics

## 36 1. Introduction

37 Harmful algal blooms (HABs) that produce biotoxins that accumulate in seafood species  
38 represent a growing threat to public health and marine fisheries and aquaculture (Hallegraeff et  
39 al., 2021). More than 200 taxa of marine algae produce biotoxins that threaten human health  
40 (Lundholm et al., 2009), with risk present in nearly all coastal waters (OBIS, 2025). Collectively,  
41 these toxins cause seven major poisoning syndromes in humans – paralytic, amnesic,  
42 diarrhetic, neurotoxic, azaspiracid, cyanotoxin, and ciguatera poisoning – with new toxins and  
43 syndromes discovered each decade (Nicolas et al., 2017). These syndromes cause symptoms  
44 ranging from gastrointestinal issues to neurological issues to death (Grattan et al., 2016). As a  
45 result, managers often close fisheries and aquaculture to protect public health, which can cause  
46 significant socioeconomic impacts from lost commercial, recreational, and cultural activities  
47 (Moore et al., 2020). HABs are expected to increase in frequency, duration, and intensity with  
48 climate change (IPCC, 2019), making them critical to study to ensure that seafood can safely  
49 remain a source of healthy, sustainable food for a growing human population.

50

51 To protect public health, many governments use biotoxin monitoring programs to track  
52 seafood safety and manage fisheries and aquaculture operations that are vulnerable to biotoxin  
53 risk (Andersen et al., 2004). In general, these programs monitor the toxicity of seafood species  
54 and trigger management actions when toxicity rises above a threshold deemed unsafe for  
55 human consumption, commonly referred to as the “action threshold” (Langlois and Morton,  
56 2018). The management action, which could be a closure or an evisceration requirement (i.e.,  
57 required removal of toxic body parts), is not ceased until toxicity falls below the action threshold,  
58 often after several successive tests to ensure safety. Ideally, all vulnerable species would be  
59 monitored to fully protect public health (Costa et al., 2017) and sampling would be highly  
60 spatially and temporally resolved to protect public health while also avoiding unnecessary  
61 management restrictions (Free et al., 2022). However, given limited resources to support  
62 expensive lab testing, expansive taxonomic, spatial, and temporal coverage is rarely possible  
63 (Langlois and Morton, 2018). Improving the cost-effectiveness of biotoxin monitoring is thus  
64 necessary to monitor more species, in more places, at more times. This could be achieved by  
65 either lowering the cost of each test (i.e., cheaper monitoring) or by lowering the number of tests  
66 required to effectively manage risk (i.e., more efficient monitoring).

67

68 One pathway for improving the efficiency of biotoxin monitoring programs is to tailor the  
69 frequency of sampling to the toxicokinetics of the monitored species (Blanco, 2009).  
70 Toxicokinetics describe the processes and rates of accumulation (a.k.a., uptake, adsorption),  
71 distribution, metabolism, and depuration (a.k.a., excretion, elimination, detoxification) of  
72 biotoxins within a species (Landrum et al., 1992). The rate at which species accumulate toxins  
73 determines how quickly monitoring should begin and proceed after a HAB is detected. For  
74 example, monitoring could begin later and advance more slowly if accumulation is slow but  
75 should begin sooner and advance more quickly if accumulation is fast. The distribution of toxin  
76 burden among different tissues is important because it determines what tissue is the most  
77 useful indicator of public health risk and whether a species could be safely consumed and  
78 successfully marketed following the evisceration (removal) of the most toxic tissue. The  
79 metabolism of the consumed toxin into new compounds, which can be either more or less toxic  
80 than the original compound (Bricelj and Shumway, 1998), contributes to the duration of seafood  
81 toxicity. Finally, the rate of depuration determines how frequently monitoring is needed after a  
82 species becomes toxic to facilitate the timely end of management actions. It can also be used to  
83 provide seafood harvesters, processors, and dealers forecasts of when management actions  
84 are likely to cease.

85

86 The use of depuration rates to design more efficient biotoxin monitoring and  
87 management is particularly promising because of the availability of good mathematical models  
88 for describing depuration and forecasting the duration of high toxicity. In general, depuration  
89 kinetics are theorized to follow either one- or two-compartment exponential decay (Blanco,  
90 2009). In a one-compartment model, biotoxins are assumed to accumulate within a single  
91 “compartment”, which can represent a single tissue, a group of tissues, or even a whole  
92 organism, and are assumed to be exponentially lost to the environment at a single rate. For  
93 example, a toxin might accumulate in the digestive system following ingestion and then be  
94 quickly eliminated through egestion. In a two-compartment model, biotoxins are assumed to  
95 accumulate in an initial compartment (e.g., the digestive system) with some transference to a  
96 second compartment (e.g., muscle) with a slower exponential depuration rate. Theoretically,  
97 depuration rates could be described using even more compartments, though statistical support  
98 for increasingly complex models to offer more parsimonious fits seems unlikely; to our  
99 knowledge, the maximum number of compartments used in practice is three (Ye et al., 2021).  
100 With knowledge of the exponential decay constants for any of these models, managers could

101 forecast depuration timelines (**Fig. 1**) and provide themselves, fishermen, and aquaculture  
102 farmers with valuable predictions of when seafood is expected to be safe for consumption.

103

104 To illustrate how knowledge of depuration rates could improve the efficiency of biotoxin  
105 monitoring, we consider a species that depurates a biotoxin at  $0.03 \text{ day}^{-1}$  ( $2.9\% \text{ day}^{-1}$ ; 23.1 day  
106 half-life) based on one-compartment depuration kinetics (**Fig. 1**). This is roughly equivalent to  
107 the rate at which Atlantic surfclams (*Spisula solidissima*) depurate paralytic shellfish toxins  
108 (PSTs) under warm conditions (Bricelj et al., 2014). After reaching peak toxicity, managers  
109 could use this depuration rate to forecast when toxicity is expected to fall below the action  
110 threshold and tailor the cadence of monitoring accordingly (**Fig. 1A**). Specifically, managers  
111 could pause regular testing while toxicity is expected to remain well above the action threshold  
112 and resume it when toxicity is expected to approach the threshold. In this example, optimized  
113 testing eliminates the need for four tests, which accumulates when applied across many  
114 management zones (e.g., 10 zones = 40 saved tests). This frees up resources to monitor new  
115 management zones or new species at the same cost as the original monitoring program.  
116 Importantly, knowledge of depuration rates can improve efficiency even before peak toxicity is  
117 attained (**Fig. 1B**). If the first test conducted after a forecast is higher than expected (because  
118 the species is still accumulating toxins from an ongoing bloom or from toxins in the food web),  
119 the forecast can be repeated and the cadence of monitoring updated accordingly.

120

121 The widespread use of depuration rates to increase the efficiency of biotoxin monitoring  
122 programs requires the consolidation of known depuration rates, identification of the factors that  
123 affect biotoxin depuration, and prioritization of depuration rates still needing study. This is  
124 partially supported by a small number of review papers. A review by Fernandez et al. (2003)  
125 provided biotoxin “retention times”, the time required for toxicity to fall below either the action  
126 threshold or the limit of detection, for 34 species-toxin combinations representing 31 bivalve  
127 species and five toxin syndromes (paralytic, diarrhetic, amnesic, neurotoxic, other). Although  
128 these values provide credible evidence that depuration rates are species- and toxin-specific,  
129 they are challenging to interpret and cannot be operationalized as rates. A review by Bricelj and  
130 Shumway (1998) provides operational PST depuration rates (% per day) for 21 species of  
131 bivalves. A handful of research papers provide non-systematically collated depuration rates to  
132 place measured depuration rates within a broader context (Garcia-Corona et al., 2024; Martins  
133 et al., 2020; Schultz et al., 2013). While valuable, these reviews collectively lack depuration

134 rates for non-bivalves, three notable biotoxin syndromes (ciguatera, cyanotoxin, azaspiracid),  
135 and over two decades of research into marine biotoxin depuration processes.

136

137 Here, we seek to empower more efficient marine biotoxin monitoring and management  
138 through a multi-pronged assessment of biotoxin depuration rates. First, we conducted a  
139 systematic literature review to collate published depuration rates, synthesize information on the  
140 factors that impact biotoxin depuration, and identify best practices for future depuration studies.  
141 Second, we prioritized species for future depuration study by identifying highly produced  
142 seafood species that are vulnerable and exposed to each biotoxin syndrome yet have no  
143 published depuration rates. Finally, we used a Bayesian regression model trained on our  
144 database of biotoxin depuration rates to predict rates for unstudied species, which can be used  
145 to guide monitoring programs until depuration studies are completed. Overall, we demonstrate  
146 how biotoxin depuration rates can forecast depuration timelines, which can be used to design  
147 more efficient monitoring programs and to support informed management and business  
148 decisions.

149 **2. Methods**

150 **2.1 Literature review**

151 **2.1.1 Database development**

152 We conducted a systematic review of marine biotoxin depuration rates following the  
153 PRISMA review protocol (**Fig. S1**) (Page et al., 2021). First, we identified 797 candidate papers  
154 by using the following search query in Web of Science on July 30, 2025: (“depurat\*” or “excret\*”  
155 or “eliminat\*” or “detox\*”) AND (“toxin\*” or “biotoxin\*” or “phycotoxin” or “domoic” or “okadaic” or  
156 “saxitoxin” or “brevetoxin” or “azaspiracid” or “cyanotoxin” or “ciguatoxin”) AND (“marine” or  
157 “ocean”). This query was designed to identify papers that study the depuration (a.k.a. excretion,  
158 elimination, or detoxification; term 1) of marine phycotoxins (term 2) from marine species (term  
159 3). We only considered papers that either quantified the depuration rates of biotoxins produced  
160 by harmful algae from marine species or presented the data required for us to externally  
161 quantify depuration rates. Thus, we excluded 643 papers that did not study a marine species,  
162 did not study a biotoxin produced by a harmful algae species, or did not quantify a depuration  
163 rate or present the data needed to externally derive a depuration rate (**Fig. S1**). We

164 supplemented this systematic review with a targeted search of the Chinese literature to identify  
 165 depuration rates not represented in the English literature; this non-systematic review added two  
 166 papers on paralytic shellfish toxin depuration rates in Manila clam (*Ruditapes philippinarum*).  
 167

168 We reviewed the resulting 156 papers (**Fig. S2**) and extracted the following attributes of  
 169 the study (**Table S1**): species studied (common and scientific name), biotoxin studied and its  
 170 causative agent, tissue studied (e.g., meat, viscera, hepatopancreas; **Table S2**), study type (lab  
 171 or field), feeding conditions during depuration (starved, fed a non-toxic diet, or foraged in the  
 172 wild), and other experimental conditions (e.g., varied temperature, salinity, diets, etc.). If the  
 173 depuration rate (exponential decay constant or half-life) was directly reported, we recorded the  
 174 rate and whether it was derived from a one- or two-compartment exponential decay model  
 175 (details below). These are also known as first- or second-order or one- or two-phase (biphasic)  
 176 decay models. We grouped the studied biotoxins into eight syndromes of shellfish poisoning  
 177 (Nicolas et al., 2017): amnesic, diarrhetic, paralytic, ciguatera, neurotoxic, azaspiracid,  
 178 cyanotoxin, and other shellfish poisoning (**Table 1**). Cyanotoxin poisoning describes toxins  
 179 formed by cyano-bacteria including microcystin, nodularin, and homoanatoxin. The other  
 180 category includes yessotoxins, pectenotoxins, tetrodotoxins, gymnodimines, and karlotoxins.

### 181 2.1.2 Deriving depuration rates

182 If the depuration rate was not directly reported as either an exponential decay constant  
 183 or half-life, we extracted the data needed to derive the depuration rate using WebPlotDigitizer  
 184 (Rohatgi, 2025). We estimated depuration rates using a one-compartment exponential decay  
 185 model fit to the depuration phase of the data. For field studies with long time series, depuration  
 186 rates were often estimated for discrete depuration events (**Fig. S3**). We calculated tissue-  
 187 specific depuration rates such that:

$$189 N_t = N_0 e^{-kt}$$

190  
 191 where toxicity at time  $t$  ( $N_t$ ) is a function of initial toxicity ( $N_0$ ) and the decay constant  $k$ .  
 192

193 We calculated the half-life, the time required for toxicity to halve, associated with each  
 194 reported or derived one-compartment model depuration rate as:

$$196 t_{1/2} = \ln(2)/k$$

197

198 If a paper reported a half-life but not the decay constant ( $k$ ), we inverted this equation to  
199 calculate the decay constant. We standardized all decay constants and half-lives to be in terms  
200 of days (i.e., some fast depuration rates were reported or derived in terms of hours). Finally, we  
201 calculated the percent daily loss of biotoxin burden as:

202

203 
$$\% \text{ daily loss} = 1 - \exp(-k)$$

204 2.2 Priority species for depuration study

205 We identified priority species for depuration study as vulnerable species that have high  
206 commercial harvests from countries with HAB exposure but that lack published depuration  
207 rates. First, we identified countries exposed to HAB species associated with each biotoxin  
208 syndrome (**Table 1**) using data from the Ocean Biodiversity Information System (OBIS) (OBIS,  
209 2025), which provides geotagged observations of HAB species (**Fig. S4**). We classified a  
210 country's waters as exposed to biotoxin syndrome if an associated species (OBIS) has ever  
211 been recorded within its Exclusive Economic Zone (EEZ) (Flanders Marine Institute, 2025). We  
212 note that this likely underestimates countries exposed to HABs as many countries, especially in  
213 Africa and the Middle East (**Fig. S4**), lack HAB monitoring programs (Andersen et al., 2004).

214

215 Second, we identified shellfish and finfish species that are vulnerable to HABs and  
216 harvested in exposed countries using national fisheries and aquaculture production data from  
217 the Food and Agriculture Organization (FAO) of the United Nations (FAO, 2024). We identified  
218 vulnerable shellfish as filter-feeding molluscs (e.g., oysters, mussels, clams, scallops), as they  
219 readily accumulate toxins by directly consuming HAB species, even within aquaculture facilities  
220 where they generally feed directly from the surrounding environment. We excluded predatory  
221 molluscs (e.g., cephalopods), grazing molluscs (e.g., gastropods), and non-mollusc shellfish  
222 (e.g., crustaceans, echinoderms), which are challenging to prioritize because their indirect  
223 biotoxin accumulation pathways make their vulnerability to biotoxins highly heterogeneous. The  
224 shellfish prioritization excludes ciguatera, which is principally a finfish biotoxin syndrome.

225

226 We identified vulnerable finfish as those vulnerable to ciguatera, the primary biotoxin  
227 syndrome affecting finfish. Ciguatera is most common in large, tropical, reef-associated,  
228 predators (Lewis and Holmes, 1993; Randall, 1958). We thus used information on habitat  
229 associations, maximum length, and trophic level from FishBase (Boettiger et al., 2012; Froese

230 and Pauly, 2025) to identify reef-associated predators larger than 25 cm that are harvested in  
231 capture fisheries. A threshold of 25 cm was selected as the smallest fish with detectable  
232 ciguatoxins in the review of (Li et al., 2023) was striated surgeonfish (*Ctenochaetus striatus*) at  
233 26 cm maximum length. Because FishBase information on trophic level is relatively sparse, we  
234 could only exclude known herbivores (i.e., we could not filter for known predators). FishBase  
235 also identifies fish with known ciguatera observations; these species were considered in the  
236 prioritization even if they did not meet the criteria above. We excluded aquaculture production  
237 from the finfish prioritization analysis because predatory finfish are generally fed non-toxic food  
238 and are thus less exposed to ciguatoxins through the food web.

239

240 Finally, we identified the 20 vulnerable species with the highest annual production  
241 (bivalves: aquaculture+fisheries; finfish: fisheries only) from 2014-2023 in EEZs exposed to  
242 each biotoxin syndrome and classified species without published depuration rates as priorities  
243 for study. We highlighted unstudied species that would provide the first depuration estimate at  
244 the order, family, or genus levels as particularly valuable. To illustrate the value of these  
245 estimates, we quantified the (1) number of currently harvested species in the taxonomic group  
246 using the FAO data and (2) total number of species in the group using FishBase and  
247 SeaLifeBase (Palomares and Pauly, 2025), which captures potential future harvest diversity.

248

249 Although we did not prioritize non-bivalve invertebrates for depuration study, we  
250 compared maximum biotoxin toxicities reported in non-bivalves by select review papers (Costa  
251 et al., 2017; Deeds et al., 2008; Lefebvre and Robertson, 2010) relative to common international  
252 action thresholds (Langlois and Morton, 2018) to assess the importance of conducting  
253 depuration studies for non-bivalve vectors of seafood poisoning syndromes. These review  
254 papers were opportunistically selected from the systematic literature search but do not  
255 constitute a systematic review of all observed non-bivalve toxicities.

## 256 2.3 Predicting bivalve PST depuration rates

257 We compared the ability for one generalized linear model and three mixed effects  
258 models to predict paralytic shellfish toxin (PST) depuration rates in marine bivalves. We focused  
259 on PST depuration rates in bivalves based on the *a priori* expectation that this was the only  
260 clade-syndrome combination with sufficient data (**Fig. 2**) to generate a model with good  
261 predictive skill. All four models predict the log depuration rate to normalize the response variable  
262 and to constrain predictions to positive depuration rates (i.e., exponential decay rather than

263 exponential growth). All four models include five fixed effects: (1) study type (lab vs. field), (2)  
264 tissue type (e.g. muscle, hepatopancreas, etc.); (3) maximum length (cm), (4) von Bertalanffy  
265 somatic growth rate (1/yr), which describes the rate at which an organism grows towards its  
266 maximum size, and (5) preferred temperature (°C). These variables were selected based on  
267 hypotheses that (a) depuration rates would be faster in the lab, where species are fed non-toxic  
268 diets; (b) depuration rates would vary by tissue; and (c) depuration rates would be faster for  
269 smaller, faster growing, warmer water species, which are expected to have faster metabolisms  
270 (Robinson et al., 1983) and therefore faster egestion. We retrieved the maximum length, growth  
271 rate, and preferred temperature from SeaLifeBase (Palomares and Pauly, 2025) using the  
272 *rfishbase* R package (Boettiger et al., 2012). When values were missing for a species, we  
273 preferentially used the genus-, family-, order-, or class-level median, depending on availability.  
274

275 The first model includes only the five fixed effects variables (the “fixed effects only”  
276 model) while the subsequent models use different approaches for incorporating taxonomic  
277 random effects. The inclusion of taxonomic random effects evaluates the hypothesis that traits  
278 besides those explicitly evaluated as fixed effects may also determine depuration rates. For  
279 example, species-specific physiology and feeding ecology may play an important role in  
280 depuration, but we lack the data to explicitly incorporate these traits as fixed effects. The  
281 “phylogenetic random effects” model evaluates the hypothesis that depuration rates are  
282 phylogenetically conserved and correlated to ancestry. This model includes species-specific  
283 random effects that were modelled using a variance-covariance matrix derived from the bivalve  
284 phylogenetic tree. We constructed a phylogenetic tree of all bivalve species using the Open  
285 Tree of Life API (Hinchliff et al., 2015) via the *rotl* R package (Michonneau et al., 2016). We  
286 estimated branch lengths using the Grafen method (Grafen, 1997), which scales internal nodes  
287 to approximate evolutionary divergence when branch-length information is incomplete,  
288 implemented through the *ape* R package (Paradis and Schliep, 2019). The “taxonomically  
289 nested model” has hierarchically nested order, family, genus, and species random effects. This  
290 model evaluates the hypothesis that depuration rates are similar within a clade but that  
291 differences between clades are not related to ancestry (as in the phylogenetic model). Finally,  
292 the “species random effects” model includes species-level random effects that are not  
293 structured by phylogeny or taxonomy. This model evaluates the hypothesis that unobserved  
294 species traits impact depuration rates but that these impacts are idiosyncratic and not related to  
295 taxonomy.  
296

297 We fit all four models using a Bayesian estimation approach implemented through the  
298 *brms* R package (Bürkner, 2017). The models were compared using efficient approximate  
299 leave-one-out cross-validation (LOO) using the *loo* R package (Vehtari et al., 2024), where the  
300 best model was identified as the one with the largest expected log predictive density (ELPD),  
301 which characterizes the ability of the model to predict the data withheld in the cross-validation.  
302 The fit of all four models was also evaluated through the estimation of a Bayesian R<sup>2</sup> (Gelman et  
303 al., 2019). We evaluated the coefficients and conditional effects of predictors in the best fitting  
304 model to understand the impact of each variable on PST depuration rates. Finally, we used the  
305 best fitting model to estimate PST depuration rates for all harvested marine bivalves, as  
306 determined through the analysis of the FAO production data (FAO, 2024) described above. We  
307 included all harvested bivalves, not just those harvested from EEZs with known PST occurrence  
308 (**Fig. S4**), given that PST may be present but undetected in many of these EEZs and the  
309 potential for the range of PST causative agents to expand in the future. The life history traits for  
310 these species were also retrieved from SeaLifeBase using the *rfishbase* R package.

### 311 3. Results

#### 312 3.1 Literature review

##### 313 3.1.1 General characteristics

314 Biotoxin depuration rates have been studied in 85 marine species spanning 66 genera,  
315 39 families, 26 orders, and 10 classes (**Fig. 2A; Table S3**). Marine invertebrates, especially  
316 bivalves, have been much more studied than marine vertebrates: only 13 papers (8%) have  
317 evaluated biotoxin depuration rates in finfish whereas 145 papers (93%) have assessed biotoxin  
318 depuration rates in invertebrates (some papers studied both an invertebrate and a vertebrate  
319 allowing this statistic to sum to >100%; this applies to other results as well). Most of the  
320 evaluated papers studied bivalves (124 papers; 80%), with a particular focus on blue mussels  
321 (31 papers; 20%), Mediterranean mussels (17 papers; 11%), Pacific oysters (13 papers; 8%),  
322 eastern oysters (8 papers; 5%), and king scallops (6 papers; 4%). Notably, blue mussels are the  
323 only species with depuration rates estimated for six of the eight biotoxin syndromes (**Fig. 2B**).  
324

325 The depuration of PSTs from marine species has been studied more than the depuration  
326 of any other biotoxin (66 papers; 42%) (**Fig. 2B**). Domoic acid (24 papers, 15%), diarrhetic

327 shellfish toxin (DST) (24 papers; 15%), and cyanotoxin (16 papers; 10%) depuration rates have  
328 received similar levels of attention. Brevetoxin depuration has been evaluated in 9 papers (6%),  
329 which evaluate four bivalve, two finfish, and one dolphin species. Ciguatoxin depuration has  
330 only been studied in four finfish species (4 papers) and azaspiracid depuration has only been  
331 measured in three bivalve species (3 papers). Eighteen papers (12%) have assessed the  
332 depuration rates of “other” biotoxins (**Table 1**), which include yessotoxins, tetrodotoxins,  
333 pectenotoxins, karlotoxins, and gymnodimines (**Fig. 2B**).

334

335 Biotoxin depuration has been studied in many tissue types (**Fig. S5**) with some papers  
336 comparing depuration rates among many tissues (**Fig. 3B**). In general, the tissues most  
337 evaluated are those that either harbor the greatest toxin burden or are consumed by people. For  
338 bivalves, studies have largely focused on the soft tissue (eaten by people) and the  
339 hepatopancreas (greatest toxin burden; Bricelj and Shumway, 1998). Similarly, crustacean  
340 depuration rates have largely been evaluated in the hepatopancreas (greatest toxin burden;  
341 Schultz et al., 2013) and the soft tissue (eaten by people). For finfish, the dominant tissues  
342 studied are the liver and muscle (eaten by people). Most gastropod studies have measured  
343 depuration in the foot (eaten by people) or the whole organism. All cephalopod studies have  
344 focused exclusively on the viscera, and all phytoplankton, zooplankton, and sea squirt studies  
345 have exclusively analysed the whole organism (**Fig. S6**).

346

347 Most depuration studies occur in the lab (71%; 110 papers), where depuration can be  
348 measured under controlled diet and environmental conditions (**Fig. 3C**). 23% (36 papers) of  
349 depuration studies occur in the field, where organisms are potentially exposed to toxic algae  
350 while depurating (i.e., depuration may be offset by uptake), but where depuration is quantified in  
351 a real-world setting. Four studies (3%) depurate organisms fed toxic algae in the lab at non-toxic  
352 field sites to mimic depuration in a natural, but non-toxic, setting. Five studies (3%) directly  
353 compared lab and field depuration rates. Houle et al. (2023) find that PST depuration in Purple-  
354 hinged rock scallop (*Crassadoma gigantea*) is 3.1 times slower in the field. Slower depuration in  
355 the field is also found for the depuration of domoic acid by Peruvian calico scallops (*Argopecten*  
356 *purpuratus*) (Alvarez et al., 2020) and variegated scallops (*Mimachlamys varia*) (Le Moan et al.,  
357 2025) and the depuration of PSTs from purple clams (*Hiatula rostrata*) (Chen and Chou, 2002)  
358 and blue mussel (*Mytilus edulis*) (Scarratt et al., 1991). Our meta-analysis confirms this result  
359 for most species with depuration rates estimated for common tissues in field and lab studies  
360 (**Fig. S6**).

361 3.1.2 Experimental results

362 Many of the evaluated papers assessed depuration rates under different experimental  
363 treatments (**Fig. 3G**). In particular, many lab studies considered the impacts of water  
364 temperature, dietary factors, and biotoxin exposure characteristics on depuration rates. A few  
365 lab studies also considered the impacts of size and/or age on depuration rates, the ability for  
366 industrial additives to enhance depuration rates, and the sensitivity of depuration rate estimates  
367 to measurement technique. Many field studies assessed depuration rates across different  
368 locations and/or years and two field studies compared depuration rates at the seafloor and  
369 surface. Five studies directly compared depuration rates in the lab, where organisms are fed a  
370 controlled non-toxic diet, versus the field, where organisms experience a natural diet that may  
371 not be completely toxin-free (**Fig. 3G**).

372 3.1.2.1 Impacts of exposure intensity

373 Because studies of biotoxin depuration rates are often conducted following studies of  
374 biotoxin accumulation (e.g. Kwong et al., 2006; Lopes et al., 2014a; Lund et al., 1997), many of  
375 the evaluated studies (n=22) included trials with different exposure intensities. However, the  
376 primary purpose of these treatments is to quantify feeding clearance rates and associated  
377 biotoxin uptake rates, which are density-dependent. Although these treatments impact the peak  
378 toxicity ( $N_c$ ) of a one-compartment depuration model, they would not be expected to affect the  
379 depuration rate constant ( $k$ ), which is, by definition, the same at any toxicity. As a result, most of  
380 these papers do not explicitly compare depuration rates across treatments and we made no  
381 attempt to make these comparisons ourselves. Most of these studies (n=16) manipulated  
382 exposure intensity by varying the density (dosage) of the causative agent. The remaining  
383 studies varied exposure intensity by varying the composition of causative agents in the diet  
384 (n=3; Bricelj et al., 1991; Jauffrais et al., 2012; Lewis et al., 2022), the duration of exposure to  
385 the causative agent (n=1; Lin et al., 2024), the nutrient conditions during exposure (n=1;  
386 Strogyloudi et al., 2006), or the method of exposure (n=1; i.e., oral exposure vs. injection;  
387 Kankaanpää et al., 2005).

388 3.1.2.2 Impacts of dietary factors

389 The eleven papers that evaluate the impact of dietary factors on biotoxin depuration  
390 rates generally find that individuals depurate faster when fed than when starved and that they  
391 depurate even faster when provided more food or when hungrier. This is generally believed to  
392 occur because depuration largely occurs through egestion of feces or pseudofeces and

393 egestion is generally higher when eating (Bricelj and Shumway, 1998). Faster depuration has  
394 been found for fed versus starved individuals for: (i) PSTs in Pacific oysters (*Crassostrea gigas*)  
395 (Medhioub et al., 2012) and Jinjiang oysters (*Ostrea rivularis*) (Yang et al., 2021); (ii) okadaic  
396 acid in blue mussels (Marcaillou et al., 2010); (iii) domoic acid in Dungeness crab (*Metacarcinus*  
397 *magister*) (Lund et al., 1997); and (iv) gymnodimines in grooved carpet shells (*Ruditapes*  
398 *decussatus*) (Medhioub et al., 2010). Blue mussels depurated okadaic acid faster when fed  
399 more food (Marcaillou et al., 2010). Relatedly, field-collected brown crabs (*Cancer pagrus*) in  
400 poor body condition (hungrier) depurated faster okadaic acid faster than lab-fed brown crabs in  
401 better body condition (less hungry). The depuration rate of okadaic acid (Svensson, 2003) and  
402 domoic acid (Wohlgeschaffen et al., 1992) from blue mussels and of domoic acid from three  
403 *Calanus* copepod species (*C. finmarchicus*, *C. glacialis*, *C. finmarchicus*) (Hardardottir et al.,  
404 2019; Leandro et al., 2010) were all so rapid that they were not affected by whether they were  
405 starved or fed. Only northern quahog (*Mercenaria mercenaria*) and constricted tagelus  
406 (*Sinonovacula constricta*) were found to depurate karlotoxins faster when starved than when fed  
407 (Li et al., 2024). The authors hypothesize that this surprising finding may be because stomach  
408 contents, including residual toxic algae, are evacuated more efficiently when starved.

#### 409 3.1.2.3 Impacts of temperature

410 The nine papers that evaluated the impact of temperature on biotoxin rates generally  
411 find that depuration is faster in warmer waters. Blue mussels (*Mytilus edulis*) depurated domoic  
412 acid faster at 11°C than 6°C (Novaczek et al., 1992) and faster at 11°C than 6°C (Scarratt et al.,  
413 1991). Similarly, wedge shells (*Donax trunculus*) depurated okadaic acid 71% faster at 20°C  
414 than at 17°C (Botelho et al., 2018). Atlantic surfclams (*Spisula solidissima*) viscera, where  
415 toxicity is highest, depurated okadaic acid faster under warmer conditions though temperature  
416 did not impact depuration rates in other tissues (Bricelj et al., 2014). On the other hand,  
417 Svensson and Förlin (2004) found that even though blue mussels (*Mytilus edulis*) eliminated  
418 lipids faster in warmer waters, water temperature did not affect the depuration rate of okadaic  
419 acid, a lipophilic phycotoxin. Farrell et al. (2015) found that Sydney rock oyster (*Saccostrea*  
420 *glomerata*) and diploid Pacific oysters (*Crassostrea gigas*) depurated PST faster at 27°C than at  
421 22°C, but that temperature did not affect depuration rates for triploid Pacific oysters. Tang et al.  
422 (2021b) found that Korean hard-shelled mussel (*Mytilus coruscus*) depurated PSTs faster at  
423 30°C than at 25°C. In the only study examining the impact of temperature on the biotoxin  
424 depuration rate of a finfish, Barbosa et al. (2019) found that gilthead seabream (*Sparus aurata*)  
425 depurated PST so quickly that an impact of temperature could not be measured. Finally, Braga

426 et al. (2018) is the only paper to find slower depuration under warming, where Mediterranean  
427 mussels depurated PSTs faster at 19°C than at 24°C.

428 3.1.2.4 Impacts of body size and age

429 The five papers that considered the impact of size or age on biotoxin depuration rates  
430 generally found that smaller/younger individuals depurate faster than larger/older individuals.  
431 Bogan et al., (2007) found that smaller king scallops (*Pecten maximus*) depurated domoic acid  
432 faster than larger scallops. Mafra et al. (2010) found that smaller Eastern oysters (*Crassostrea*  
433 *virginica*) depurated domoic acid faster than larger oysters but that size did not affect the  
434 domoic acid depuration rates of blue mussels (*Mytilus edulis*). Similarly, Duinker et al. (2007a)  
435 found no difference in the okadaic acid depuration rates of 1- and 2-year-old blue mussels.  
436 Finally, Min et al. (2018) show that cyanotoxin depuration began earlier for juvenile mysid  
437 crustaceans (*Neomysis awatschensis*) and thus progressed faster.

438 3.1.2.5 Impacts of depuration enhancers

439 A few papers examined the ability for additives to enhance the depuration process. Xie  
440 et al. (2013) found that supplementing Jinjiang oyster (*Ostrea rivularis*) diets with chitosan, a  
441 natural polymer that adsorbs PST toxins and prevents their reuptake by depurating filter  
442 feeders, significantly accelerated their PST depuration. Qiu et al. (2018) found that adding  
443 activated carbon, which also adsorbs PST toxins and prevents their reuptake by depurating filter  
444 feeders, to depuration tanks significantly accelerated PST depuration from both Mediterranean  
445 mussels (*Mytilus galloprovincialis*) and Farrer's scallops (*Chlamys farreri*). Activated carbon is a  
446 highly effective biotoxin adsorbent because of its high porosity, surface area, and cationic  
447 charge. Similarly, Peña-Llopis et al. (2014) found that adding N-Acetylcysteine, which boosts  
448 the production of compounds central to the detoxification process, resulted in a four-fold  
449 increase in the depuration of domoic acid from king scallops (*Pecten maximus*), one of the  
450 slowest depurating bivalve species (Blanco et al., 2002). On the other hand, Leal et al. (2023)  
451 found that adding cation-exchange resins (CER), which adsorb positively charged toxic  
452 compounds, did not significantly accelerate PST depuration in blue mussel (*Mytilus edulis*).

453 3.1.3 Depuration rates by species

454 Only 41% (n=64) of the evaluated studies reported biotoxin depuration rates in terms of  
455 exponential decay constants or half-lives, which are quantitative values that can be directly  
456 compared across studies, species, tissues, experimental conditions, biotoxins, etc. (**Fig. 3E**).

457 The remaining 59% of studies (n=92) described depuration rates in bespoke terms that are not  
458 directly comparable across studies, such as “*after 14 days, the [domoic acid] concentration in*  
459 *the fed crabs decreased by 73%*” (Lund et al., 1997) or “[toxicity decreased] from 3.1 µg  
460 [*okadaic acid*] g<sup>-1</sup> .... at day 1 to 1.51 µg [*okadaic acid*] g<sup>-1</sup> at day 32” (Svensson, 2003). Among  
461 the 66 studies that reported exponential decay constants or half-lives, 50 (76%) estimated these  
462 values using one-compartment exponential decay models, 3 (5%) estimated these values using  
463 two-compartment models (Choi et al., 2003; Schultz et al., 2008; Yu et al., 2005), 8 (12%)  
464 compared the results of one- and two-compartment models (Alvarez et al., 2020; Blanco et al.,  
465 1999; Jauffrais et al., 2012; Lopes et al., 2014; Mafra et al., 2010; Moroño et al., 2003; Nielsen  
466 et al., 2016; Woofter et al., 2005), and one compared the results of one-, two-, and three-  
467 compartment models (Kennedy et al., 1992). Only four of the studies comparing one- and multi-  
468 compartment models found significantly more support for the multi-compartment model (Alvarez  
469 et al., 2020; Jauffrais et al., 2012; Kennedy et al., 1992; Woofter et al., 2005). These  
470 comparisons were made on a mixture of expert judgement and comparison of R<sup>2</sup> values, which  
471 also involved extensive expert judgement (**Fig. 3F**). Note that many studies (n=39) compared  
472 depuration rates among different tissues (**Fig. 3B**), which also provides information on multi-  
473 compartment depuration rates.

474

475 Depuration rates varied from 22.3 day<sup>-1</sup> (0.03 day half-life) for microcystin from whole  
476 *Eurytemora affinis* copepods (Karjalainen et al., 2006) to 0.0005 day<sup>-1</sup> (1269 day half-life) for  
477 domoic acid from the gills of Dungeness crab (*Metacarcinus magister*) (Schultz et al., 2013)  
478 (**Fig. 4**). Depuration rates appeared relatively similar among species of the same genus (**Fig. 4**),  
479 motivating the taxonomic regression analysis described in *Section 2.3*.

### 480 3.2 Priority species for depuration study

481 Thirteen of the top-20 most harvested marine filter-feeding mollusc species from  
482 countries exposed to PSTs have had their PST depuration rates studied (**Fig. 5A**), the highest  
483 of any of the biotoxin types (**Fig. 5**). However, three of the top-5 species have not had their PST  
484 depuration rates examined: constricted tagelus (*Sinonovacula constricta*) and blood cockle  
485 (*Tegillarca granosa*). PST depuration rates for 1 new order, 2 new families, and 4 new genera  
486 could be gained through the evaluation of 7 of the 10 unstudied species (**Table S4**). In  
487 particular, evaluation of blood cockle (*Tegillarca granosa*) would provide information for 8  
488 harvested and 360 total species in the Arcoida order.

489

490 Only six of the top-20 most harvested marine filter-feeding mollusc species from  
491 countries exposed to domoic acid have had their domoic acid depuration rates studied (**Fig.**  
492 **5B**). Notably, none of the four most intensely harvested species have had their domoic acid  
493 depuration rates examined: Manila clam, constricted tagelus, blood cockle (*Tegillarca granosa*),  
494 or Chilean mussel (*Mytilus chilensis*). Domoic acid depuration rates for 1 new order, 4 new  
495 families, and 2 new genera could be gained through the evaluation of 11 of the 14 unstudied  
496 species (**Table S4**). In particular, evaluation of Manila clam (*Ruditapes philippinarum*), striped  
497 venus (*Chamelea gallina*), or northern quahog (*Mercenaria mercenaria*) would provide  
498 information for 22 harvested and 428 total species in the Veneridae family.  
499

500 Only four of the top-20 most harvested marine filter-feeding mollusc species from  
501 countries exposed to DSTs have had their DST depuration rates studied (**Fig. 5C**). Notably, six  
502 of the seven most intensely harvested species have had their DST depuration rates examined:  
503 constricted tagelus, Pacific oyster (*Magallana gigas*), Japanese scallop (*Mizuhopecten*  
504 *yessoensis*), blood cockle, Chilean mussel, and Atlantic sea scallop (*Placopecten*  
505 *magellanicus*). DST depuration rates for 2 new orders, 3 new families, and 7 new genera could  
506 be gained through the evaluation of 14 of the 17 unstudied species (**Table S4**). In particular,  
507 evaluation of blood cockle would provide information for 8 harvested and 360 total species in  
508 the Arcoida order.  
509

510 Only five of the top-20 most harvested marine filter-feeding mollusc species from  
511 countries exposed to cyanotoxins have had their cyanotoxin depuration rates studied (**Fig. 5D**).  
512 Notably, neither of the two most intensely harvested species have had their cyanotoxin  
513 depuration rates examined: Chilean mussel or Atlantic sea scallop. Cyanotoxin depuration rates  
514 for 4 new families, and 2 new genera could be gained through the evaluation of 14 of the 16  
515 unstudied species (**Table S4**). In particular, evaluation of Atlantic sea scallop (*Placopecten*  
516 *magellanicus*), Patagonian scallop (*Zygochlamys patagonica*), or king scallop (*Pecten maximus*)  
517 would provide information for 20 harvested and 297 total species in the Pectinidae family.  
518

519 Only two of the top-20 most harvested marine filter-feeding mollusc species from  
520 countries exposed to brevetoxins have had their brevetoxin depuration rates studied (**Fig. 5E**).  
521 Notably, none of the six most intensely harvested species have had their brevetoxin depuration  
522 rates examined: Manila clam, constricted tagelus, Japanese scallop, blood cockle, Chilean  
523 mussel, or Pacific oyster. Brevetoxin depuration rates for 2 new orders, 5 new families, and 5

524 new genera could be gained through the evaluation of 17 of the 18 unstudied species (**Table**  
525 **S4**). In particular, evaluation of Japanese scallop (*Mizuhopecten yessoensis*), Atlantic sea  
526 scallop, king scallop, or queen scallop (*Aequipecten opercularis*) would provide information for  
527 20 harvested and 297 total species in the Pectinidae family.

528

529 Only one of the top-20 most harvested marine filter-feeding mollusc species from  
530 countries exposed to azaspiracids have had their azaspiracid depuration rates studied (**Fig. 5F**).  
531 Notably, none of the seven most intensely harvested species have had their azaspiracid  
532 depuration rates examined: Manila clam, constricted tagelus, blood cockle, greenshell mussel  
533 (*Perna canaliculus*), Mediterranean mussel (*Mytilus galloprovincialis*), Peruvian calico scallop  
534 (*Argopecten purpuratus*), or Patagonian scallop (*Zygochlamys patagonica*). Azaspiracid  
535 depuration rates for 4 new orders and 2 new genera could be gained through the evaluation of  
536 17 of the 19 unstudied species (**Table S4**). In particular, evaluation of Manila clam, constricted  
537 tagelus, striped venus, common cockle (*Cerastoderma edule*), grooved carpet shell (*Ruditapes*  
538 *decussatus*), triangular tivela (*Tivela mactroides*), or smooth callista (*Callista chione*) would  
539 provide information for 58 harvested and 2549 total species in the Veneroida order.

540

541 Striped mullet (*Mugil cephalus*) is the only finfish in the top-50 most harvested finfish  
542 with known or hypothesized vulnerability to ciguatera from countries exposed to ciguatera to  
543 have had its ciguatera depuration rates studied (Ledreux et al., 2014) (**Fig. S7**). Otherwise,  
544 ciguatera depuration rates have only been quantified for minor fisheries species. Pinfish  
545 (*Lagodon rhomboides*) (Bennett and Robertson, 2021), orange-spotted grouper (*Epinephelus*  
546 *coioides*) (Li et al., 2020), and lionfish (*Pterois volitans*) (Leite et al., 2021) have had depuration  
547 rates measured but are the 88<sup>th</sup>, 99<sup>th</sup>, and 114<sup>th</sup> most important large, predatory, reef-associated  
548 fisheries species occurring in countries where ciguatera is known to occur.

549

550 Although only 34 non-bivalves species have had their depuration rates studied, many  
551 non-bivalves have been observed within toxicities exceeding action thresholds (**Fig. S8**),  
552 highlighting the importance of studying biotoxin depuration in more non-bivalve species. In  
553 particular, a large number of harvested gastropods and crustaceans have been observed with  
554 PST toxicities far above the PST action threshold.

555 3.3 Predicting bivalve PST depuration rates

556 All four models exhibited good convergence ( $\hat{R} < 1.01$ , no divergent transitions) and  
557 passed posterior predictive checks (**Figure S9**). The models with taxonomic random effects  
558 significantly outperformed the model with only life history, location, and tissue fixed effects  
559 ( $\Delta\text{ELPD} > 26$ ;  $\Delta R^2=0.18$ ; **Table S5**). The models with taxonomic random effects exhibited  
560 similar performance with the greatest statistical support for the taxonomically random effects  
561 model ( $\text{ELPD}=-229.4$ ,  $R^2=0.67$ ) followed by the non-phylogenetic random effects model  
562 ( $\Delta\text{ELPD}=0.3$ ,  $\Delta\text{ELPD-SE}=0.3$ ,  $\Delta R^2=0.01$ ) then the phylogenetic random effects model  
563 ( $\Delta\text{ELPD}=1.3$ ,  $\Delta\text{ELPD-SE}=0.0$ ,  $\Delta R^2=0.02$ ). The taxonomic random effects model was therefore  
564 selected as the best performing model.

565

566 The taxonomic random effects model estimated that depuration rates are significantly  
567 slower (smaller) in the field relative to the lab (**Fig. 6A; Fig. S10A**). On average, field depuration  
568 rates are 2.5 times slower than lab depuration rates. The model estimated non-significant  
569 impacts of the three life history variables, which exhibited a mixture of non-significant positive  
570 (growth rate) and negative (maximum length, preferred temperature) effects. The model  
571 estimated significant differences in PST depuration rates among bivalve tissues with the  
572 hepatopancreas and soft tissues exhibiting faster depuration rates than other tissues. The  
573 conditional effects of the fixed effects variable, which estimate the depuration rate with all other  
574 effects estimated at their average, are shown in **Fig. S10**. The greater statistical support for this  
575 model over the “fixed effects only” model indicates a significant impact of taxonomy on  
576 depuration rates with the relative impacts of taxonomy on depuration rates illustrated in **Fig. 6B**.  
577 The greater support of this model over the phylogenetic model suggests that, based on the  
578 current data, while depuration rates vary by clade, they do not vary based on the relatedness of  
579 clades (**Table S5**).  
580

581 The field-based PST depuration rates for species included in model fitting were  
582 estimated to vary from  $0.0009 \text{ day}^{-1}$  for smooth clam (*Callista chione*) to  $0.20 \text{ day}^{-1}$  for noble  
583 scallop (*Mimachlamys crassicostata*) (**Fig. 7; Table S6**). The field-based PST depuration rates  
584 for all harvested bivalves were estimated to vary from  $0.0009 \text{ day}^{-1}$  for smooth clam to  $1.94 \text{ day}^{-1}$   
585 for Pacific calico scallop (*Argopecten ventricosus*) (**Fig. 8; Table S7**), after excluding  
586 exceptionally high and uncertain estimated depuration rates for giant clam (*Tridacna gigas*) and  
587 mangrove cupped oyster (*Crassostrea rhizophorae*). Giant clam ( $91.5 \text{ day}^{-1}$ ) and mangrove  
588 copper oyster ( $16.7 \text{ day}^{-1}$ ) exhibited high depuration rates because of their exceptionally large

589 maximum size (137 cm) and fast growth rate ( $2.8 \text{ yr}^{-1}$ ), respectively. Because no species in the  
590 Arcida or Limida order were available in the training dataset, predictions for species in this  
591 order are not informed by taxonomic information. The lab- and field-based depuration rates  
592 predicted for harvested marine bivalves are provided in **Table S7**.

## 593 4. Discussion

594 Ensuring the safety of marine seafood is a daunting task. An estimated ~200 taxa  
595 produce biotoxins that accumulate in marine food webs and threaten public health (Lundholm et  
596 al., 2009). These taxa produce a diverse range of toxins, which require independent chemical  
597 assays to detect and monitor (Hallegraeff et al., 2004). With over 3,000 species of marine fish  
598 and invertebrates harvested by commercial fisheries and aquaculture along hundreds of  
599 thousands of kilometers of coastline (FAO, 2024), it is impossible for biotoxin monitoring to  
600 cover all species, toxins, and locations. Thus, managers need every tool in the toolbox to design  
601 cost-effective biotoxin monitoring programs that protect public health while also limiting closures  
602 to commercially, recreationally, and culturally important coastal food systems.

603  
604 Forecasting depuration timelines using depuration rates offers one such tool. With  
605 knowledge of how quickly a species eliminates toxins, managers can predict when toxicity will  
606 fall to levels deemed safe for human consumption. This information is valuable for several  
607 reasons. First, it provides seafood businesses with predictions of how long production is likely to  
608 be delayed, which can empower adaptive business decisions. For example, during long delays,  
609 harvesters may decide to pivot to new species, fishing grounds, or even alternative livelihoods  
610 (Moore et al., 2020). Second, such predictions could help managers decide whether to close  
611 fisheries, which could be preferred during short depuration timelines, or let them operate under  
612 an “evisceration order” that requires the removal of toxic viscera before sale, which can lower  
613 product value (Hackett et al., 2003), but may be preferable to closures during long depuration  
614 timelines. Finally, as described in the introduction, such predictions could be used to improve  
615 the efficiency of biotoxin monitoring (Blanco, 2009). Eliminating unnecessary tests would free up  
616 limited resources to allow monitoring of more sites or species, which has large economic and  
617 public health benefits. Monitoring more sites increases the resolution of biotoxin management  
618 and could lead to less restrictive fisheries closures (Free et al., 2022) while monitoring  
619 previously unmonitored species could more fully protect public health (Costa et al., 2017).

620

621 Our results show that depuration is slower in the field than in the lab, which has  
622 important implications for the application of lab-based depuration rates in natural settings. While  
623 lab studies quantify depuration rates while organisms are either starved or fed a non-toxic diet,  
624 field studies quantify depuration while organisms continue the uptake of biotoxins from  
625 dwindling blooms (Rourke et al., 2021), residual biotoxins in the food web (Yang et al., 2016), or  
626 dormant benthic cysts, which can be directly consumed by detritivores or planktivores if  
627 resuspended (Persson et al., 2006). This means that depuration timelines projected using lab-  
628 base depuration rates are likely to be optimistic (i.e., forecast faster declines in toxicity than  
629 reality). Fortunately, this is a favorable bias as testing sooner than necessary protects public  
630 health without unnecessarily delaying openings to fisheries or aquaculture operations (Free et  
631 al., 2022). The opposite bias (slower declines than reality) would be less favorable as it could  
632 delay testing until after toxicity has fallen below the action threshold, resulting in unnecessarily  
633 long closures to fisheries and aquaculture operations. However, managers may want to assume  
634 slower depuration rates than predicted by lab studies as more accurate forecasts will result in  
635 higher cost savings while still protecting public health and avoiding unnecessary closures. For  
636 example, managers could assume that depuration occurs 2.5 times more slowly in the field, the  
637 average estimated by our best performing Bayesian regression model.

638

639 Managers may also adjust the expected depuration rate and associated cadence of  
640 monitoring based on observations of temperature, food availability, body condition, or other  
641 factors that impact depuration rates. For example, managers may expect faster than average  
642 depuration rates if temperatures are warm (Bricelj et al., 2014), food availability and  
643 consumption is high (Bricelj and Shumway, 1998), or body condition is poor (Castberg et al.,  
644 2004). However, caution is necessary as these factors can have confounding impacts on bloom  
645 toxicity and biotoxin uptake. If warm water stimulates HAB productivity and toxicity (McKibben et  
646 al., 2017), elevated uptake may offset accelerated depuration. Similarly, if consumption is high  
647 due to either high food availability or low body condition, then rapid toxin uptake may offset  
648 accelerated depuration. Adjusting depuration rates based on these considerations may  
649 therefore be most useful once there is evidence that the bloom has abated and there is  
650 significantly less biotoxin available for uptake. Then, managers can use knowledge of recent  
651 temperature, food availability, or body condition to adjust the expected depuration rate and  
652 recalculate the optimized cadence of biotoxin monitoring.

653

Our review indicates that aquaculture farmers can take several actions to accelerate biotoxin depuration. Because depuration rates increase with food ingestion and egestion (Bricelj and Shumway, 1998), farms can enhance depuration by increasing food availability and/or stimulating food consumption. In the case of fed aquaculture for finfish and crustaceans, this could involve providing more food than usual. In the case of unfed bivalve aquaculture, consumption could be stimulated by reducing stocking density to reduce competition for ambient food (Cubillo et al., 2012). Another strategy could be to limit or inhibit feeding during a bloom to avoid biotoxin accumulation but also to reduce body condition and increase hunger to stimulate rapid consumption and depuration after the bloom abates (Castberg et al., 2004). Because depuration rates increase with temperature, which increases metabolism, consumption, and egestion (Bricelj et al., 2014; Novaczek et al., 1992), farmers could move racks, lines, rafts, or nets into warmer areas after a HAB to accelerate depuration. Furthermore, if warm water does not result in increased mortality, disease, HAB risk, or other detrimental effects, aquaculture could be strategically sited in warm areas to enhance depuration when necessary. Relatedly, aquaculture species with fast depuration rates (and slow uptake rates) may be good candidates for areas with high HAB risk. Finally, there is evidence that a number of industrial additives can be used to enhance depuration rates (Bian et al., 2024; Martinez-Albores et al., 2020), but these are often cost prohibitive or not allowed by regulation (Leal and Cristiano, 2024).

Biotoxin depuration rates of marine seafood species are understudied, especially for non-filter feeders. Higher trophic level species, including herbivorous gastropods, detritivorous crustaceans, and carnivorous fish, are particularly understudied, despite observations of unsafe levels of toxicity in these species (Costa et al., 2017; Deeds et al., 2008; Lefebvre and Robertson, 2010). The quantification of depuration rates for vulnerable gastropods, crustaceans, and finfish and their broader inclusion in biotoxin monitoring programs, where they are often overlooked (Costa et al., 2017), is thus important for fully protecting public health. It is frequently asserted that biotoxins in finfish pose minimum human health risk because the toxins do not accumulate in muscle tissue (e.g., Deeds et al., 2008; Lefebvre et al., 2002); however, the consumption of non-muscle tissue is common in many cultures and many preparation techniques use the whole fish (Golden et al., 2021). Furthermore, the processing of planktivorous forage fish into fish meal and fish oil uses the whole fish, presenting a potential pathway for unmonitored toxins to enter aquaculture and livestock feed (Adeyemo-Eleyode et al., 2025). Finally, the study of species that are not harvested by humans but represent important nodes in marine food webs is critical to understanding the trophic transfer of biotoxins

688 (Holmes and Lewis, 2022; Lefebvre et al., 2002). Besides three unharvested copepod species  
689 (*Calanus finmarchicus* are harvested in Norway; FAO, 2024), we found that only two  
690 unharvested species (opossum shrimp, *Neomysis awatschensis* and Pacific mole crab, *Emerita*  
691 *analogica*) have had their depuration rates studied.

692

693 Although bivalves have undergone the most study, depuration rates have still not been  
694 quantified for most bivalve species harvested in commercial fisheries and aquaculture. For  
695 example, PST depuration rates are unquantified for 104 species, 60 entire genera, 12 entire  
696 families, and 2 entire orders of harvested marine bivalves. To our knowledge, we provide the  
697 first evidence that PST depuration rates are structured by bivalve taxonomy, meaning that  
698 closely related species exhibit similar depuration rates. Although we did not find evidence that  
699 PST depuration rates are phylogenetically conserved, this may be due to low taxonomic  
700 representation in current depuration studies, given that nested taxonomic identity was found to  
701 be an important predictor of PST depuration rates. As a result, managers can use either our  
702 predicted depuration rates or collated observed depuration rates from related species as proxies  
703 for species without known depuration rates. This finding also highlights the immense value of  
704 empirically quantifying PST depuration rates for a new order, family, or genus to provide  
705 guidance on depuration rates for the greatest number of new species. The expanded  
706 quantification of depuration rates would be useful to confirm whether depuration rates are  
707 taxonomically structured, or even phylogenetically conserved, across other toxins and  
708 taxonomic classes (i.e., not just a result for PSTs in bivalves). We suspect this is the case given  
709 the similarity in physiology and feeding ecology among related organisms (Leahy et al., 2025).

710

711 Biotoxin monitoring programs present a direct and underutilized data source for  
712 measuring depuration rates under natural conditions. Although marine biotoxin monitoring  
713 programs are used by many wealthy coastal countries (Andersen et al., 2004), our literature  
714 review found only 18 papers that directly reported depuration rates quantified from monitoring  
715 programs. These programs document the rise and fall of biotoxins in diverse species across  
716 many sites and years, representing a large and informative store of already collected data on  
717 seafood toxicokinetics. The analysis of these data would yield depuration rates for new species  
718 and toxins (e.g., McGuire et al. (2025) provide the only source of DST depuration rates for  
719 eastern oyster, *Crassostrea virginica*) and would quantify the variability in depuration rates  
720 stemming from different environmental conditions (e.g., Blanco et al. (1997) show that impacts  
721 of salinity, temperature, light availability, and primary productivity on PST depuration in

722 mussels), all without additional field or lab costs. As a start, we quantified depuration rates for  
723 45 species-toxin combinations from 30 field studies that did not directly estimate depuration  
724 rates but were discovered in our systematic review due to the inclusion of depuration-related  
725 words in their abstract or keywords (e.g., Haya et al., 2003; Kvrgić et al., 2022; Rourke et al.,  
726 2021). However, this still overlooks the likely large number of biotoxin monitoring programs that  
727 are either not documented, are documented without these keywords, or are only documented in  
728 the grey or non-English literature. The optimization of monitoring programs using depuration  
729 rates derived from their own data would free up resources to expand monitoring to new species,  
730 thereby funding the iterative derivation of depuration rates and optimization of monitoring.

731

732 The utility of new depuration studies would be maximized through the adoption of a few  
733 best practices. In particular, surprisingly few of the evaluated studies (41% of papers) directly  
734 quantified depuration rates using standard depuration models, which complicates comparisons  
735 between studies and limits utility to managers. New studies should use standard depuration  
736 models (see Blanco, 2009) to quantify depuration rates to ease interpretability and use. If  
737 comparing one- and multi-compartment models, we recommend the use of Akaike information  
738 criterion (AIC) to select the most parsimonious model, recognizing that multi-compartment  
739 models have more parameters and should nearly always generate tighter, though not  
740 necessarily more parsimonious, fits (Burnham and Anderson, 2004). All of the studies  
741 comparing one- and multi-compartment models compared fits used either  $R^2$  (e.g., Nielsen et  
742 al., 2016), which is biased to favor more complex models, or subjective judgements of fit and  
743 parsimony (e.g., Kennedy et al., 1992), which is not replicable. Next, given that depuration in  
744 real-world fisheries and aquaculture settings is likely to occur while feeding, new studies should  
745 always include a scenario in which the treated organism is fed during the depuration phase.  
746 24% of the evaluated studies only considered depuration under starved conditions (e.g.,  
747 Duinker et al., 2007b), limiting their relevance to real-world settings. Finally, depuration studies  
748 should consider management-relevant tissues to maximize utility. For example, 10% of the  
749 evaluated studies did not generate a depuration rate for tissues targeted for consumption by  
750 people or with the greatest toxin burden (e.g., focused only on the hemolymph; Schultz et al.,  
751 2008).

752

753 As the public health risk posed by HABs worsens under the combined effects of  
754 eutrophication and climate change (IPCC, 2019), managers will need every tool in the toolbox to  
755 improve the cost effectiveness of biotoxin monitoring. The use of depuration rates to adjust the

756 cadence of monitoring during the depuration phase of HAB events is only one such tool. For  
757 example, the development of reliable early warning indicators of HAB risk could be used to  
758 more efficiently time the onset of biotoxin monitoring, sparing the need for testing while risk is  
759 low (Anderson et al., 2019). Similarly, knowledge of biotoxin uptake rates by seafood species  
760 could be used to optimize the cadence of testing during the uptake phase of HAB events. These  
761 advances will be critical to fully protecting public health while simultaneously avoiding  
762 unnecessary fisheries and aquaculture closures in a rapidly changing ocean.

## 763 Acknowledgements

764 This work is the result of research funded by NOAA's National Centers for Coastal Ocean  
 765 Science Competitive Research Program, Climate Program Office, Ocean Acidification Program,  
 766 and the U.S. Integrated Ocean Observing System Office under award NA22NOS4780171 to  
 767 Oregon State University, and to NOAA's Pacific Marine Environmental Laboratory.

## 768 References

- 769 Adeyemo-Eleyode, V.O., Adetuyi, B.O., Olajide, P.A., Chidume, C.C., Okunlola, F.O., Oni, P.G.,  
 770 Awe, A.I., 2025. Exploring the Origin and Epidemiology of Biotoxins in Foods and Feeds:  
 771 An Updated Perspective, in: *Biotoxins in Food*. CRC Press.
- 772 Alvarez, G., Rengel, J., Araya, M., Alvarez, F., Pino, R., Uribe, E., Diaz, P.A., Rossignoli, A.E.,  
 773 Lopez-Rivera, A., Blanco, J., 2020. Rapid Domoic Acid Depuration in the Scallop  
 774 *Argopecten purpuratus* and Its Transfer from the Digestive Gland to Other Organs.  
 775 *Toxins*. <https://doi.org/10.3390/toxins12110698>
- 776 Andersen, P., Enevoldsen, H., Anderson, D., 2004. Harmful algal monitoring programme and  
 777 action plan design, in: *Manual on Harmful Marine Algae*. UNESCO Publishing, Paris,  
 778 France.
- 779 Anderson, C.R., Berdalet, E., Kudela, R.M., Cusack, C.K., Silke, J., O'Rourke, E., Dugan, D.,  
 780 McCammon, M., Newton, J.A., Moore, S.K., Paige, K., Ruberg, S., Morrison, J.R.,  
 781 Kirkpatrick, B., Hubbard, K., Morell, J., 2019. Scaling Up From Regional Case Studies to  
 782 a Global Harmful Algal Bloom Observing System. *Front. Mar. Sci.*  
 783 <https://doi.org/10.3389/fmars.2019.00250>
- 784 Arnich, N., Thébault, A., 2018. Dose-Response Modelling of Paralytic Shellfish Poisoning (PSP)  
 785 in Humans. *Toxins* 10, 141. <https://doi.org/10.3390/toxins10040141>
- 786 Barbosa, V., Santos, M., Anacleto, P., Maulvault, A.L., Pousao-Ferreira, P., Costa, P.R.,  
 787 Marques, A., 2019. Paralytic Shellfish Toxins and Ocean Warming: Bioaccumulation and  
 788 Ecotoxicological Responses in Juvenile Gilthead Seabream (*Sparus aurata*). *Toxins*.  
 789 <https://doi.org/10.3390/toxins11070408>
- 790 Bennett, C.T., Robertson, A., 2021. Depuration Kinetics and Growth Dilution of Caribbean  
 791 Ciguatoxin in the Omnivore *Lagodon rhomboides*: Implications for Trophic Transfer and  
 792 Ciguatera Risk. *Toxins*. <https://doi.org/10.3390/toxins13110774>
- 793 Bian, Y., Feng, X., Zhang, Y., Du, C., Wen, Y., 2024. Marine toxins in environment: Recent  
 794 updates on depuration techniques. *Ecotoxicol. Environ. Saf.*  
 795 <https://doi.org/10.1016/j.ecoenv.2024.116990>
- 796 Blanco, J., 2009. Modelling as a mitigation strategy for harmful algal blooms. *Shellfish Saf.*  
 797 Qual., Woodhead Publishing Series in Food Science Technology and Nutrition.
- 798 Blanco, J., Acosta, C.P., Bermúdez de la Puente, M., Salgado, C., 2002. Depuration and  
 799 anatomical distribution of the amnesic shellfish poisoning (ASP) toxin domoic acid in the  
 800 king scallop *Pecten maximus*. *Aquat. Toxicol.* 60, 111–121.  
 801 [https://doi.org/10.1016/S0166-445X\(01\)00274-0](https://doi.org/10.1016/S0166-445X(01)00274-0)
- 802 Blanco, J., Fernández, M., Míguez, A., Moroño, A., 1999. Okadaic acid depuration in the mussel  
 803 *Mytilus galloprovincialis*: one- and two-compartment models and the effect of  
 804 environmental conditions. *Mar. Ecol. Prog. Ser.* <https://doi.org/10.3354/meps176153>
- 805 Blanco, J., Morono, A., Franco, J., Reyero, M., 1997. PSP detoxification kinetics in the mussel  
 806 *Mytilus galloprovincialis*. One- and two-compartment models and the effect of some  
 807 environmental variables. *Mar. Ecol. Prog. Ser.* <https://doi.org/10.3354/meps158165>
- 808 Boettiger, C., Lang, D.T., Wainwright, P.C., 2012. rfishbase: exploring, manipulating and

- 809 visualizing FishBase data from R. J. Fish Biol. 81, 2030–2039.  
 810 <https://doi.org/10.1111/j.1095-8649.2012.03464.x>
- 811 Bogan, Y.M., Harkin, A.L., Gillespie, J., Kennedy, D.J., Hess, P., Slater, J.W., 2007. The  
 812 influence of size on domoic acid concentration in king scallop, *Pecten maximus* (L.).  
 813 Harmful Algae. <https://doi.org/10.1016/j.hal.2006.05.005>
- 814 Botelho, M.J., Vale, C., Joaquim, S., Costa, S.T., Soares, F., Roque, C., Matias, D., 2018.  
 815 Combined effect of temperature and nutritional regime on the elimination of the lipophilic  
 816 toxin okadaic acid in the naturally contaminated wedge shell *Donax trunculus*.  
 817 Chemosphere. <https://doi.org/10.1016/j.chemosphere.2017.09.100>
- 818 Braga, A.C., Camacho, C., Marques, A., Gago-Martinez, A., Pacheco, M., Costa, P.R., 2018.  
 819 Combined effects of warming and acidification on accumulation and elimination  
 820 dynamics of paralytic shellfish toxins in mussels *Mytilus galloprovincialis*. Environ. Res.  
 821 <https://doi.org/10.1016/j.envres.2018.03.045>
- 822 Bricelj, V.M., Cembella, A.D., Laby, D., 2014. Temperature effects on kinetics of paralytic  
 823 shellfish toxin elimination in Atlantic surfclams, *Spisula solidissima*. Deep-Sea Res. Part  
 824 II-Top. Stud. Oceanogr. <https://doi.org/10.1016/j.dsr2.2013.05.014>
- 825 Bricelj, V.M., Shumway, S.E., 1998. Paralytic Shellfish Toxins in Bivalve Molluscs: Occurrence,  
 826 Transfer Kinetics, and Biotransformation. Rev. Fish. Sci.  
 827 <https://doi.org/10.1080/10641269891314294>
- 828 Bürkner, P.-C., 2017. brms: An R Package for Bayesian Multilevel Models Using Stan. J. Stat.  
 829 Softw. 80, 1–28. <https://doi.org/10.18637/jss.v080.i01>
- 830 Burnham, K.P., Anderson, D.R., 2004. Multimodel Inference: Understanding AIC and BIC in  
 831 Model Selection. Sociol. Methods Res. 33, 261–304.  
 832 <https://doi.org/10.1177/0049124104268644>
- 833 Castberg, T., Torgersen, T., Aasen, J., Aune, T., Naustvoll, L., 2004. Diarrhoetic shellfish  
 834 poisoning toxins in Cancer pagurus Linnaeus, 1758 (Brachyura, Cancridae) in  
 835 Norwegian waters. Sarsia. <https://doi.org/10.1080/00364820410002550>
- 836 Chen, C., Chou, H., 2002. Fate of paralytic shellfish poisoning toxins in purple clam *Hiatala*  
 837 *rostrata*, in outdoor culture and laboratory culture. Mar. Pollut. Bull.  
 838 [https://doi.org/10.1016/S0025-326X\(01\)00307-1](https://doi.org/10.1016/S0025-326X(01)00307-1)
- 839 Choi, M., Hsieh, D., Lam, P., Wang, W., 2003. Field depuration and biotransformation of  
 840 paralytic shellfish toxins in scallop *Chlamys nobilis* and green-lipped mussel *Perna*  
 841 *viridis*. Mar. Biol. <https://doi.org/10.1007/s00227-003-1148-y>
- 842 Costa, P.R., Costa, S.T., Braga, A.C., Rodrigues, S.M., Vale, P., 2017. Relevance and  
 843 challenges in monitoring marine biotoxins in non-bivalve vectors. Food Control.  
 844 <https://doi.org/10.1016/j.foodcont.2016.12.038>
- 845 Cubillo, A.M., Peteiro, L.G., Fernández-Reiriz, M.J., Labarta, U., 2012. Influence of stocking  
 846 density on growth of mussels (*Mytilus galloprovincialis*) in suspended culture.  
 847 Aquaculture 342–343, 103–111. <https://doi.org/10.1016/j.aquaculture.2012.02.017>
- 848 Deeds, J.R., Landsberg, J.H., Etheridge, S.M., Pitcher, G.C., Longan, S.W., 2008. Non-  
 849 Traditional Vectors for Paralytic Shellfish Poisoning. Mar. Drugs 6, 308–348.  
 850 <https://doi.org/10.3390/md6020308>
- 851 Duinker, A., Bergslien, M., Strand, O., Olseng, C.D., Svartdal, A., 2007a. The effect of size and  
 852 age on depuration rates of diarrhetic shellfish toxins (DST) in mussels (*Mytilus edulis* L.).  
 853 Harmful Algae. <https://doi.org/10.1016/j.hal.2006.10.003>
- 854 Duinker, A., Bergslien, M., Strand, O., Olseng, C.D., Svartdal, A., 2007b. The effect of size and  
 855 age on depuration rates of diarrhetic shellfish toxins (DST) in mussels (*Mytilus edulis* L.).  
 856 Harmful Algae. <https://doi.org/10.1016/j.hal.2006.10.003>
- 857 FAO, 2024. The State of World Fisheries and Aquaculture 2024. FAO, Rome.
- 858 Farrell, H., Seebacher, F., O'Connor, W., Zammit, A., Harwood, D.T., Murray, S., 2015. Warm  
 859 temperature acclimation impacts metabolism of paralytic shellfish toxins from

- 860                   Alexandrium minutum in commercial oysters. *Glob. Change Biol.*  
 861                   <https://doi.org/10.1111/gcb.12952>
- 862 Fernandez, M., Shumway, S., Blanco, J., 2003. Management of shellfish resources.  
 863 Flanders Marine Institute, 2025. *MarineRegions.org*.
- 864 Free, C.M., Moore, S.K., Trainer, V.L., 2022. The value of monitoring in efficiently and  
 865 adaptively managing biotoxin contamination in marine fisheries. *Harmful Algae* 114,  
 866 102226. <https://doi.org/10.1016/j.hal.2022.102226>
- 867 Froese, R., Pauly, D., 2025. FishBase [WWW Document]. URL [www.fishbase.org](http://www.fishbase.org)
- 868 Garcia-Corona, J.L., Fabiou, C., Vanmaldergem, J., Petek, S., Derrien, A., Terre-Terrillon, A.,  
 869 Bressolier, L., Breton, F., Hegaret, H., 2024. The amnesic shellfish poisoning toxin,  
 870 domoic acid: The tattoo of the king scallop *Pecten maximus*. *Harmful Algae*.  
 871 <https://doi.org/10.1016/j.hal.2024.102607>
- 872 Gelman, A., Goodrich, B., Gabry, J., Vehtari, A., 2019. R-squared for Bayesian Regression  
 873 Models. *Am. Stat.* 73, 307–309. <https://doi.org/10.1080/00031305.2018.1549100>
- 874 Gibble, C.M., Peacock, M.B., Kudela, R.M., 2016. Evidence of freshwater algal toxins in marine  
 875 shellfish: Implications for human and aquatic health. *Harmful Algae*.  
 876 <https://doi.org/10.1016/j.hal.2016.09.007>
- 877 Golden, C.D., Koehn, J.Z., Shepon, A., Passarelli, S., Free, C.M., Viana, D.F., Matthey, H.,  
 878 Eurich, J.G., Gephart, J.A., Fluet-Chouinard, E., Nyboer, E.A., Lynch, A.J., Kjellevold,  
 879 M., Bromage, S., Charlebois, P., Barange, M., Vannuccini, S., Cao, L., Kleisner, K.M.,  
 880 Rimm, E.B., Danaei, G., DeSisto, C., Kelahan, H., Fiorella, K.J., Little, D.C., Allison,  
 881 E.H., Fanzo, J., Thilsted, S.H., 2021. Aquatic foods to nourish nations. *Nature* 598, 315–  
 882 320. <https://doi.org/10.1038/s41586-021-03917-1>
- 883 Grafen, A., 1997. The phylogenetic regression. *Philos. Trans. R. Soc. Lond. B Biol. Sci.* 326,  
 884 119–157. <https://doi.org/10.1098/rstb.1989.0106>
- 885 Grattan, L.M., Holobaugh, S., Morris, J.G., 2016. Harmful algal blooms and public health.  
 886 Harmful Algae, Harmful Algal Blooms and Public Health 57, 2–8.  
 887 <https://doi.org/10.1016/j.hal.2016.05.003>
- 888 Hackett, S.C., Krachey, M.J., Dewees, C.M., 2003. An economic overview of Dungeness crab  
 889 (Cancer magister) processing in California 44, 8.
- 890 Hallegraeff, G.M., Anderson, D.M., Belin, C., Bottein, M.-Y.D., Bresnan, E., Chinain, M.,  
 891 Enevoldsen, H., Iwataki, M., Karlson, B., McKenzie, C.H., Sunesen, I., Pitcher, G.C.,  
 892 Provoost, P., Richardson, A., Schweibold, L., Tester, P.A., Trainer, V.L., Yñiguez, A.T.,  
 893 Zingone, A., 2021. Perceived global increase in algal blooms is attributable to intensified  
 894 monitoring and emerging bloom impacts. *Commun. Earth Environ.* 2, 117.  
 895 <https://doi.org/10.1038/s43247-021-00178-8>
- 896 Hallegraeff, G.M., Anderson, D.M., Cembella, A.D. (Eds.), 2004. Manual on Harmful Marine  
 897 Algae. UNESCO Publishing, Paris, France.
- 898 Hardardottir, S., Hjort, D.M., Wohlrab, S., Krock, B., John, U., Nielsen, T.G., Lundholm, N.,  
 899 2019. Trophic interactions, toxicokinetics, and detoxification processes in a domoic acid-  
 900 producing diatom and two copepod species. *Limnol. Oceanogr.*  
 901 <https://doi.org/10.1002/limo.11078>
- 902 Haya, K., Martin, JL, Robinson, S., Martin, JD, Khots, A., 2003. Does uptake of Alexandrium  
 903 fundyense cysts contribute to the levels of PSP toxin found in the sea scallop,  
 904 *Placopecten magellanicus*? *Harmful Algae*. [https://doi.org/10.1016/S1568-9883\(02\)00068-9](https://doi.org/10.1016/S1568-9883(02)00068-9)
- 905 Hinchliff, C.E., Smith, S.A., Allman, J.F., Burleigh, J.G., Chaudhary, R., Coghill, L.M., Crandall,  
 906 K.A., Deng, J., Drew, B.T., Gazis, R., Gude, K., Hibbett, D.S., Katz, L.A.,  
 907 Laughinghouse, H.D., McTavish, E.J., Midford, P.E., Owen, C.L., Ree, R.H., Rees, J.A.,  
 908 Soltis, D.E., Williams, T., Cranston, K.A., 2015. Synthesis of phylogeny and taxonomy  
 909 into a comprehensive tree of life. *Proc. Natl. Acad. Sci.* 112, 12764–12769.
- 910

- 911 https://doi.org/10.1073/pnas.1423041112  
 912 Holmes, M.J., Lewis, R.J., 2022. Origin of Ciguateric Fish: Quantitative Modelling of the Flow of  
 913 Ciguatoxin through a Marine Food Chain. Toxins.  
 914 https://doi.org/10.3390/toxins14080534  
 915 Houle, K.C., Bill, B.D., Christy, A., Davis, J.P., Leighfield, T.A., Morton, S.L., Shumway, S.E.,  
 916 Trainer, V.L., Vadopalas, B., Hudson, B., 2023. Biotoxin uptake, retention, and  
 917 depuration trends in purple-hinged rock scallops, *Crassadoma gigantea* (Gray 1825). J.  
 918 SHELLFISH Res. https://doi.org/10.2983/035.042.0209  
 919 IPCC, 2019. IPCC Special Report on the Ocean and Cryosphere in a Changing Climate.  
 920 Jauffrais, T., Marcaillou, C., Herrenknecht, C., Truquet, P., Sechet, V., Nicolau, E., Tillmann, U.,  
 921 Hess, P., 2012. Azaspiracid accumulation, detoxification and biotransformation in blue  
 922 mussels (*Mytilus edulis*) experimentally fed Azadinium spinosum. Toxicon.  
 923 https://doi.org/10.1016/j.toxicon.2012.04.351  
 924 Karjalainen, M., Kozlowsky-Suzuki, B., Lehtiniemi, M., Engström-Öst, J., Kankaanpää, H.,  
 925 Viitasalo, M., 2006. Nodularin accumulation during cyanobacterial blooms and  
 926 experimental depuration in zooplankton. Mar. Biol. https://doi.org/10.1007/s00227-005-  
 927 0126-y  
 928 Kennedy, C.J., Schulman, L., Baden, D.G., Walsh, P.J., 1992. Toxicokinetics of brevetoxin  
 929 PBTX-3 in the Gulf toadfish, *Opsanus beta*, following intravenous administration. Aquat.  
 930 Toxicol. https://doi.org/10.1016/0166-445X(92)90032-I  
 931 Kim, B.-M., Haque, Md.N., Lee, D.-H., Nam, S.-E., Rhee, J.-S., 2018. Comparative  
 932 Toxicokinetics and Antioxidant Response in the Microcystin-LR-Exposed Gill of Two  
 933 Marine Bivalves, *Crassostrea gigas* and *Mytilus edulis*. J. Shellfish Res. 37, 497–506.  
 934 https://doi.org/10.2983/035.037.0305  
 935 Kim, Y.D., Kim, W.J., Shin, Y.K., Lee, D.-H., Kim, Y.-J., Kim, J.K., Rhee, J.-S., 2017.  
 936 Microcystin-LR bioconcentration induces antioxidant responses in the digestive gland of  
 937 two marine bivalves *Crassostrea gigas* and *Mytilus edulis*. Aquat. Toxicol.  
 938 https://doi.org/10.1016/j.aquatox.2017.05.003  
 939 Kvrgić, K., Lešić, T., Džafić, N., Pleadin, J., 2022. Occurrence and Seasonal Monitoring of  
 940 Domoic Acid in Three Shellfish Species from the Northern Adriatic Sea 12.  
 941 Landrum, P.F., Lydy, M.J., Lee, H., 1992. Toxicokinetics in aquatic systems: Model  
 942 comparisons and use in hazard assessment. Environ. Toxicol. Chem. 11, 1709–1725.  
 943 https://doi.org/10.1002/etc.5620111205  
 944 Langlois, G.W., Morton, S.L., 2018. Marine Biotoxin and Harmful Algae Monitoring and  
 945 Management, in: Harmful Algal Blooms. John Wiley & Sons, Ltd, pp. 377–418.  
 946 https://doi.org/10.1002/9781118994672.ch10  
 947 Le Moan, E., Derrien, A., Terre-Terrillon, A., Fabiouix, C., Jean, F., Lassudrie, M., Flye-Sainte-  
 948 Marie, J., Hegaret, H., 2025. Low contamination and rapid depuration of domoic acid in  
 949 the variegated scallop, *Mimachlamys varia*. Mar. Pollut. Bull.  
 950 https://doi.org/10.1016/j.marpolbul.2025.117946  
 951 Leahy, L., Chown, S.L., Riskas, H.L., Wright, I.J., Carlesso, A.G., Hammer, I.J., Sanders, N.J.,  
 952 Bishop, T.R., Parr, C.L., Gibb, H., 2025. Metabolic traits are shaped by phylogenetic  
 953 conservatism and environment, not just body size. Proc. Natl. Acad. Sci. 122,  
 954 e2501541122. https://doi.org/10.1073/pnas.2501541122  
 955 Leal, J.F., Bombo, G., Amado, P.S.M., Pereira, H., Cristiano, M.L.S., 2023. Cation-Exchange  
 956 Resin Applied to Paralytic Shellfish Toxins Depuration from Bivalves Exposed to  
 957 *Gymnodinium catenatum*. Foods. https://doi.org/10.3390/foods12040768  
 958 Leal, J.F., Cristiano, M.L.S., 2024. Why are bivalves not detoxified? Curr. Opin. Food Sci.  
 959 https://doi.org/10.1016/j.cofs.2024.101162  
 960 Leandro, L.F., Teegarden, G.J., Roth, P.B., Wang, Z., Doucette, G.J., 2010. The copepod  
 961 *Calanus finmarchicus*: A potential vector for trophic transfer of the marine algal biotoxin,

- 962 domoic acid. *J. Exp. Mar. Biol. Ecol.* <https://doi.org/10.1016/j.jembe.2009.11.002>
- 963 Ledreux, A., Brand, H., Chinain, M., Bottein, M.-Y.D., Ramsdell, J.S., 2014. Dynamics of  
964 ciguatoxins from *Gambierdiscus polynesiensis* in the benthic herbivore *Mugil cephalus*:  
965 Trophic transfer implications. *HARMFUL ALGAE*.  
966 <https://doi.org/10.1016/j.hal.2014.07.009>
- 967 Lefebvre, K., Silver, M., Coale, S., Tjeerdema, R., 2002. Domoic acid in planktivorous fish in  
968 relation to toxic *Pseudo-nitzschia* cell densities. *Mar. Biol.*  
969 <https://doi.org/10.1007/s00227-001-0713-5>
- 970 Lefebvre, K.A., Bargu, S., Kieckhefer, T., Silver, M.W., 2002. From sanddabs to blue whales:  
971 the pervasiveness of domoic acid. *Toxicon* 40, 971–977. [https://doi.org/10.1016/S0041-0101\(02\)00093-4](https://doi.org/10.1016/S0041-0101(02)00093-4)
- 972 Lefebvre, K.A., Robertson, A., 2010. Domoic acid and human exposure risks: A review.  
973 *Toxicon, Toxins in Seafood* 56, 218–230. <https://doi.org/10.1016/j.toxicon.2009.05.034>
- 974 Leite, I. do P., Sdiri, K., Taylor, A., Viallon, J., Gharbia, H.B., Mafra Junior, L.L., Swarzenski, P.,  
975 Oberhaensli, F., Darius, H.T., Chinain, M., Bottein, M.-Y.D., 2021. Experimental  
976 Evidence of Ciguatoxin Accumulation and Depuration in Carnivorous Lionfish. *Toxins*.  
977 <https://doi.org/10.3390/toxins13080564>
- 978 Lewis, A.M., Dean, K.J., Hartnell, D.M., Percy, L., Turner, A.D., Lewis, J.M., 2022. The value of  
979 toxin profiles in the chemotaxonomic analysis of paralytic shellfish toxins in determining  
980 the relationship between British *Alexandrium* spp. and experimentally contaminated  
981 *Mytilus* sp. *Harmful Algae*. <https://doi.org/10.1016/j.hal.2021.102131>
- 982 Lewis, R., Holmes, M., 1993. Origin and transfer of toxins involved in ciguatera. *Comp.*  
983 *Biochem. Physiol. C-Pharmacol. Toxicol. Endocrinol.* [https://doi.org/10.1016/0742-8413\(93\)90217-9](https://doi.org/10.1016/0742-8413(93)90217-9)
- 984 Li, J., Mak, Y.L., Chang, Y.-H., Xiao, C., Chen, Y.-M., Shen, J., Wang, Q., Ruan, Y., Lam,  
985 P.K.S., 2020. Uptake and Depuration Kinetics of Pacific Ciguatoxins in Orange-Spotted  
986 Grouper (*Epinephelus coioides*). *Environ. Sci. Technol.*  
987 <https://doi.org/10.1021/acs.est.9b07888>
- 988 Li, Q., Mahmudiono, T., Mohammadi, H., Nematollahi, A., Hoseinvandtabar, S., Mehri, F.,  
989 Hasanzadeh, V., Limam, I., Fakhri, Y., Thai, V.N., 2023. Concentration ciguatoxins in  
990 fillet of fish: A global systematic review and meta-analysis. *Heliyon* 9.  
991 <https://doi.org/10.1016/j.heliyon.2023.e18500>
- 992 Li, Y., Chen, R., Zhu, Z., Mu, T., Ran, Z., Xu, J., Zhou, C., Yan, X., 2024. Accumulation and  
993 depuration of 4,5-dihydro-KmTx2 from *Karlodinium veneficum* in the bivalves,  
994 *Mercenaria mercenaria* and *Sinonovacula constricta*. *Harmful Algae*.  
995 <https://doi.org/10.1016/j.hal.2024.102736>
- 996 Lopes, V.M., Baptista, M., Repolho, T., Rosa, R., Costa, P.R., 2014. Uptake, transfer and  
997 elimination kinetics of paralytic shellfish toxins in common octopus (*Octopus vulgaris*).  
998 *Aquat. Toxicol.* <https://doi.org/10.1016/j.aquatox.2013.11.011>
- 999 Lund, J.A.K., Barnett, H.J., Hatfield, C.L., Gauglitz, E.J., Wekell, J.C., Rasco, B., 1997. Domoic  
1000 acid uptake and depuration in Dungeness crab (*Cancer magister Dana 1852*). *J.*  
1001 *Shellfish Res.* 16, 225–231.
- 1002 Lundholm, N., Bernard, C., Churro, C., Escalera, L., Fraga, S., Hoppenrath, M., Iwataki, M.,  
1003 Larsen, J., Mertens, K., Moestrup, Ø., Murray, S., Salas, R., Tillmann, U., Zingone, A.,  
1004 2009. IOC-UNESCO Taxonomic Reference List of Harmful Micro Algae. Accessed at  
1005 <https://www.marinespecies.org/hab> on yyyy-mm-dd. <https://doi.org/10.14284/362>
- 1006 Mafra, L.L., Jr., Bricelj, V.M., Fennel, K., 2010. Domoic acid uptake and elimination kinetics in  
1007 oysters and mussels in relation to body size and anatomical distribution of toxin. *Aquat.*  
1008 *Toxicol.* <https://doi.org/10.1016/j.aquatox.2010.07.002>
- 1009 Marcaillou, C., Haure, J., Mondeguer, F., Courcoux, A., Dupuy, B., Penisson, C., 2010. Effect of  
1010 food supply on the detoxification in the blue mussel, *Mytilus edulis*, contaminated by
- 1011
- 1012

- 1013 diarrhetic shellfish toxins. *Aquat. Living Resour.* <https://doi.org/10.1051/alr/2010026>
- 1014 Martinez-Albores, A., Lopez-Santamarina, A., Rodriguez, J.A., Ibarra, I.S., Mondragón, A. del  
1015 C., Miranda, J.M., Lamas, A., Cepeda, A., 2020. Complementary Methods to Improve  
1016 the Depuration of Bivalves: A Review. *Foods* 9, 129.  
1017 <https://doi.org/10.3390/foods9020129>
- 1018 Martins, J.C., Dominguez-Perez, D., Azevedo, C., Braga, A.C., Costae, P.R., Osorio, H.,  
1019 Vasconcelos, V., Campos, A., 2020. Molecular Responses of Mussel *Mytilus*  
1020 *galloprovincialis* Associated to Accumulation and Depuration of Marine Biotoxins  
1021 Okadaic Acid and Dinophysistoxin-1 Revealed by Shotgun Proteomics. *Front. Mar. Sci.*  
1022 <https://doi.org/10.3389/fmars.2020.589822>
- 1023 McGuire, B.T., Sanderson, M.P., Smith, J.L., Gobler, C.J., 2025. Clearance rates and toxin  
1024 accumulation by North Atlantic bivalves during harmful algal blooms caused by the  
1025 dinoflagellate, *Dinophysis acuminata*, in estuaries. *Harmful Algae*.  
1026 <https://doi.org/10.1016/j.hal.2024.102745>
- 1027 McKibben, S.M., Peterson, W., Wood, A.M., Trainer, V.L., Hunter, M., White, A.E., 2017.  
1028 Climatic regulation of the neurotoxin domoic acid. *Proc. Natl. Acad. Sci.* 114, 239–244.  
1029 <https://doi.org/10.1073/pnas.1606798114>
- 1030 Medhioub, W., Gueguen, M., Lassus, P., Bardouil, M., Truquet, P., Sibat, M., Medhioub, N.,  
1031 Soudant, P., Kraiem, M., Amzil, Z., 2010. Detoxification enhancement in the  
1032 gymnodimine-contaminated grooved carpet shell, *Ruditapes decussatus* (Linne).  
1033 *Harmful Algae*. <https://doi.org/10.1016/j.hal.2009.10.002>
- 1034 Medhioub, W., Lassus, P., Truquet, P., Bardouil, M., Amzil, Z., Sechet, V., Sibat, M., Soudant,  
1035 P., 2012. Spirolide uptake and detoxification by *Crassostrea gigas* exposed to the toxic  
1036 dinoflagellate *Alexandrium ostenfeldii*. *Aquaculture*.  
1037 <https://doi.org/10.1016/j.aquaculture.2012.06.023>
- 1038 Michonneau, F., Brown, J.W., Winter, D.J., 2016. rotl: an R package to interact with the Open  
1039 Tree of Life data. *Methods Ecol. Evol.* 7, 1476–1481. <https://doi.org/10.1111/2041-210X.12593>
- 1041 Min, B.-H., Ravikumar, Y., Lee, D.-H., Choi, K.S., Kim, B.-M., Rhee, J.-S., 2018. Age-dependent  
1042 antioxidant responses to the bioconcentration of microcystin-LR in the mysid crustacean,  
1043 *Neomysis awatschensis*. *Environ. Pollut.* <https://doi.org/10.1016/j.envpol.2017.09.050>
- 1044 Moore, S.K., Dreyer, S.J., Ekstrom, J.A., Moore, K., Norman, K., Klinger, T., Allison, E.H.,  
1045 Jardine, S.L., 2020. Harmful algal blooms and coastal communities: Socioeconomic  
1046 impacts and actions taken to cope with the 2015 U.S. West Coast domoic acid event.  
1047 *Harmful Algae* 96, 101799. <https://doi.org/10.1016/j.hal.2020.101799>
- 1048 Moroño, A., Arévalo, F., Fernández, M., Maneiro, J., Pazos, Y., Salgado, C., Blanco, J., 2003.  
1049 Accumulation and transformation of DSP toxins in mussels *Mytilus galloprovincialis*  
1050 during a toxic episode caused by *Dinophysis acuminata*. *Aquat. Toxicol.*  
1051 [https://doi.org/10.1016/S0166-445X\(02\)00105-4](https://doi.org/10.1016/S0166-445X(02)00105-4)
- 1052 Nicolas, J., Hoogenboom, R.L.A.P., Hendriksen, P.J.M., Bodero, M., Bovee, T.F.H., Rietjens,  
1053 I.M.C.M., Gerssen, A., 2017. Marine biotoxins and associated outbreaks following  
1054 seafood consumption: Prevention and surveillance in the 21st century. *Glob. Food  
1055 Secur.* 15, 11–21. <https://doi.org/10.1016/j.gfs.2017.03.002>
- 1056 Nielsen, L.T., Hansen, P.J., Krock, B., Vismann, B., 2016. Accumulation, transformation and  
1057 breakdown of DSP toxins from the toxic dinoflagellate *Dinophysis acuta* in blue mussels,  
1058 *Mytilus edulis*. *Toxicon*. <https://doi.org/10.1016/j.toxicon.2016.03.021>
- 1059 Novaczek, I., Madhyastha, M., Ablett, R., Donald, A., Johnson, G., Nijjar, M., Sims, D., 1992.  
1060 Depuration of domoic acid from live blue mussels (*Mytilus edulis*). *Can. J. Fish. Aquat.  
1061 Sci.* <https://doi.org/10.1139/f92-035>
- 1062 OBIS, 2025. OBIS HAB node.
- 1063 Page, M.J., McKenzie, J.E., Bossuyt, P.M., Boutron, I., Hoffmann, T.C., Mulrow, C.D.,

- 1064 Shamseer, L., Tetzlaff, J.M., Akl, E.A., Brennan, S.E., Chou, R., Glanville, J., Grimshaw,  
 1065 J.M., Hróbjartsson, A., Lalu, M.M., Li, T., Loder, E.W., Mayo-Wilson, E., McDonald, S.,  
 1066 McGuinness, L.A., Stewart, L.A., Thomas, J., Tricco, A.C., Welch, V.A., Whiting, P.,  
 1067 Moher, D., 2021. The PRISMA 2020 statement: an updated guideline for reporting  
 1068 systematic reviews. *BMJ* 372, n71. <https://doi.org/10.1136/bmj.n71>
- 1069 Palomares, M.L.D., Pauly, D., 2025. SeaLifeBase.
- 1070 Paradis, E., Schliep, K., 2019. ape 5.0: an environment for modern phylogenetics and  
 1071 evolutionary analyses in R. *Bioinformatics* 35, 526–528.  
<https://doi.org/10.1093/bioinformatics/bty633>
- 1073 Peña-Llopis, S., Serrano, R., Pitarch, E., Beltran, E., Ibanez, M., Hernandez, F., Pena, J.B.,  
 1074 2014. N-Acetylcysteine boosts xenobiotic detoxification in shellfish. *Aquat. Toxicol.*  
<https://doi.org/10.1016/j.aquatox.2014.05.006>
- 1076 Persson, A., Smith, B.C., Wikfors, G.H., Quilliam, M., 2006. Grazing on toxic *Alexandrium  
 1077 fundyense* resting cysts and vegetative cells by the eastern oyster (*Crassostrea  
 1078 virginica*). *Harmful Algae* 5, 678–684. <https://doi.org/10.1016/j.hal.2006.02.004>
- 1079 Qiu, J., Fan, H., Liu, T., Liang, X., Meng, F., Quilliam, M.A., Li, A., 2018. Application of activated  
 1080 carbon to accelerate detoxification of paralytic shellfish toxins from mussels *Mytilus  
 1081 galloprovincialis* and scallops *Chlamys farreri*. *Ecotoxicol. Environ. Saf.*  
<https://doi.org/10.1016/j.ecoenv.2017.10.005>
- 1083 Randall, J.E., 1958. A Review of Ciguatera, Tropical Fish Poisoning, with a Tentative  
 1084 Explanation of its Cause. *Bull. Mar. Sci.* 8, 236–267.
- 1085 Robinson, W.R., Peters, R.H., Zimmermann, J., 1983. The effects of body size and temperature  
 1086 on metabolic rate of organisms. *Can. J. Zool.* 61, 281–288. <https://doi.org/10.1139/z83-037>
- 1088 Rohatgi, A., 2025. WebPlotDigitizer.
- 1089 Rourke, W.A., Justason, A., Martin, J.L., Murphy, C.J., 2021. Shellfish Toxin Uptake and  
 1090 Depuration in Multiple Atlantic Canadian Molluscan Species: Application to Selection of  
 1091 Sentinel Species in Monitoring Programs. *Toxins*.  
<https://doi.org/10.3390/toxins13020168>
- 1093 SCARRATT, D., GILGAN, M., POCKLINGTON, R., CASTEL, J., 1991. DETOXIFICATION OF  
 1094 BIVALVE MOLLUSKS NATURALLY CONTAMINATED WITH DOMOIC ACID.  
 1095 MOLLUSCAN SHELLFISH DEPURATION.
- 1096 Schultz, I.R., Skillman, A., Sloan-Evans, S., Woodruff, D., 2013. Domoic acid toxicokinetics in  
 1097 Dungeness crabs: New insights into mechanisms that regulate bioaccumulation. *Aquat.  
 1098 Toxicol.* <https://doi.org/10.1016/j.aquatox.2013.04.011>
- 1099 Schultz, I.R., Skillman, A., Woodruff, D., 2008. Domoic acid excretion in dungeness crabs, razor  
 1100 clams and mussels. *Mar. Environ. Res.*, Pollutant Responses in Marine Organisms  
 1101 (PRIMO 14 66, 21–23. <https://doi.org/10.1016/j.marenvres.2008.02.012>
- 1102 Sephton, D.H., Haya, X., Martin, J.L., LeGresley, M.M., Page, F.H., 2007. Paralytic shellfish  
 1103 toxins in zooplankton, mussels, lobsters and caged Atlantic salmon, *Salmo salar*, during  
 1104 a bloom of *Alexandrium fundyense* off Grand Manan Island, in the Bay of Fundy.  
 1105 Harmful Algae. <https://doi.org/10.1016/j.hal.2007.03.002>
- 1106 Svensson, S., 2003. Depuration of Okadaic acid (Diarrhetic Shellfish Toxin) in mussels, *Mytilus  
 1107 edulis* (*Linnaeus*), feeding on different quantities of nontoxic algae. *Aquaculture*.  
[https://doi.org/10.1016/S0044-8486\(02\)00504-5](https://doi.org/10.1016/S0044-8486(02)00504-5)
- 1109 Svensson, S., Förlin, L., 2004. Analysis of the importance of lipid breakdown for elimination of  
 1110 okadaic acid (diarrhetic shellfish toxin) in mussels, *Mytilus edulis*:: results from a field  
 1111 study and a laboratory experiment. *Aquat. Toxicol.*  
<https://doi.org/10.1016/j.aquatox.2003.11.002>
- 1113 Tang, Y., Zhang, H., Wang, Y., Fan, C., Shen, X., 2021a. Combined Effects of Temperature and  
 1114 Toxic Algal Abundance on Paralytic Shellfish Toxic Accumulation, Tissue Distribution

- 1115 and Elimination Dynamics in Mussels *Mytilus coruscus*. Toxins.  
1116 <https://doi.org/10.3390/toxins13060425>
- 1117 Tang, Y., Zhang, H., Wang, Y., Fan, C., Shen, X., 2021b. Combined Effects of Temperature and  
1118 Toxic Algal Abundance on Paralytic Shellfish Toxic Accumulation, Tissue Distribution  
1119 and Elimination Dynamics in Mussels *Mytilus coruscus*. Toxins.  
1120 <https://doi.org/10.3390/toxins13060425>
- 1121 Vehtari, A., Gabry, J., Magnusson, M., Yao, Y., Bürkner, P., Paananen, T., Gelman, A., 2024.  
1122 loo: Efficient leave-one-out cross-validation and WAIC for Bayesian models.
- 1123 Wohlgeschaffen, G., Mann, K., Rao, D., Pocklington, R., 1992. Dynamics of the phycotoxin  
1124 domoic acid - accumulation and excretion in 2 commercially important bivalves. *J. Appl.*  
1125 *Phycol.* <https://doi.org/10.1007/BF02185786>
- 1126 Woofter, R., Brendtro, K., Ramsdell, J., 2005. Uptake and elimination of brevetoxin in blood of  
1127 striped mullet (*Mugil cephalus*) after aqueous exposure to *Karenia brevis*. *Environ.*  
1128 *Health Perspect.* <https://doi.org/10.1289/ehp.7274>
- 1129 Xie, W., Liu, X., Yang, X., Zhang, C., Bian, Z., 2013. Accumulation and depuration of paralytic  
1130 shellfish poisoning toxins in the oyster *Ostrea rivularis* Gould – Chitosan facilitates the  
1131 toxin depuration. *Food Control* 30, 446–452.  
1132 <https://doi.org/10.1016/j.foodcont.2012.07.035>
- 1133 Yang, X., Hu, X., Dong, Z., Li, M., Zheng, Z., Xie, W., 2021. Effect of carboxymethyl chitosan on  
1134 the detoxification and biotransformation of paralytic shellfish toxins in oyster *Ostrea*  
1135 *rivularis*. *Toxicon*. <https://doi.org/10.1016/j.toxicon.2021.03.006>
- 1136 Yang, Z., Luo, Q., Liang, Y., Mazumder, A., 2016. Processes and pathways of ciguatoxin in  
1137 aquatic food webs and fish poisoning of seafood consumers. *Environ. Rev.* 24, 144–150.  
1138 <https://doi.org/10.1139/er-2015-0054>
- 1139 Ye, L., Liu, J., Wang, Y., Sun, L., Fang, Z., Deng, Q., Qiu, M., Zhao, J., 2021. Development of a  
1140 three-compartment toxicokinetic model for T-2 toxin in shrimp by blindfold particle swarm  
1141 optimization algorithm. *Ecotoxicol. Environ. Saf.*  
1142 <https://doi.org/10.1016/j.ecoenv.2020.111698>
- 1143 Yu, K., Choi, M., Shen, X., Wu, R., Wang, W., Lam, P., 2005. Modeling of depuration of  
1144 paralytic shellfish toxins in *Chlamys nobilis* and *Perna viridis*. *Mar. Pollut. Bull.*  
1145 <https://doi.org/10.1016/j.marpolbul.2005.01.019>

1146 **Tables and Figures**

1147 **Table 1.** Marine biotoxin poisoning syndromes and their causative organisms.

1148

Syndrome	Biotoxin	Causative organisms
Amnesic (ASP)	Domoic acid (DA)	Diatom: <i>Pseudo-nitzschia</i> spp.
Diarrhetic (DSP)	Diarrhetic shellfish toxins (DSTs)	Dinoflagellate: <i>Dinophysis</i> spp., <i>Prorocentrum</i> spp.
Paralytic (PSP)	Paralytic shellfish toxins (PSTs) <sup>2</sup>	Dinoflagellate: <i>Alexandrium</i> spp., <i>Pyrodinium bahamense</i> , <i>Gymnodinium catenatum</i>
Azaspiracid (AZP)	Azaspiracid (AZA)	Dinoflagellate: <i>Azadinium</i> spp., <i>Amphidoma spinosum</i>
Ciguatera (CFP)	Ciguatoxin (CTX)	Dinoflagellate: <i>Gambierdiscus</i> spp., <i>Fukuyoa</i> spp.
Neurotoxic (NSP)	Brevetoxin (PbTx)	Dinoflagellate: <i>Karenia</i> spp.
Cyanotoxin	Cyanotoxins <sup>3</sup>	Cyanobacteria
Other	Other phycotoxins <sup>4</sup>	Dinoflagellate: <i>Protoceratium reticulatum</i> , <i>Lingulodinium polyedra</i> , <i>Gonyaulax</i> spp.

1149

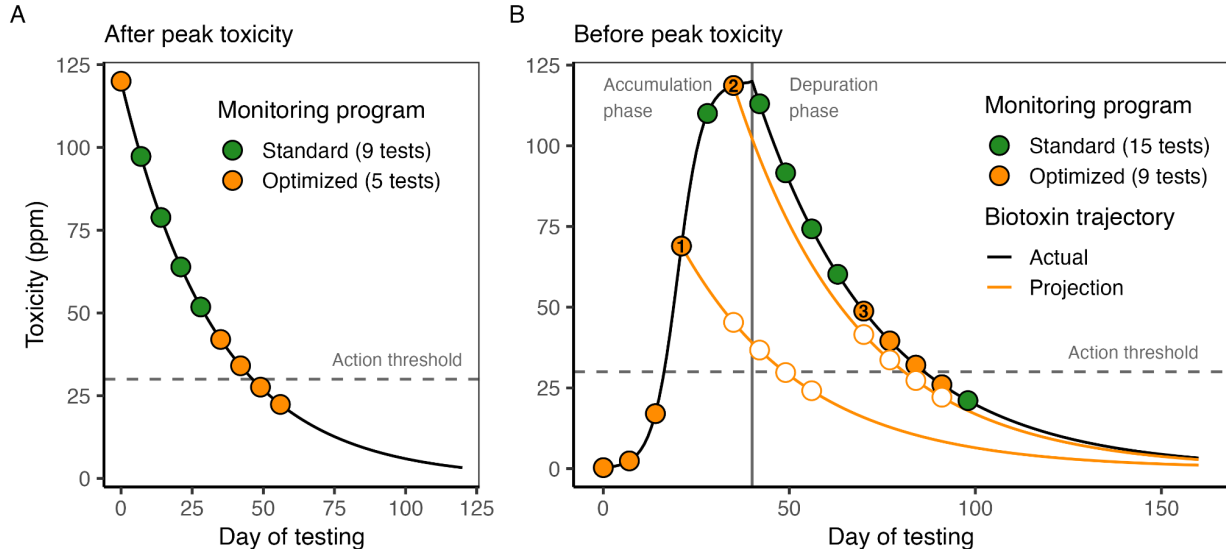
1150 <sup>1</sup> Okadaic acid (OA), dinophysistoxin (DTX)

1151 <sup>2</sup> Saxitoxin (STX), gonyautoxin (GTX)

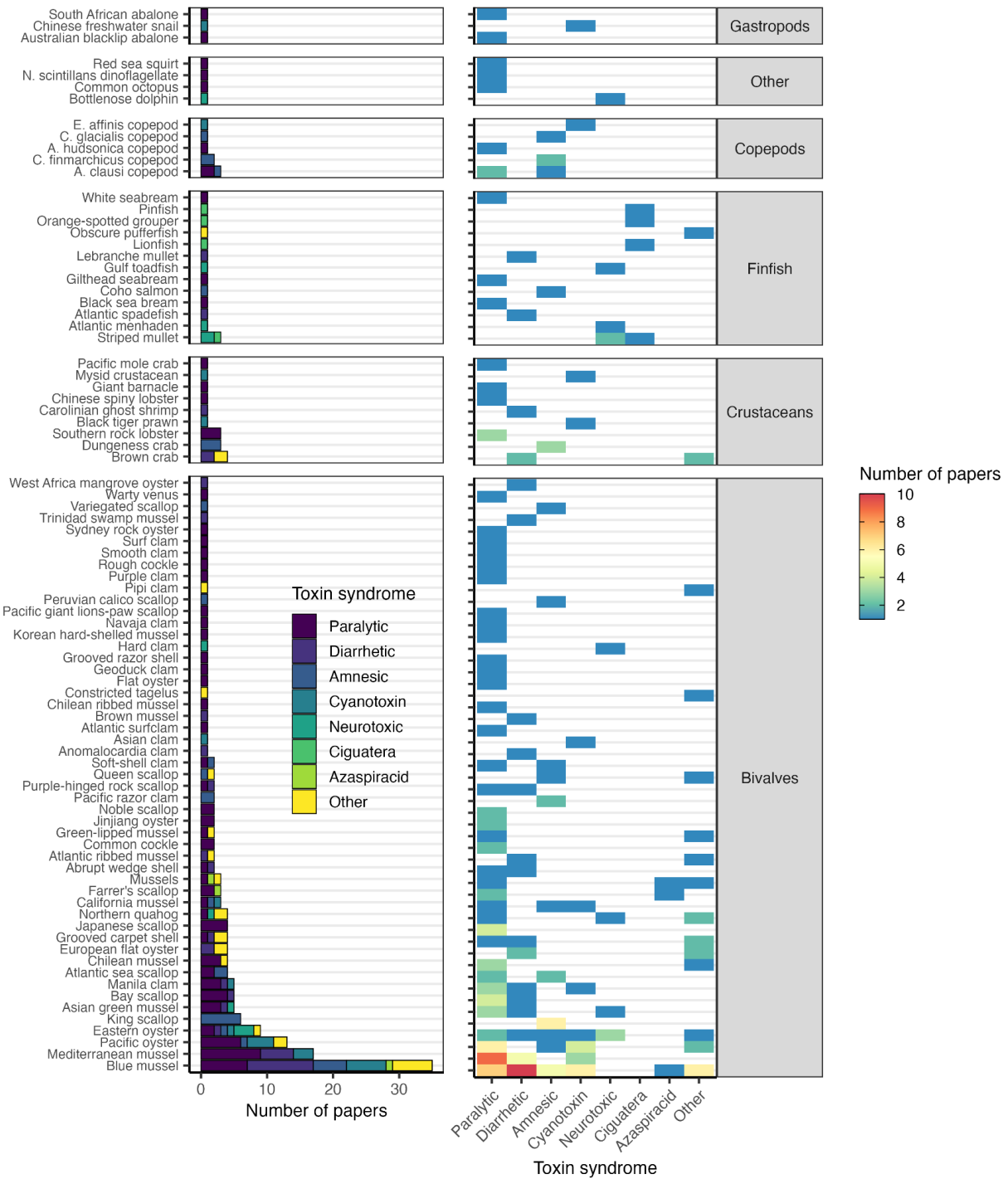
1152 <sup>3</sup> Microcystin, nodularin, homoanatoxin, cylindrospermopsin

1153 <sup>4</sup> Yessotoxin (YTX), pectenotoxin (PTX, associated with DSTs but do not cause DSP), tetrodotoxin (TTX),

1154 gymnodimine (GYM), karlotoxin

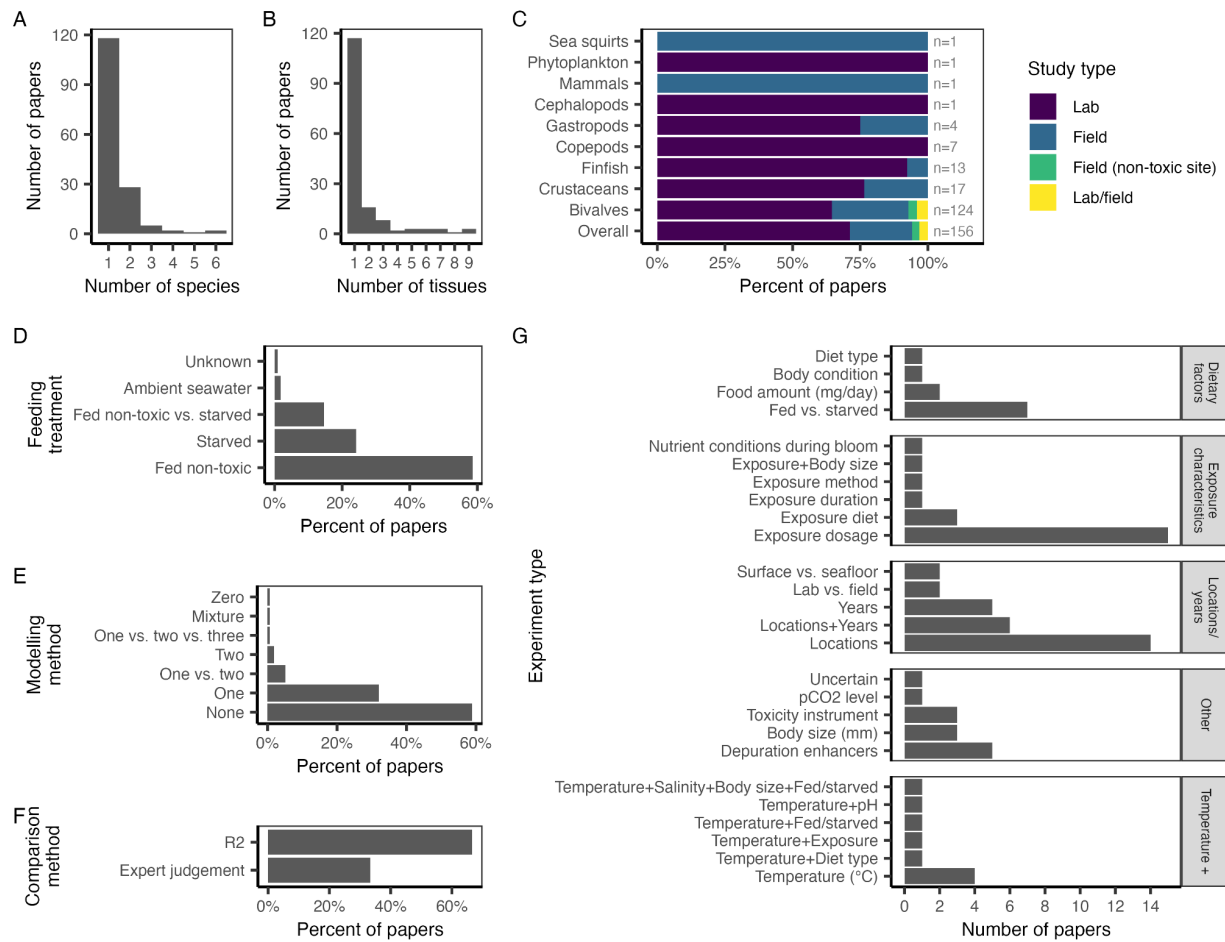


1155  
1156 **Figure 1.** An illustration of the value of biotoxin depuration rates in efficiently monitoring and  
1157 managing biotoxin risk both **(A)** after and **(B)** before peak toxicity is attained. In both panels, the  
1158 black curve shows a hypothetical accumulation (B only) and depuration trajectory for a marine  
1159 seafood species that depurates at  $0.03 \text{ day}^{-1}$ . The points indicate weekly sampling that ceases  
1160 once toxicity falls below the management action threshold (horizontal dashed line) in two  
1161 consecutive weeks, a common requirement for opening a fishery closed due to biotoxin risk. In  
1162 **(A)**, standard weekly sampling would require nine tests (all points), but pausing testing until two  
1163 weeks before toxicity is projected to fall below the action threshold would require only five tests  
1164 (orange points only). In **(B)**, scheduling tests based on three projections (marked by numbers)  
1165 eliminates the need for six tests. The white circles indicate the projected testing schedule that is  
1166 updated when toxicity is found to be higher than expected.

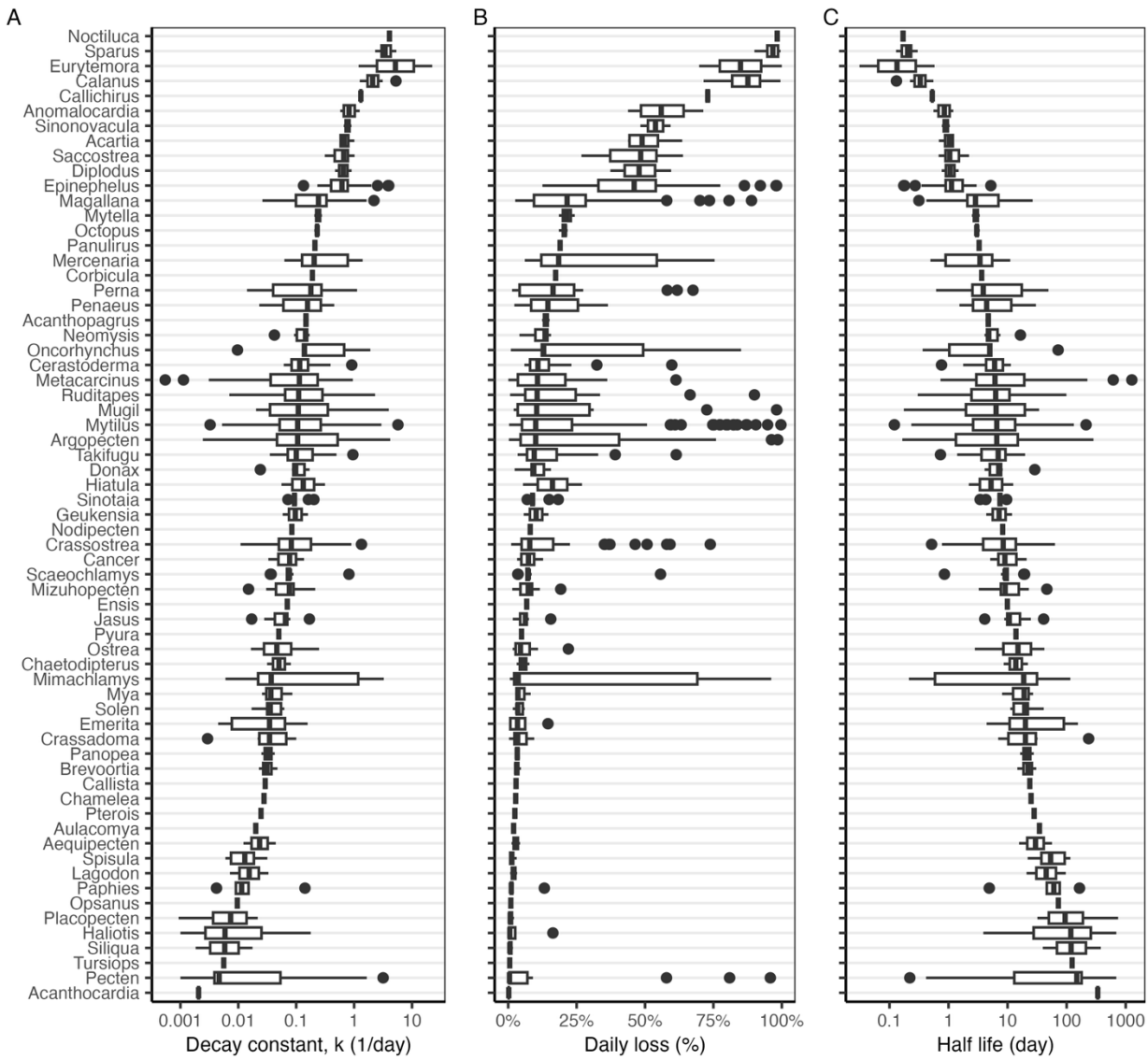


1167  
1168  
1169  
1170  
1171

**Figure 2.** The number of papers measuring depuration rates by species and biotoxin. Species are grouped by taxonomic class and are ordered by increasing sample size (bottom to top). Biotoxins are also ordered by increasing sample size (left to right). See **Table S3** for the scientific names of all species shown here.

1172  
1173

**Figure 3.** Characteristics of papers measuring biotoxin depuration in marine species. Panel **A** shows the number of species studied in a paper. Panel **B** shows the number of tissues evaluated in a paper. Panel **C** shows the percent of papers that conduct lab and/or field studies of depuration rates; a few studies conduct depuration studies at non-toxic field sites. Panel **D** shows the feeding treatment used during the depuration phase of each study; all field studies use wild diets. Panel **E** shows the modeling method used to quantify depuration rates (i.e., one- or two-compartment exponential decay models). Panel **F** shows the method used to compare models with different numbers of compartments in papers making such comparisons. Panel **G** shows the number of studies conducting experiments to measure depuration rates under different conditions. Experiment types are grouped into broader categories.



1184

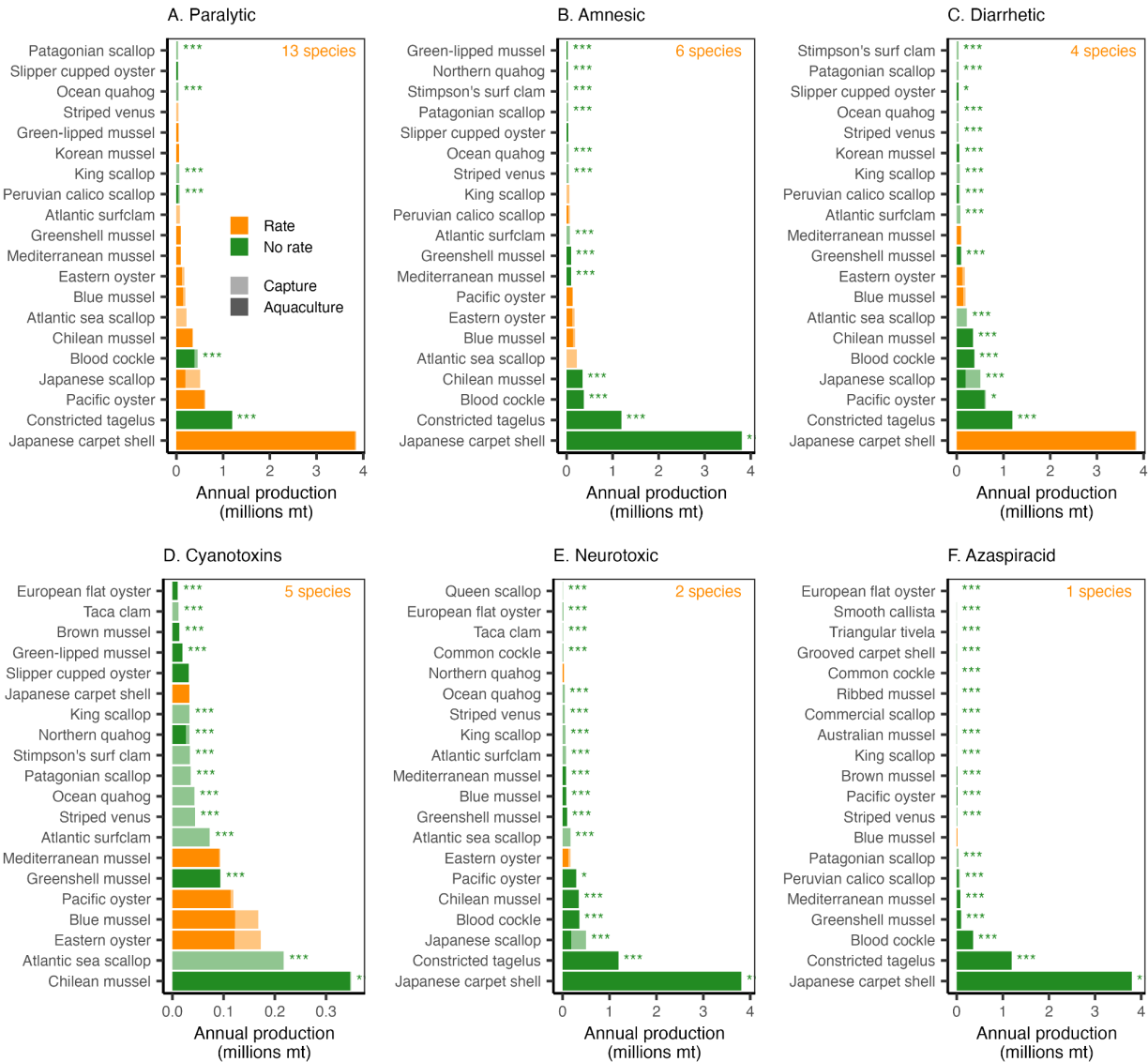
1185

**Figure 4.** The (A) exponential decay constant ( $k$ , day<sup>-1</sup>), (B) daily percent loss (%), and (C) half-life (days) of marine biotoxins by genus. In the boxplots, the solid line indicates the median, the box indicates the interquartile range (IQR; 25th to 75th percentiles), the whiskers indicate 1.5 times the IQR, and points indicate outliers.

1186

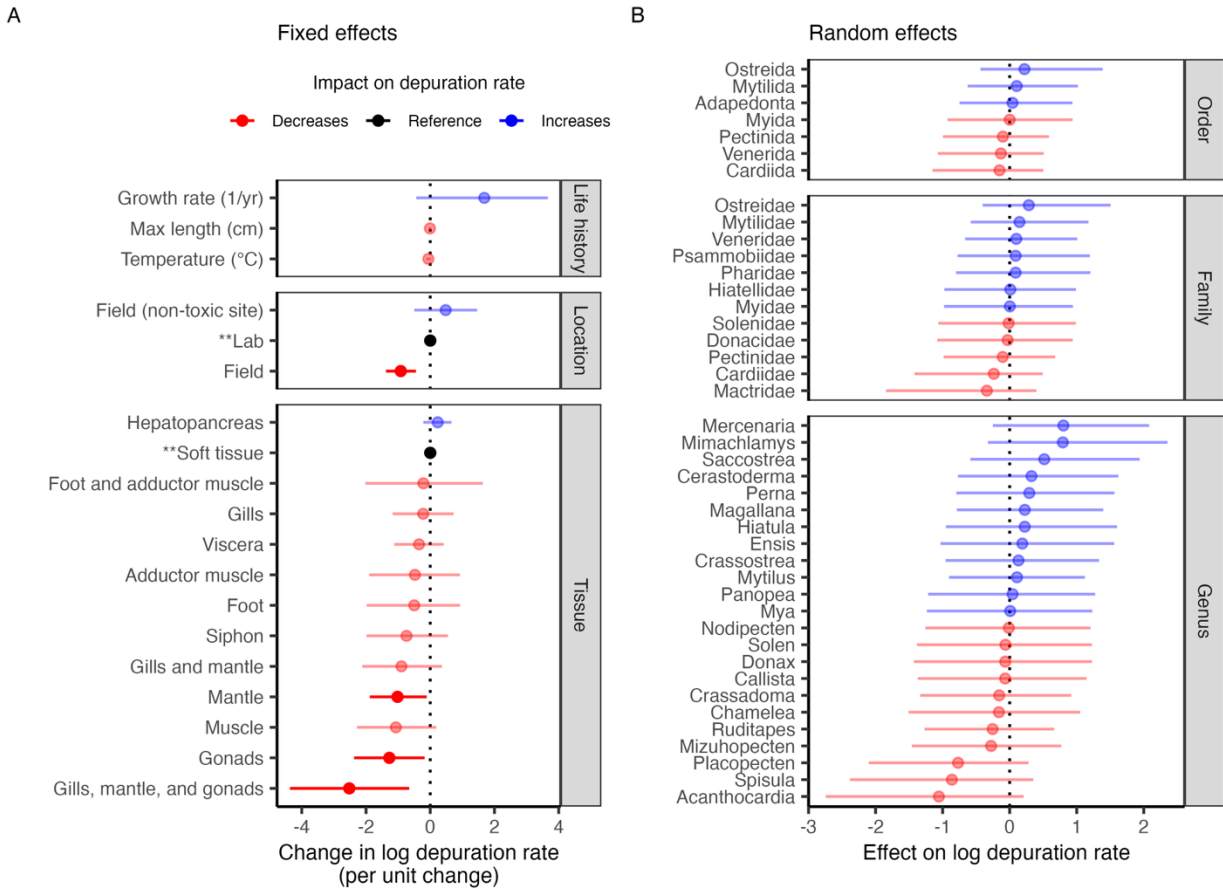
1187

1188



1189

1190 **Figure 5.** The twenty filter-feeding marine mollusc species with the greatest annual production  
1191 (millions mt, 2014-2023) within Exclusive Economic Zones (**Fig. S5**) exposed to harmful algal  
1192 blooms causing each of the evaluated biotoxin syndromes and an indication of whether (orange)  
1193 or not (green) the depuration rate of the causative biotoxin has been studied. The species are  
1194 sorted in order of decreasing annual production across both aquaculture (solid) and fisheries  
1195 (transparent). The number of species whose depuration rates have been studied is printed in  
1196 the top-right corner of each plot. The asterisks mark species whose depuration rate would  
1197 contribute a new order (\*\*), family (\*\*), or genus (\*) if studied. Ciguatera is evaluated separately  
1198 because it is more strongly associated with large, predatory, tropical reef fish (**Fig. S7**).



1199

1200

**Figure 6.** The (A) fixed effects and (B) random effects coefficients estimated by the final model. Points indicate the median estimate and lines indicate the 95% credible interval. Color indicates the impact of the point estimate of the effect on depuration rates. Transparency indicates whether the 95% credible intervals overlap with zero (solid=no overlap, transparent=overlap). The categorical fixed effects (location and tissue) are estimated relative to a reference level, which is marked with asterisks and is indicated in black. The conditional effects of the fixed effects variables are shown in **Fig. S10**.

1201

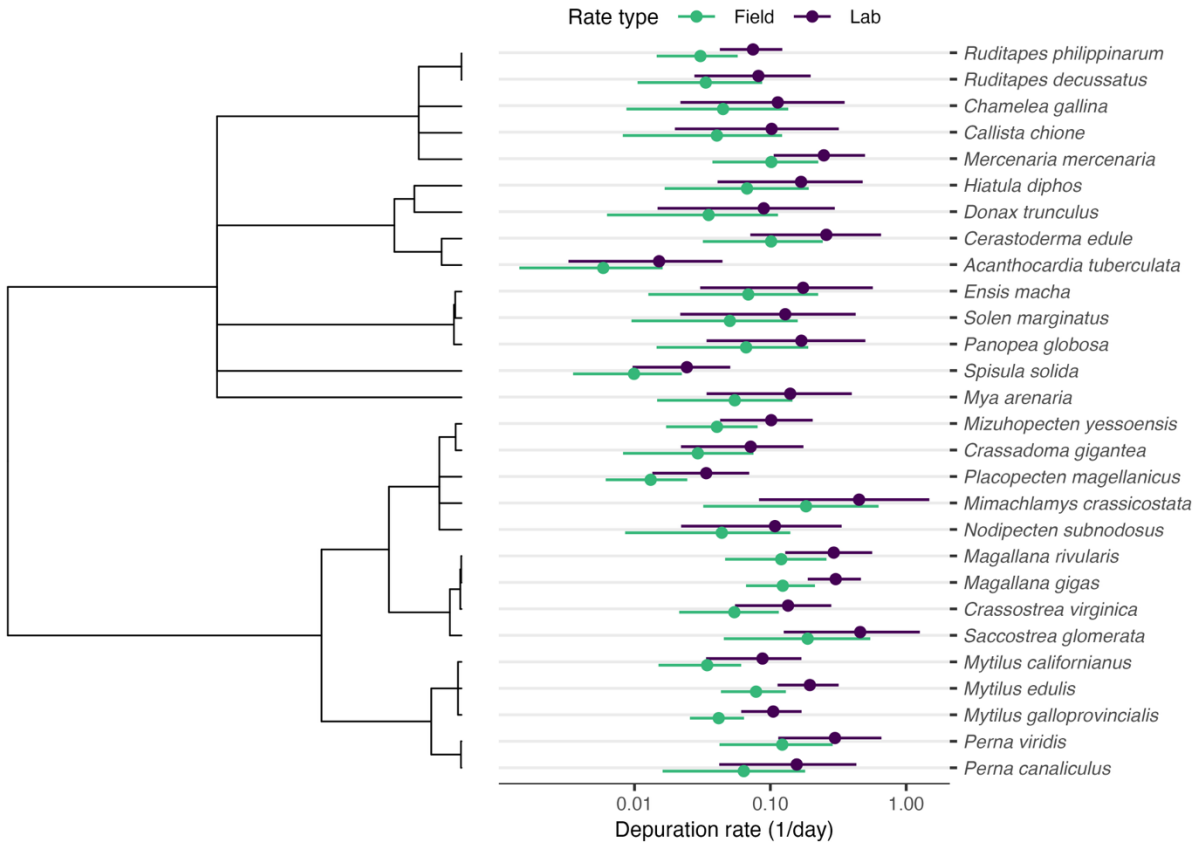
1202

1203

1204

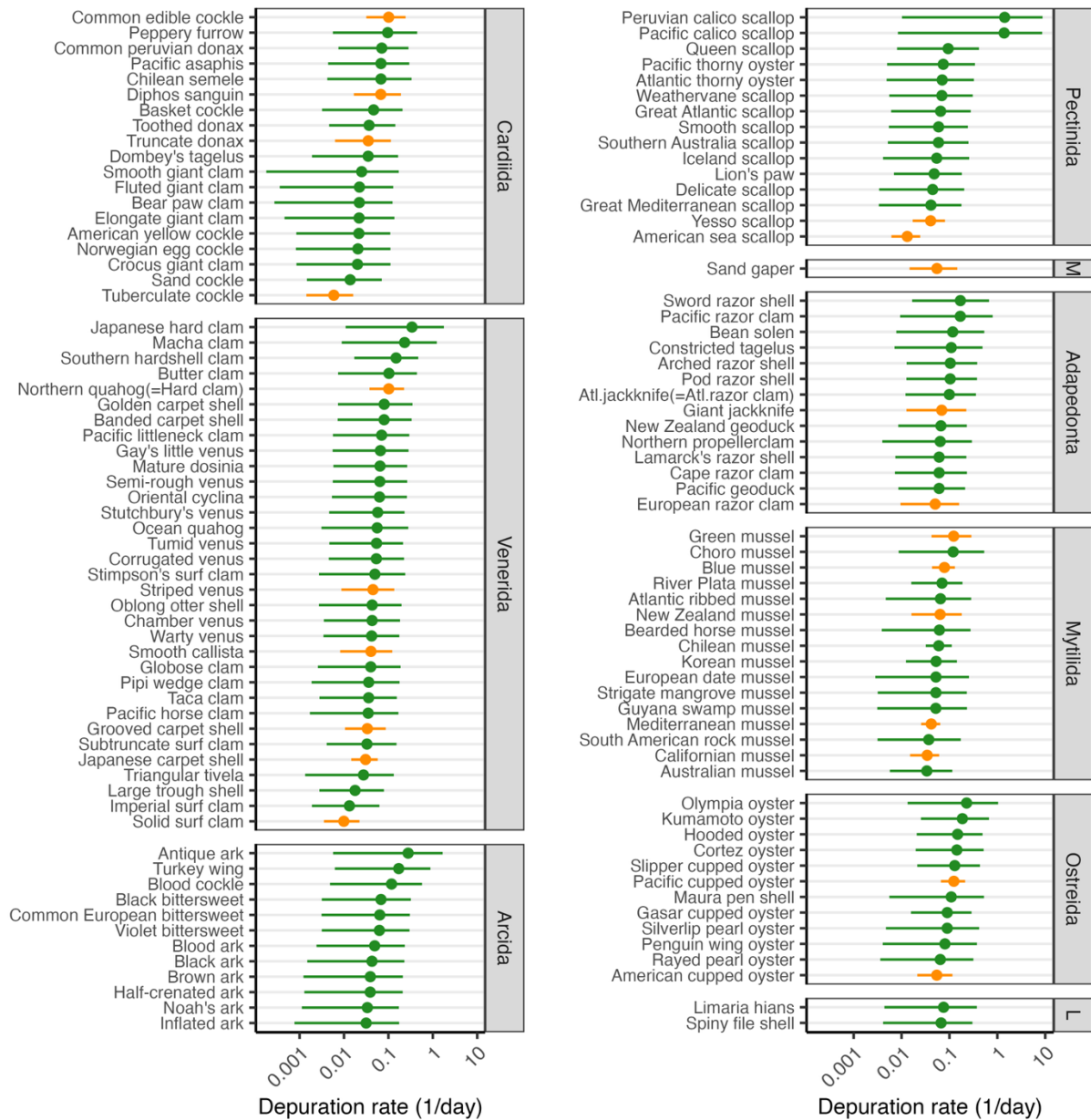
1205

1206



1207  
1208  
1209  
1210  
1211

**Figure 7.** Paralytic shellfish toxin (PST) depuration rate estimates for species with measured depuration rates from the final regression model. Species are organized by phylogeny. Points indicate the median estimate and lines indicate the 95% credible interval. See **Table S6** for details.



1212

1213 **Figure 8.** Paralytic shellfish toxin (PST) depuration rates for harvest marine bivalve species  
 1214 predicted by the final regression model. Species are organized by taxonomic order (M=Myida,  
 1215 L=Limida). Points indicate the median estimate and lines indicate the 95% credible interval.  
 1216 Species represented in the training data are marked in blue. Large predicted depuration rates  
 1217 for giant clam (*Tridacna gigas*) and mangrove cupped oyster (*Crassostrea rhizophorae*) are  
 1218 suppressed to ease visualization. See **Table S7** for details on the predicted depuration rates.

1219    **Supplemental Tables and Figures**

1220    **Supplemental Tables**

1221    **Table S1.** Attributes of papers that conduct studies of biotoxin depuration for aquatic organisms  
 1222    collected for the literature review analysis.

1223

<b>Column</b>	<b>Description</b>	<b>Details</b>
paper_id	Paper id	Example: Lund et al. (1997)
comm_name	Common name	Example: Dungeness crab
sci_name	Scientific name	Example: Metacarcinus magister
syndrome	Syndrome	Amnesic, Diarrhetic, Paralytic, Azaspiracid, Ciguatera, Neurotoxic, Cyanotoxin
hab_species	HAB species	Examples: Pseudo-nitzschia australis
biotoxin	Biotoxin	Domoic acid, DSTs,PSTs, Azaspiracid, Ciguatoxin, Brevetoxin, Cyanotoxin, Other
subtoxin	Sub-biotoxin	Examples: dcSTX, GTX3, okadaic acid, etc
study_type	Study type	Llab, field, field (non-toxic)
exp_type	Experiment type	Examples: Temperature, Exposure, Diet type, etc.
treatment	Experimental treatment	Examples: 18°C, 20°C, 30 psu, 35 psu, etc.
feed_scenario	Feeding scenario	Fed clean, starved, ambient seawater, wild
tissue	Tissue type	Examples: digestive gland, hepatopancreas
source	Source of depuration rate	Examples: Figure 1, Table 1, Supplemental Data 1, Results 3.2
rate_type	Derivation of depuration rate	provided, derived, digitized
ncomp	Number of compartments	None, zero, one, two, one vs. two, one vs. two vs. three
rate_hr	Depuration rate (1/hr)	
hlife_hr	half-life (hr)	
rate_d	Depuration rate (1/day)	
hlife_d	half-life (day)	
notes	General notes	

1224

1225 **Table S2.** Tissue harmonization by class.

1226

Harmonized tissue	Synonyms
<i>Malacostraca</i>	
Hepatopancreas	Hepatopancreas, digestive gland
Soft tissue	Soft tissue, whole
<i>Gastropoda</i>	
Foot	Foot, muscle
Hepatopancreas	Hepatopancreas, digestive gland
<i>Bivalvia</i>	
Hepatopancreas	Hepatopancreas, digestive gland
Soft tissue	Soft tissue, tissue, edible tissue, edible portion, meat, flesh, whole flesh, whole, whole tissue, total tissue, non-viscera

1227

1228 **Table S3.** The number of papers providing depuration rates by species and syndrome  
 1229 (par=paralytic; amn=amnesic; dia=diahretic; cya=cyanotoxin; neu=neurotoxic; cig=ciguatera;  
 1230 aza=azaspiracid; oth=other).

1231

Class	Family	Scientific name	Common name	Par	Amn	Dia	Cya	Neu	Cig	Aza	Oth
Asidiaceae	Pyridae	<i>Pyura chilensis</i>	Red sea squirt	1							
Bivalvia	Cardiidae	<i>Acanthocardia tuberculata</i>	Rough cockle	1							
Bivalvia	Cardiidae	<i>Cerastoderma edule</i>	Common cockle	2							
Bivalvia	Cyrenidae	<i>Corbicula fluminea</i>	Asian clam				1				
Bivalvia	Donacidae	<i>Donax trunculus</i>	Abrupt wedge shell	1		1					
Bivalvia	Hiatellidae	<i>Panopea globosa</i>	Geoduck clam	1							
Bivalvia	Mactridae	<i>Spisula solida</i>	Surf clam	1							
Bivalvia	Mactridae	<i>Spisula solidissima</i>	Atlantic surfclam	1							
Bivalvia	Mesodesmatidae	<i>Paphies australis</i>	Pipi clam							1	
Bivalvia	Myidae	<i>Mya arenaria</i>	Soft-shell clam	1	1						
Bivalvia	Mytilidae	<i>Aulacomya atra</i>	Chilean ribbed mussel	1							
Bivalvia	Mytilidae	<i>Geukensia demissa</i>	Atlantic ribbed mussel			1				1	
Bivalvia	Mytilidae	<i>Mytella guyanensis</i>	Trinidad swamp mussel			1					
Bivalvia	Mytilidae	<i>Mytilus californianus</i>	California mussel	1	1		1				
Bivalvia	Mytilidae	<i>Mytilus chilensis</i>	Chilean mussel	3							1
Bivalvia	Mytilidae	<i>Mytilus coruscus</i>	Korean hard-shelled mussel	1							
Bivalvia	Mytilidae	<i>Mytilus edulis</i>	Blue mussel	7	5	10	6			1	6
Bivalvia	Mytilidae	<i>Mytilus galloprovincialis</i>	Mediterranean mussel	9		5	3				
Bivalvia	Mytilidae	<i>Mytilus spp.</i>	Mussels	1						1	1
Bivalvia	Mytilidae	<i>Perna canaliculus</i>	Green-lipped mussel	1							1
Bivalvia	Mytilidae	<i>Perna perna</i>	Brown mussel			1					
Bivalvia	Mytilidae	<i>Perna viridis</i>	Asian green mussel	3		1		1			
Bivalvia	Ostreidae	<i>Crassostrea tulipa</i>	West Africa mangrove oyster			1					
Bivalvia	Ostreidae	<i>Crassostrea virginica</i>	Eastern oyster	2	1	1	1	3			1
Bivalvia	Ostreidae	<i>Magallana gigas</i>	Pacific oyster	6	1		4				2
Bivalvia	Ostreidae	<i>Magallana rivularis</i>	Jinjiang oyster	2							
Bivalvia	Ostreidae	<i>Ostrea chilensis</i>	Flat oyster	1							
Bivalvia	Ostreidae	<i>Ostrea edulis</i>	European flat oyster			2					2
Bivalvia	Ostreidae	<i>Saccostrea glomerata</i>	Sydney rock oyster	1							
Bivalvia	Pectinidae	<i>Aequipecten opercularis</i>	Queen scallop		1						1
Bivalvia	Pectinidae	<i>Argopecten irradians</i>	Bay scallop	4		1					
Bivalvia	Pectinidae	<i>Argopecten purpuratus</i>	Peruvian calico scallop		1						
Bivalvia	Pectinidae	<i>Crassadoma gigantea</i>	Purple-hinged rock scallop	1		1					
Bivalvia	Pectinidae	<i>Mimachlamys crassicornata</i>	Noble scallop	2							
Bivalvia	Pectinidae	<i>Mimachlamys varia</i>	Variegated scallop		1						
Bivalvia	Pectinidae	<i>Mizuhopecten yessoensis</i>	Japanese scallop	4							
Bivalvia	Pectinidae	<i>Nodipecten subnodosus</i>	Pacific giant lions-paw scallop	1							
Bivalvia	Pectinidae	<i>Pecten maximus</i>	King scallop		6						
Bivalvia	Pectinidae	<i>Placopecten magellanicus</i>	Atlantic sea scallop	2	2						
Bivalvia	Pectinidae	<i>Scaeochlamys farreri</i>	Farrer's scallop	2							1
Bivalvia	Pharidae	<i>Ensis macha</i>	Navaja clam	1							
Bivalvia	Pharidae	<i>Siliqua patula</i>	Pacific razor clam		2						
Bivalvia	Pharidae	<i>Sinonovacula constricta</i>	Constricted tagelus							1	
Bivalvia	Psammobiidae	<i>Hiatula diphos</i>	Purple clam	1							
Bivalvia	Solenidae	<i>Solen marginatus</i>	Grooved razor shell	1							
Bivalvia	Veneridae	<i>Anomalocardia flexuosa</i>	Anomalocardia clam			1					
Bivalvia	Veneridae	<i>Callista chione</i>	Smooth clam	1							
Bivalvia	Veneridae	<i>Chamelea gallina</i>	Warty venus	1							
Bivalvia	Veneridae	<i>Mercenaria campechiensis</i>	Hard clam					1			
Bivalvia	Veneridae	<i>Mercenaria mercenaria</i>	Northern quahog	1			1				2
Bivalvia	Veneridae	<i>Ruditapes decussatus</i>	Grooved carpet shell	1		1					2
Bivalvia	Veneridae	<i>Ruditapes philippinarum</i>	Manila clam	3		1	1				
Cephalopoda	Octopodidae	<i>Octopus vulgaris</i>	Common octopus	1							
Copepoda	Acartiidae	<i>Acartia clausi</i>	A. clausi copepod	2	1						
Copepoda	Acartiidae	<i>Acartia hudsonica</i>	A. hudsonica copepod	1							
Copepoda	Calanidae	<i>Calanus finmarchicus</i>	C. finmarchicus copepod		2						
Copepoda	Calanidae	<i>Calanus glacialis</i>	C. glacialis copepod		1						
Copepoda	Temoridae	<i>Eurytemora affinis</i>	E. affinis copepod				1				
Dinophyceae	Noctilucaceae	<i>Noctiluca scintillans</i>	N. scintillans dinoflagellate	1							
Gastropoda	Haliotidae	<i>Haliotis midae</i>	South African abalone	1							
Gastropoda	Haliotidae	<i>Haliotis rubra</i>	Australian blacklip abalone	1							
Gastropoda	Viviparidae	<i>Sinotaia quadrata</i>	Chinese freshwater snail				1				

Malacostraca	Callichiridae	<i>Callichirus major</i>	Carolinian ghost shrimp	1	
Malacostraca	Cancridae	<i>Cancer pagurus</i>	Brown crab	2	
Malacostraca	Cancridae	<i>Metacarcinus magister</i>	Dungeness crab	3	
Malacostraca	Hippidae	<i>Emerita analoga</i>	Pacific mole crab	1	
Malacostraca	Mysidae	<i>Neomysis awatschensis</i>	Mysid crustacean		1
Malacostraca	Palinuridae	<i>Jasus edwardsii</i>	Southern rock lobster	3	
Malacostraca	Palinuridae	<i>Panulirus stimsoni</i>	Chinese spiny lobster	1	
Malacostraca	Penaeidae	<i>Penaeus monodon</i>	Black tiger prawn		1
Mammalia	Delphinidae	<i>Tursiops truncatus</i>	Bottlenose dolphin		1
Teleostei	Alosidae	<i>Brevoortia tyrannus</i>	Atlantic menhaden		1
Teleostei	Batrachoididae	<i>Opsanus beta</i>	Gulf toadfish		1
Teleostei	Ephippidae	<i>Chaetodipterus faber</i>	Atlantic spadefish	1	
Teleostei	Epinephelidae	<i>Epinephelus coioides</i>	Orange-spotted grouper		1
Teleostei	Mugilidae	<i>Mugil cephalus</i>	Striped mullet	2	1
Teleostei	Mugilidae	<i>Mugil liza</i>	Lebranché mullet		1
Teleostei	Salmonidae	<i>Oncorhynchus kisutch</i>	Coho salmon	1	
Teleostei	Scorpaenidae	<i>Pterois volitans</i>	Lionfish		1
Teleostei	Sparidae	<i>Acanthopagrus schlegelii</i>	Black sea bream	1	
Teleostei	Sparidae	<i>Diplodus sargus</i>	White seabream	1	
Teleostei	Sparidae	<i>Lagodon rhomboides</i>	Pinfish		1
Teleostei	Sparidae	<i>Sparus aurata</i>	Gilthead seabream	1	
Teleostei	Tetraodontidae	<i>Takifugu obscurus</i>	Obscure pufferfish		1
Thecostraca	Balanidae	<i>Austromegabalanus psittacus</i>	Giant barnacle	1	

1233  
1234**Table S4.** Diversity of orders, families, and genera of harvested marine molluscs.

Syndrome	Type	Group	Species	Production (1000s mt)	Number of species Harvested	Total	
Amnesic	Order	Arcoida	Blood cockle ( <i>Tegillarca granosa</i> )	375.1	8	360	
		Veneridae	Manila clam ( <i>Ruditapes philippinarum</i> ), Striped venus ( <i>Chamelea gallina</i> ), Northern quahog ( <i>Mercenaria mercenaria</i> )	3885.3	22	428	
		Solecurtidae	Constricted tagelus ( <i>Sinonovacula constricta</i> )	1191.3	2	26	
		Mactridae	Atlantic surfclam ( <i>Spisula solidissima</i> ), Stimpson's surf clam ( <i>Mactromeris polynyma</i> )	106.1	10	116	
		Arcticidae	Ocean quahog ( <i>Arctica islandica</i> )	42.8	1	1	
	Genus	Perna	Greenshell mussel ( <i>Perna canaliculus</i> ), Green-lipped mussel ( <i>Perna viridis</i> )	118.9	3	5	
		Zygochlamys	Patagonian scallop ( <i>Zygochlamys patagonica</i> )	35.5	2	1	
		Veneroida	Manila clam ( <i>Ruditapes philippinarum</i> ), Constricted tagelus ( <i>Sinonovacula constricta</i> ), Striped venus ( <i>Chamelea gallina</i> ), Common cockle ( <i>Cerastoderma edule</i> ), Grooved carpet shell ( <i>Ruditapes decussatus</i> ), Triangular tivela ( <i>Tivela mactroides</i> ), Smooth callista ( <i>Callista chione</i> )	5015.8	58	2549	
	Azaspiracid	Order	Arcoida	Blood cockle ( <i>Tegillarca granosa</i> )	356.8	8	360
		Ostreoida	Peruvian calico scallop ( <i>Argopecten purpuratus</i> ), Patagonian scallop ( <i>Zygochlamys patagonica</i> ), King scallop ( <i>Pecten maximus</i> ), Commercial scallop ( <i>Pecten fumatus</i> ), European flat oyster ( <i>Ostrea edulis</i> )	107.5	26	548	
		Genus	Ostreida	Pacific oyster ( <i>Magallana gigas</i> )	16.3	5	88
			Perna	Greenshell mussel ( <i>Perna canaliculus</i> ), Brown mussel ( <i>Perna perna</i> )	107.2	3	5
			Aulacomya	Ribbed mussel ( <i>Aulacomya atra</i> )	2.5	1	3
		Genus	Pectinidae	Atlantic sea scallop ( <i>Placopecten magellanicus</i> ), Patagonian scallop ( <i>Zygochlamys patagonica</i> ), King scallop ( <i>Pecten maximus</i> )	286.3	20	297
			Veneridae	Striped venus ( <i>Chamelea gallina</i> ), Northern quahog ( <i>Mercenaria mercenaria</i> ), Manila clam ( <i>Ruditapes philippinarum</i> ), Taca clam ( <i>Leukoma thaca</i> )	122.0	22	428
			Mactridae	Atlantic surfclam ( <i>Spisula solidissima</i> ), Stimpson's surf clam ( <i>Mactromeris polynyma</i> )	106.1	10	116
			Arcticidae	Ocean quahog ( <i>Arctica islandica</i> )	42.8	1	1
			Perna	Greenshell mussel ( <i>Perna canaliculus</i> ), Green-lipped mussel ( <i>Perna viridis</i> ), Brown mussel ( <i>Perna perna</i> )	126.5	3	5
	Diarrhetic	Order	Ostrea	European flat oyster ( <i>Ostrea edulis</i> )	10.6	3	20
			Ostreida	Pacific oyster ( <i>Magallana gigas</i> ), Slipper cupped oyster ( <i>Magallana bilineata</i> )	657.5	5	88
			Arcoida	Blood cockle ( <i>Tegillarca granosa</i> )	375.7	8	360
			Family	Constricted tagelus ( <i>Sinonovacula constricta</i> )	1191.3	2	26
			Mactridae	Atlantic surfclam ( <i>Spisula solidissima</i> ), Stimpson's surf clam ( <i>Mactromeris polynyma</i> )	106.1	10	116
		Genus	Arcticidae	Ocean quahog ( <i>Arctica islandica</i> )	42.8	1	1
			Ruditapes	Manila clam ( <i>Ruditapes philippinarum</i> )	3848.4	2	4
			Mizuhopecten	Japanese scallop ( <i>Mizuhopecten yessoensis</i> )	505.8	1	1
			Placopecten	Atlantic sea scallop ( <i>Placopecten magellanicus</i> )	217.5	1	1
			Perna	Greenshell mussel ( <i>Perna canaliculus</i> )	93.5	3	5
	Neurotoxic	Order	Pecten	King scallop ( <i>Pecten maximus</i> )	62.2	4	18
			Chamelea	Striped venus ( <i>Chamelea gallina</i> )	46.1	1	3
			Zygochlamys	Patagonian scallop ( <i>Zygochlamys patagonica</i> )	35.5	2	1
			Arcoida	Blood cockle ( <i>Tegillarca granosa</i> )	357.1	8	360
			Ostreida	Pacific oyster ( <i>Magallana gigas</i> )	293.1	5	88
		Family	Solecurtidae	Constricted tagelus ( <i>Sinonovacula constricta</i> )	1191.3	2	26
			Pectinidae	Japanese scallop ( <i>Mizuhopecten yessoensis</i> ), Atlantic sea scallop ( <i>Placopecten magellanicus</i> ), King scallop ( <i>Pecten maximus</i> ), Queen scallop ( <i>Aequipecten opercularis</i> )	734.1	20	297
			Mactridae	Atlantic surfclam ( <i>Spisula solidissima</i> )	71.8	10	116
		Genus	Arcticidae	Ocean quahog ( <i>Arctica islandica</i> )	42.8	1	1
			Cardiidae	Common cockle ( <i>Cerastoderma edule</i> )	14.3	13	222
			Ruditapes	Manila clam ( <i>Ruditapes philippinarum</i> )	3813.6	2	4
			Mytilus	Chilean mussel ( <i>Mytilus chilensis</i> ), Blue mussel ( <i>Mytilus edulis</i> ), Mediterranean mussel ( <i>Mytilus galloprovincialis</i> )	503.5	7	12
			Chamelea	Striped venus ( <i>Chamelea gallina</i> )	45.7	1	3
	Paralytic	Order	Leukoma	Taca clam ( <i>Leukoma thaca</i> )	11.9	2	3
			Ostrea	European flat oyster ( <i>Ostrea edulis</i> )	11.0	3	20
			Arcoida	Blood cockle ( <i>Tegillarca granosa</i> )	453.6	8	360
		Family	Solecurtidae	Constricted tagelus ( <i>Sinonovacula constricta</i> )	1191.3	2	26
			Arcticidae	Ocean quahog ( <i>Arctica islandica</i> )	42.8	1	1
			Genus	Argopecten	Peruvian calico scallop ( <i>Argopecten purpuratus</i> )	70.2	3
		Genus	Pecten	King scallop ( <i>Pecten maximus</i> )	62.2	4	18
			Chamelea	Striped venus ( <i>Chamelea gallina</i> )	46.1	1	3
			Zygochlamys	Patagonian scallop ( <i>Zygochlamys patagonica</i> )	35.5	2	1

1235

1236 **Table S5.** Performance statistics used in model selection.

1237

Model	$\Delta\text{ELPD}$	ELPD (sd)	LOOIC (sd)	P (sd)	$R^2$ (CI)
Taxonomically nested random effects	0	-229.4 (9.2)	458.8 (18.3)	27 (2.6)	0.67 (0.6-0.72)
Species random effects	-0.3	-229.7 (9)	459.4 (18.1)	26.9 (2.5)	0.66 (0.59-0.71)
Phylogenetic random effects	-1.3	-230.8 (9.2)	461.5 (18.5)	25.1 (2.6)	0.65 (0.57-0.71)
Fixed effects only	-26	-255.4 (9.5)	510.8 (19)	16.5 (2.2)	0.49 (0.4-0.56)

1238

1239 \* ELPD = expected log predictive density (higher = better); LOOIC = leave-one-out information  
 1240 criterion (lower = better);  $R^2$  = Bayesian  $R^2$  (higher = better); P = effective number of  
 1241 parameters; SE = standard error; CI = 95% confidence interval

1242 **Table S6.** Field- and lab-based paralytic shellfish toxin depuration rates predicted by the best performing regression model for  
 1243 species included in model training along with the required predictor variables.  
 1244

Order	Family	Genus	Scientific name	Common name	Length (cm)	K (1/yr)	Temp (°C)	Field (95% CI)	Lab (95% CI)
Adapedonta	Pharidae	Ensis	<i>Ensis macha</i>	Navaja clam	16.5	0.225	11	0.069 (0.013-0.225)	0.174 (0.03-0.568)
Adapedonta	Hiatellidae	Panopea	<i>Panopea globosa</i>	Geoduck clam	19.8	0.33	8	0.066 (0.015-0.19)	0.169 (0.034-0.501)
Adapedonta	Solenidae	Solen	<i>Solen marginatus</i>	Grooved razor shell	17	0.28	10	0.05 (0.009-0.159)	0.129 (0.022-0.425)
Cardiida	Cardiidae	Acanthocardia	<i>Acanthocardia tuberculata</i>	Rough cockle	9	0.669	26.5	0.006 (0.001-0.016)	0.015 (0.003-0.044)
Cardiida	Cardiidae	Cerastoderma	<i>Cerastoderma edule</i>	Common cockle	5.6	0.62	10	0.101 (0.032-0.243)	0.258 (0.071-0.653)
Cardiida	Donacidae	Donax	<i>Donax trunculus</i>	Abrupt wedge shell	4.4	0.7	26.5	0.035 (0.006-0.114)	0.089 (0.015-0.298)
Cardiida	Psammobiidae	Hiatula	<i>Hiatula diplos</i>	Purple clam	6	0.825	26.5	0.067 (0.017-0.192)	0.168 (0.041-0.478)
Myida	Myidae	Mya	<i>Mya arenaria</i>	Soft-shell clam	10	0.3	10	0.055 (0.015-0.146)	0.14 (0.034-0.397)
Mytilida	Mytilidae	Mytilus	<i>Mytilus californianus</i>	California mussel	25.5	0.25	15	0.034 (0.015-0.061)	0.088 (0.034-0.169)
Mytilida	Mytilidae	Mytilus	<i>Mytilus edulis</i>	Blue mussel	11	0.24	8	0.078 (0.043-0.13)	0.195 (0.113-0.318)
Mytilida	Mytilidae	Mytilus	<i>Mytilus galloprovincialis</i>	Mediterranean mussel	16.5	0.26	17	0.042 (0.026-0.064)	0.105 (0.061-0.17)
Mytilida	Mytilidae	Perna	<i>Perna canaliculus</i>	Green-lipped mussel	15	0.6	26	0.064 (0.016-0.18)	0.156 (0.042-0.43)
Mytilida	Mytilidae	Perna	<i>Perna viridis</i>	Asian green mussel	16.5	1.07	26	0.122 (0.042-0.287)	0.299 (0.114-0.657)
Ostreida	Ostreidae	Crassostrea	<i>Crassostrea virginica</i>	Eastern oyster	30	0.565	24	0.054 (0.021-0.115)	0.135 (0.055-0.281)
Ostreida	Ostreidae	Magallana	<i>Magallana gigas</i>	Pacific oyster	45	0.68	13	0.123 (0.066-0.213)	0.303 (0.189-0.464)
Ostreida	Ostreidae	Magallana	<i>Magallana rivularis</i>	Jinjiang oyster	20.88	0.84	20.5	0.12 (0.046-0.259)	0.293 (0.129-0.562)
Ostreida	Ostreidae	Saccostrea	<i>Saccostrea glomerata</i>	Sydney rock oyster	5	0.7625	24	0.188 (0.045-0.544)	0.458 (0.125-1.26)
Pectinida	Pectinidae	Crassadoma	<i>Crassadoma gigantea</i>	Purple-hinged rock scallop	25	0.5035	16	0.029 (0.008-0.075)	0.072 (0.022-0.175)
Pectinida	Pectinidae	Mimachlamys	<i>Mimachlamys crassicostata</i>	Noble scallop	9.49	0.6626	17	0.183 (0.032-0.626)	0.45 (0.082-1.479)
Pectinida	Pectinidae	Mizuhopecten	<i>Mizuhopecten yessoensis</i>	Japanese scallop	25	0.925	18	0.04 (0.017-0.081)	0.101 (0.043-0.205)
Pectinida	Pectinidae	Nodipecten	<i>Nodipecten subnodosus</i>	Pacific giant lions-paw scallop	15	0.5035	16	0.044 (0.009-0.14)	0.108 (0.022-0.335)
Pectinida	Pectinidae	Placopecten	<i>Placopecten magellanicus</i>	Atlantic sea scallop	20	0.28	8	0.013 (0.006-0.024)	0.034 (0.014-0.07)
Venerida	Veneridae	Callista	<i>Callista chione</i>	Smooth clam	11	0.24	12	0.04 (0.008-0.122)	0.102 (0.02-0.319)
Venerida	Veneridae	Chamelea	<i>Chamelea gallina</i>	Warty venus	5	0.415	14	0.045 (0.009-0.135)	0.113 (0.022-0.352)
Venerida	Veneridae	Mercenaria	<i>Mercenaria mercenaria</i>	Northern quahog	13	0.3257	17	0.102 (0.037-0.225)	0.248 (0.106-0.498)
Venerida	Veneridae	Ruditapes	<i>Ruditapes decussatus</i>	Grooved carpet shell	8	0.48	17	0.033 (0.011-0.087)	0.082 (0.028-0.198)
Venerida	Veneridae	Ruditapes	<i>Ruditapes philippinarum</i>	Manila clam	8	0.52	18	0.031 (0.015-0.058)	0.075 (0.042-0.122)
Venerida	Mactridae	Spisula	<i>Spisula solidia</i>	Surf clam	5	0.3307	11	0.01 (0.004-0.022)	0.024 (0.01-0.051)

1245

1246 **Table S7.** Field- and lab-based paralytic shellfish toxin depuration rates predicted by the best performing regression model for all  
 1247 harvested bivalve species along with the required predictor variables.  
 1248

Order	Family	Genus	Scientific name	Common name	Length (cm)	K (1/yr)	Temp (°C)	Field (95% CI)	Lab (95% CI)
Adapedonta	Hiatellidae	Cyrtodaria	<i>Cyrtodaria siliqua</i>	Northern propellerclam	11	0.07	8	0.064 (0.004-0.294)	0.161 (0.01-0.75)
Adapedonta	Pharidae	Ensis	<i>Ensis ensis</i>	Pod razor shell	16.5	0.4625	11	0.104 (0.013-0.376)	0.261 (0.031-0.944)
Adapedonta	Pharidae	Ensis	<i>Ensis leei</i>	Atl.jackknife(=Atl.razor clam)	20	0.4625	11	0.099 (0.012-0.357)	0.25 (0.028-0.897)
Adapedonta	Pharidae	Ensis	<i>Ensis macha</i>	Giant jackknife	16.5	0.225	11	0.069 (0.013-0.225)	0.174 (0.03-0.568)
Adapedonta	Pharidae	Ensis	<i>Ensis magnus</i>	Arched razor shell	16.5	0.4625	11	0.104 (0.013-0.379)	0.261 (0.03-0.951)
Adapedonta	Pharidae	Ensis	<i>Ensis siliqua</i>	Sword razor shell	15.5	0.7	11	0.169 (0.017-0.671)	0.421 (0.039-1.644)
Adapedonta	Hiatellidae	Panopea	<i>Panopea generosa</i>	Pacific geoduck	17.5	0.199	8	0.061 (0.009-0.213)	0.154 (0.02-0.537)
Adapedonta	Hiatellidae	Panopea	<i>Panopea zelandica</i>	New Zealand geoduck	17.5	0.25	8	0.066 (0.009-0.23)	0.168 (0.02-0.594)
Adapedonta	Pharidae	Pharus	<i>Pharus legumen</i>	Bean solen	9.982	0.4075	9	0.117 (0.008-0.533)	0.291 (0.019-1.295)
Adapedonta	Pharidae	Siliqua	<i>Siliqua patula</i>	Pacific razor clam	18	0.59	7	0.169 (0.009-0.798)	0.422 (0.023-1.969)
Adapedonta	Pharidae	Sinonovacula	<i>Sinonovacula constricta</i>	Constricted tagelus	15.5	0.4075	9	0.109 (0.007-0.49)	0.272 (0.018-1.215)
Adapedonta	Solenidae	Solen	<i>Solen capensis</i>	Cape razor clam	11	0.28	10	0.061 (0.007-0.231)	0.153 (0.017-0.587)
Adapedonta	Solenidae	Solen	<i>Solen lamarckii</i>	Lamarck's razor shell	10	0.28	10	0.061 (0.007-0.225)	0.154 (0.018-0.574)
Adapedonta	Solenidae	Solen	<i>Solen marginatus</i>	European razor clam	17	0.28	10	0.05 (0.009-0.159)	0.129 (0.022-0.425)
Arcida	Arcidae	Anadara	<i>Anadara antiquata</i>	Antique ark	10.5	1.54	31.75	0.278 (0.006-1.666)	0.676 (0.014-3.854)
Arcida	Arcidae	Anadara	<i>Anadara broughtonii</i>	Inflated ark	8	0.2359	31.75	0.031 (0.001-0.175)	0.078 (0.002-0.422)
Arcida	Arcidae	Anadara	<i>Anadara kagoshimensis</i>	Half-crenated ark	6.2	0.428	31.75	0.039 (0.001-0.209)	0.096 (0.003-0.506)
Arcida	Arcidae	Anadara	<i>Anadara similis</i>	Brown ark	8	0.428	31.75	0.039 (0.001-0.211)	0.096 (0.003-0.516)
Arcida	Arcidae	Anadara	<i>Anadara tuberculosa</i>	Black ark	8	0.515	31.75	0.043 (0.001-0.229)	0.105 (0.004-0.552)
Arcida	Arcidae	Arca	<i>Arca noae</i>	Noah's ark	7	0.165	26.5	0.034 (0.001-0.172)	0.082 (0.003-0.419)
Arcida	Arcidae	Arca	<i>Arca zebra</i>	Turkey wing	10	1.2	26.5	0.171 (0.006-0.882)	0.416 (0.016-2.085)
Arcida	Glycymerididae	Glycymeris	<i>Glycymeris glycymeris</i>	Common European bittersweet	6.5	0.11	12	0.064 (0.003-0.304)	0.158 (0.007-0.747)
Arcida	Glycymerididae	Glycymeris	<i>Glycymeris nummaria</i>	Violet bittersweet	7	0.11	12	0.063 (0.003-0.298)	0.155 (0.007-0.718)
Arcida	Glycymerididae	Glycymeris	<i>Glycymeris ovata</i>	Black bittersweet	4.15	0.11	12	0.068 (0.003-0.32)	0.167 (0.008-0.785)
Arcida	Arcidae	Lunarcia	<i>Lunarcia ovalis</i>	Blood ark	7.6	0.45	25	0.049 (0.002-0.234)	0.122 (0.006-0.566)
Arcida	Arcidae	Tegillarca	<i>Tegillarca granosa</i>	Blood cockle	9	1.055	28	0.118 (0.005-0.571)	0.289 (0.012-1.424)
Cardiida	Cardiidae	Acanthocardia	<i>Acanthocardia spinosa</i>	Sand cockle	8.25	0.669	26.5	0.014 (0.001-0.071)	0.034 (0.003-0.175)
			<i>Acanthocardia</i>						
Cardiida	Cardiidae	Acanthocardia	<i>tuberculata</i>	Tuberculate cockle	9	0.669	26.5	0.006 (0.001-0.016)	0.015 (0.003-0.044)
Cardiida	Psammobiidae	Asaphis	<i>Asaphis violascens</i>	Pacific asaphis	11	0.825	26.5	0.068 (0.004-0.295)	0.167 (0.011-0.729)
Cardiida	Cardiidae	Cerastoderma	<i>Cerastoderma edule</i>	Common edible cockle	5.6	0.62	10	0.101 (0.032-0.243)	0.258 (0.071-0.653)
Cardiida	Cardiidae	Clinocardium	<i>Clinocardium nuttallii</i>	Basket cockle	14	0.1525	7	0.046 (0.003-0.208)	0.118 (0.008-0.533)
Cardiida	Cardiidae	Dallocardia	<i>Dallocardia muricata</i>	American yellow cockle	6	0.1525	26.5	0.022 (0.001-0.11)	0.055 (0.002-0.277)
Cardiida	Donacidae	Donax	<i>Donax dentifer</i>	Toothed donax	3.05	0.62	26.5	0.037 (0.005-0.143)	0.092 (0.011-0.374)
Cardiida	Donacidae	Donax	<i>Donax obesulus</i>	Common peruvian donax	3.9	1	26.5	0.071 (0.007-0.283)	0.178 (0.018-0.723)
Cardiida	Donacidae	Donax	<i>Donax trunculus</i>	Truncate donax	4.4	0.7	26.5	0.035 (0.006-0.114)	0.089 (0.015-0.298)
Cardiida	Psammobiidae	Hiatula	<i>Hiatula diphos</i>	Diphos sanguin	6	0.825	26.5	0.067 (0.017-0.192)	0.168 (0.041-0.478)

Cardiida	Cardiidae	Hippopus	<i>Hippopus hippopus</i>	Bear paw clam	50	0.14	26.5	0.022 (0-0.124)	0.056 (0.001-0.311)
Cardiida	Cardiidae	Laevicardium	<i>Laevicardium crassum</i>	Norwegian egg cockle	7.5	0.1525	26.5	0.021 (0.001-0.111)	0.052 (0.002-0.268)
Cardiida	Semelidae	Scrobicularia	<i>Scrobicularia plana</i>	Peppery furrow	6.5	0.36	8	0.096 (0.006-0.445)	0.242 (0.013-1.126)
Cardiida	Semelidae	Semele	<i>Semele solida</i>	Chilean seumele	3.035	0.297	12	0.068 (0.004-0.332)	0.171 (0.01-0.84)
Cardiida	Solecurtidae	Tagelus	<i>Tagelus dombeii</i>	Dombey's tagelus	7.8	0.4	26.5	0.035 (0.002-0.165)	0.088 (0.005-0.414)
Cardiida	Cardiidae	Tridacna	<i>Tridacna crocea</i>	Crocus giant clam	15	0.165	26.5	0.02 (0.001-0.111)	0.051 (0.002-0.288)
Cardiida	Cardiidae	Tridacna	<i>Tridacna derasa</i>	Smooth giant clam	60	0.109	26.5	0.025 (0-0.171)	0.062 (0-0.404)
Cardiida	Cardiidae	Tridacna	<i>Tridacna gigas</i>	Giant clam	137	0.07	26.5	5.402 (0-0.994)	12.555 (0-2.478)
Cardiida	Cardiidae	Tridacna	<i>Tridacna maxima</i>	Elongate giant clam	41.7	0.235	26.5	0.022 (0-0.136)	0.055 (0.001-0.336)
Cardiida	Cardiidae	Tridacna	<i>Tridacna squamosa</i>	Fluted giant clam	45	0.165	26.5	0.022 (0-0.128)	0.055 (0.001-0.325)
Limida	Limidae	Lima	<i>Lima lima</i>	Spiny file shell	9	0.43	17	0.067 (0.004-0.301)	0.166 (0.01-0.747)
Limida	Limidae	Limaria	<i>Limaria hians</i>	Limaria hians	0.605	0.43	17	0.075 (0.004-0.373)	0.188 (0.011-0.89)
Myida	Myidae	Mya	<i>Mya arenaria</i>	Sand gaper	10	0.3	10	0.055 (0.015-0.146)	0.14 (0.034-0.397)
Mytilida	Mytilidae	Choromytilus	<i>Choromytilus chorus</i>	Choro mussel	26	0.58	12	0.119 (0.009-0.531)	0.296 (0.022-1.281)
Mytilida	Mytilidae	Geukensia	<i>Geukensia demissa</i>	Atlantic ribbed mussel	12	0.26	16	0.065 (0.005-0.284)	0.161 (0.011-0.673)
Mytilida	Mytilidae	Lithophaga	<i>Lithophaga lithophaga</i>	European date mussel	5.6	0.044	16	0.052 (0.003-0.255)	0.131 (0.007-0.622)
Mytilida	Mytilidae	Modiolus	<i>Modiolus barbatus</i>	Bearded horse mussel	6.611	0.1955	16	0.062 (0.004-0.275)	0.152 (0.01-0.698)
Mytilida	Mytilidae	Mytella	<i>Mytella guyanensis</i>	Guyana swamp mussel	6	0.128	18	0.052 (0.003-0.232)	0.129 (0.007-0.56)
Mytilida	Mytilidae	Mytella	<i>Mytella strigata</i>	Strigate mangrove mussel	6	0.128	18	0.052 (0.003-0.23)	0.131 (0.008-0.566)
Mytilida	Mytilidae	Mytilus	<i>Mytilus californianus</i>	Californian mussel	25.5	0.25	15	0.034 (0.015-0.061)	0.088 (0.034-0.169)
Mytilida	Mytilidae	Mytilus	<i>Mytilus chilensis</i>	Chilean mussel	18	0.25	12	0.06 (0.032-0.111)	0.149 (0.081-0.268)
Mytilida	Mytilidae	Mytilus	<i>Mytilus coruscus</i>	Korean mussel	10.5	0.25	15	0.053 (0.012-0.143)	0.132 (0.029-0.351)
Mytilida	Mytilidae	Mytilus	<i>Mytilus edulis</i>	Blue mussel	11	0.24	8	0.078 (0.043-0.13)	0.195 (0.113-0.318)
Mytilida	Mytilidae	Mytilus	<i>Mytilus galloprovincialis</i>	Mediterranean mussel	16.5	0.26	17	0.042 (0.026-0.064)	0.105 (0.061-0.17)
Mytilida	Mytilidae	Mytilus	<i>Mytilus planulatus</i>	Australian mussel	6	0.25	26	0.034 (0.006-0.115)	0.084 (0.014-0.283)
Mytilida	Mytilidae	Mytilus	<i>Mytilus platensis</i>	River Plata mussel	9	0.38	14	0.07 (0.016-0.187)	0.174 (0.038-0.444)
Mytilida	Mytilidae	Perna	<i>Perna canaliculus</i>	New Zealand mussel	15	0.6	26	0.064 (0.016-0.18)	0.156 (0.042-0.43)
Mytilida	Mytilidae	Perna	<i>Perna perna</i>	South American rock mussel	17	0.13	26	0.037 (0.003-0.172)	0.091 (0.008-0.418)
Mytilida	Mytilidae	Perna	<i>Perna viridis</i>	Green mussel	16.5	1.07	26	0.122 (0.042-0.287)	0.299 (0.114-0.657)
Ostreida	Pinnidae	Atrina	<i>Atrina maura</i>	Maura pen shell	29.75	0.77	20	0.109 (0.006-0.526)	0.269 (0.014-1.26)
Ostreida	Ostreidae	Crassostrea	<i>Crassostrea corteziensis</i>	Cortez oyster	25	1.09	27	0.142 (0.02-0.517)	0.347 (0.051-1.17)
Ostreida	Ostreidae	Crassostrea	<i>Crassostrea rhizophorae</i>	Mangrove cupped oyster	12	2.79	27	29.998 (0.018-169.971)	70.492 (0.047-391.851)
Ostreida	Ostreidae	Crassostrea	<i>Crassostrea tulipa</i>	Gasar cupped oyster	25	0.845	27	0.09 (0.016-0.289)	0.22 (0.039-0.691)
Ostreida	Ostreidae	Crassostrea	<i>Crassostrea virginica</i>	American cupped oyster	30	0.565	24	0.054 (0.021-0.115)	0.135 (0.055-0.281)
Ostreida	Ostreidae	Magallana	<i>Magallana bilineata</i>	Slipper cupped oyster	20.88	1	28	0.129 (0.021-0.433)	0.31 (0.055-0.988)
Ostreida	Ostreidae	Magallana	<i>Magallana gigas</i>	Pacific cupped oyster	45	0.68	13	0.123 (0.066-0.213)	0.303 (0.189-0.464)
Ostreida	Ostreidae	Magallana	<i>Magallana sikamea</i>	Kumamoto oyster	6	0.84	20.5	0.186 (0.025-0.67)	0.449 (0.064-1.496)
Ostreida	Ostreidae	Ostrea	<i>Ostrea conchaphila</i>	Olympia oyster	9	0.7625	14.5	0.228 (0.013-1.04)	0.557 (0.033-2.498)
Ostreida	Margaritidae	Pinctada	<i>Pinctada maxima</i>	Silverlip pearl oyster	30	0.74	22	0.09 (0.005-0.417)	0.219 (0.012-1.014)
Ostreida	Margaritidae	Pinctada	<i>Pinctada radiata</i>	Rayed pearl oyster	10.05	0.414	22	0.064 (0.004-0.315)	0.158 (0.009-0.753)
Ostreida	Pteriidae	Pteria	<i>Pteria penguin</i>	Penguin wing oyster	30	0.69	22	0.08 (0.004-0.375)	0.199 (0.01-0.904)
Ostreida	Ostreidae	Saccostrea	<i>Saccostrea cucullata</i>	Hooded oyster	20	0.7625	24	0.148 (0.021-0.491)	0.362 (0.052-1.147)
Pectinida	Pectinidae	Aequipecten	<i>Aequipecten opercularis</i>	Queen scallop	11	0.645	12	0.094 (0.008-0.413)	0.231 (0.02-0.999)
Pectinida	Pectinidae	Argopecten	<i>Argopecten purpuratus</i>	Peruvian calico scallop	12	1.995	21	1.42 (0.01-8.773)	3.459 (0.026-21.509)

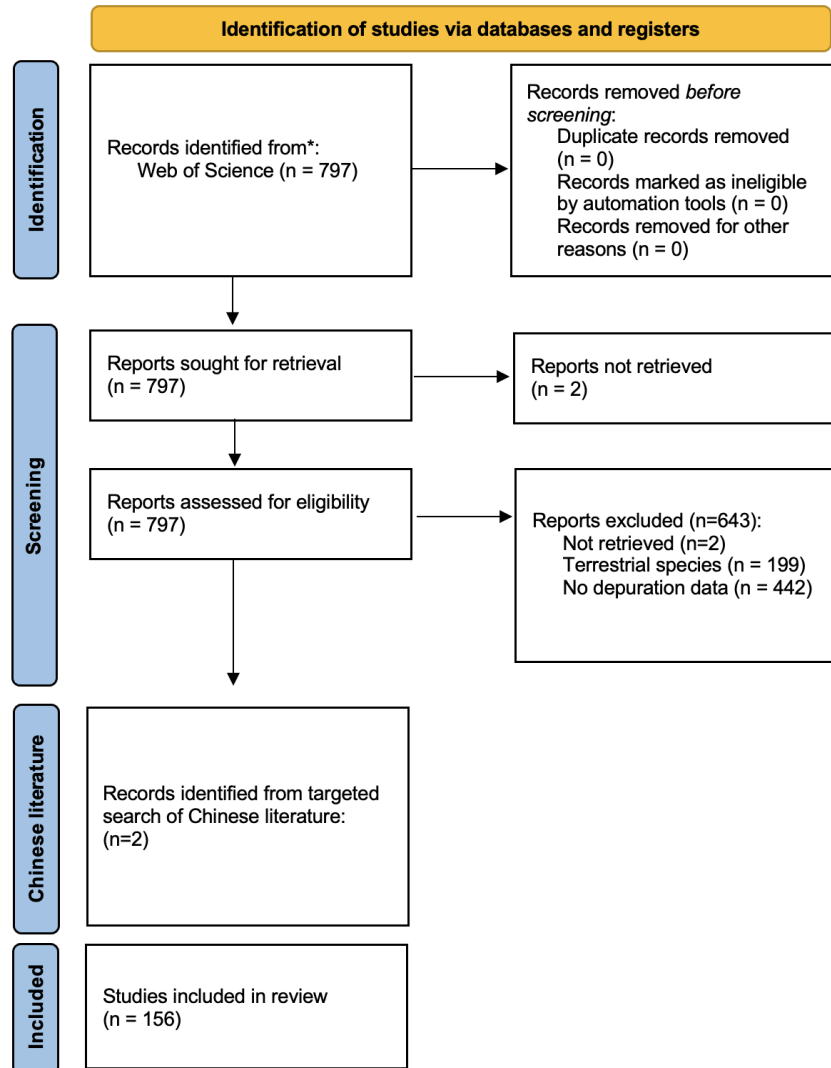
Pectinida	Pectinidae	Argopecten	<i>Argopecten ventricosus</i>	Pacific calico scallop	10	2.1	26	1.388 (0.008-8.634)	3.322 (0.021-21.089)
Pectinida	Pectinidae	Chlamys	<i>Chlamys islandica</i>	Iceland scallop	11	0.139	8	0.054 (0.004-0.257)	0.135 (0.01-0.617)
Pectinida	Pectinidae	Flexopecten	<i>Flexopecten glaber</i>	Smooth scallop	8.66	0.5035	16	0.059 (0.005-0.243)	0.147 (0.013-0.602)
Pectinida	Pectinidae	Mizuhopecten	<i>yessoensis</i>	Yesso scallop	25	0.925	18	0.04 (0.017-0.081)	0.101 (0.043-0.205)
Pectinida	Pectinidae	Nodipecten	<i>Nodipecten nodosus</i>	Lion's paw	15	0.5035	16	0.048 (0.007-0.181)	0.118 (0.018-0.421)
Pectinida	Pectinidae	Patinopecten	<i>Patinopecten caurinus</i>	Weathervane scallop	28	0.413	8	0.069 (0.006-0.306)	0.173 (0.014-0.754)
Pectinida	Pectinidae	Pecten	<i>Pecten fumatus</i>	Southern Australia scallop	9.3	0.5	16	0.059 (0.005-0.249)	0.146 (0.013-0.607)
Pectinida	Pectinidae	Pecten	<i>Pecten jacobaeus</i>	Great Mediterranean scallop	25	0.5	20	0.041 (0.003-0.178)	0.102 (0.008-0.426)
Pectinida	Pectinidae	Pecten	<i>Pecten maximus</i>	Great Atlantic scallop	17	0.475	12	0.065 (0.006-0.278)	0.162 (0.015-0.687)
Pectinida	Pectinidae	Placopecten	<i>magellanicus</i>	American sea scallop	20	0.28	8	0.013 (0.006-0.024)	0.034 (0.014-0.07)
Pectinida	Spondylidae	Spondylus	<i>Spondylus americanus</i>	Atlantic thorny oyster	11.2	0.5	16	0.07 (0.005-0.325)	0.175 (0.012-0.763)
Pectinida	Spondylidae	Spondylus	<i>crassisquama</i>	Pacific thorny oyster	8.85	0.5	16	0.074 (0.005-0.341)	0.184 (0.012-0.822)
Pectinida	Pectinidae	Zygochlamys	<i>Zygochlamys delicatula</i>	Delicate scallop	7.8	0.187	13	0.045 (0.003-0.203)	0.112 (0.008-0.495)
Venerida	Arcticidae	Arctica	<i>Arctica islandica</i>	Ocean quahog	13	0.0605	8	0.056 (0.003-0.28)	0.138 (0.008-0.669)
Venerida	Veneridae	Austrovenus	<i>Austrovenus stutchburyi</i>	Stutchbury's venus	4.9	0.3115	15	0.057 (0.005-0.231)	0.141 (0.011-0.573)
Venerida	Veneridae	Callista	<i>Callista chione</i>	Smooth callista	11	0.24	12	0.04 (0.008-0.122)	0.102 (0.02-0.319)
Venerida	Veneridae	Chamelea	<i>Chamelea gallina</i>	Striped venus	5	0.415	14	0.045 (0.009-0.135)	0.113 (0.022-0.352)
Venerida	Veneridae	Cyclina	<i>Cyclina sinensis</i>	Oriental cyclina	5	0.421	16	0.063 (0.005-0.261)	0.157 (0.013-0.612)
Venerida	Veneridae	Dosinia	<i>Dosinia exoleta</i>	Mature dosinia	4.615	0.448	16	0.065 (0.006-0.265)	0.16 (0.014-0.637)
Venerida	Veneridae	Gafrarium	<i>Gafrarium tumidum</i>	Tumid venus	4	0.32565	16	0.054 (0.005-0.213)	0.133 (0.011-0.52)
Venerida	Veneridae	Ilioichione	<i>Ilioichione subrugosa</i>	Semi-rough venus	4.485	0.421	16	0.064 (0.006-0.265)	0.159 (0.014-0.627)
Venerida	Veneridae	Leukoma	<i>Leukoma staminea</i>	Pacific littleneck clam	7.5	0.21105	8	0.07 (0.006-0.295)	0.174 (0.014-0.718)
Venerida	Veneridae	Leukoma	<i>Leukoma thaca</i>	Taca clam	8	0.174	19	0.036 (0.003-0.154)	0.089 (0.007-0.372)
Venerida	Mactridae	Lutraria	<i>Lutraria magna</i>	Oblong otter shell	5.115	0.1975	11	0.043 (0.003-0.198)	0.107 (0.007-0.493)
Venerida	Mactridae	Mactra	<i>Mactra quadrangularis</i>	Globose clam	6.05	0.15	11	0.04 (0.003-0.188)	0.099 (0.006-0.461)
Venerida	Mactromeris	Mactromeris	<i>polynyma</i>	Stimpson's surf clam	16	0.0801	4	0.05 (0.003-0.239)	0.124 (0.007-0.591)
			<i>Mercenaria</i>						
Venerida	Veneridae	Mercenaria	<i>campechiensis</i>	Southern hardshell clam	13	0.64	17	0.149 (0.017-0.47)	0.363 (0.041-1.081)
Venerida	Veneridae	Mercenaria	<i>Mercenaria mercenaria</i>	Northern quahog(=Hard clam)	13	0.3257	17	0.102 (0.037-0.225)	0.248 (0.106-0.498)
Venerida	Veneridae	Meretrix	<i>Meretrix lusoria</i>	Japanese hard clam	5	1.26	17	0.34 (0.011-1.774)	0.828 (0.028-4.243)
Venerida	Mesodesmatidae	Mesodesma	<i>Mesodesma donacium</i>	Macha clam	7	1.13	17	0.232 (0.009-1.229)	0.569 (0.022-2.981)
Venerida	Mesodesmatidae	Paphies	<i>Paphies australis</i>	Pipi wedge clam	8	0.16	20	0.036 (0.002-0.178)	0.089 (0.005-0.432)
Venerida	Veneridae	Polititapes	<i>Polititapes aureus</i>	Golden carpet shell	6	0.421	12	0.08 (0.007-0.348)	0.198 (0.017-0.816)
Venerida	Veneridae	Polititapes	<i>Polititapes rhombooides</i>	Banded carpet shell	6	0.421	12	0.08 (0.007-0.332)	0.197 (0.018-0.794)
Venerida	Veneridae	Ruditapes	<i>Ruditapes decussatus</i>	Grooved carpet shell	8	0.48	17	0.033 (0.011-0.087)	0.082 (0.028-0.198)
Venerida	Veneridae	Ruditapes	<i>Ruditapes philippinarum</i>	Japanese carpet shell	8	0.52	18	0.031 (0.015-0.058)	0.075 (0.042-0.122)
Venerida	Veneridae	Saxidomus	<i>Saxidomus gigantea</i>	Butter clam	13	0.421	7	0.103 (0.007-0.439)	0.255 (0.019-1.057)
Venerida	Mactridae	Spisula	<i>Spisula murchisoni</i>	Large trough shell	5	0.3307	12.5	0.018 (0.003-0.079)	0.043 (0.007-0.192)
Venerida	Mactridae	Spisula	<i>Spisula sachalinensis</i>	Imperial surf clam	5	0.3307	18	0.013 (0.002-0.063)	0.032 (0.005-0.149)
Venerida	Mactridae	Spisula	<i>Spisula solida</i>	Solid surf clam	5	0.3307	11	0.01 (0.004-0.022)	0.024 (0.01-0.051)
Venerida	Mactridae	Spisula	<i>Spisula subtruncata</i>	Subtruncate surf clam	3	0.67	12.5	0.033 (0.004-0.152)	0.079 (0.011-0.36)

Venerida	Veneridae	Tawera	<i>Tawera elliptica</i>	Gay's little venus	2.803	0.288	12	0.066 (0.006-0.284)	0.163 (0.014-0.682)
Venerida	Veneridae	Tivela	<i>Tivela mactroides</i>	Triangular tivela	3.4	0.15	27	0.027 (0.001-0.132)	0.068 (0.003-0.32)
Venerida	Mactridae	Tresus	<i>Tresus nuttallii</i>	Pacific horse clam	25.4	0.153	11	0.035 (0.002-0.168)	0.087 (0.004-0.422)
Venerida	Veneridae	Venerupis	<i>Venerupis corrugata</i>	Corrugated venus	7.7	0.226	13	0.053 (0.005-0.225)	0.133 (0.011-0.535)
Venerida	Veneridae	Venus	<i>Venus casina</i>	Chamber venus	5	0.26	19	0.043 (0.004-0.183)	0.106 (0.008-0.442)
Venerida	Veneridae	Venus	<i>Venus verrucosa</i>	Warty venus	7	0.26	19	0.042 (0.003-0.176)	0.103 (0.009-0.434)

1249

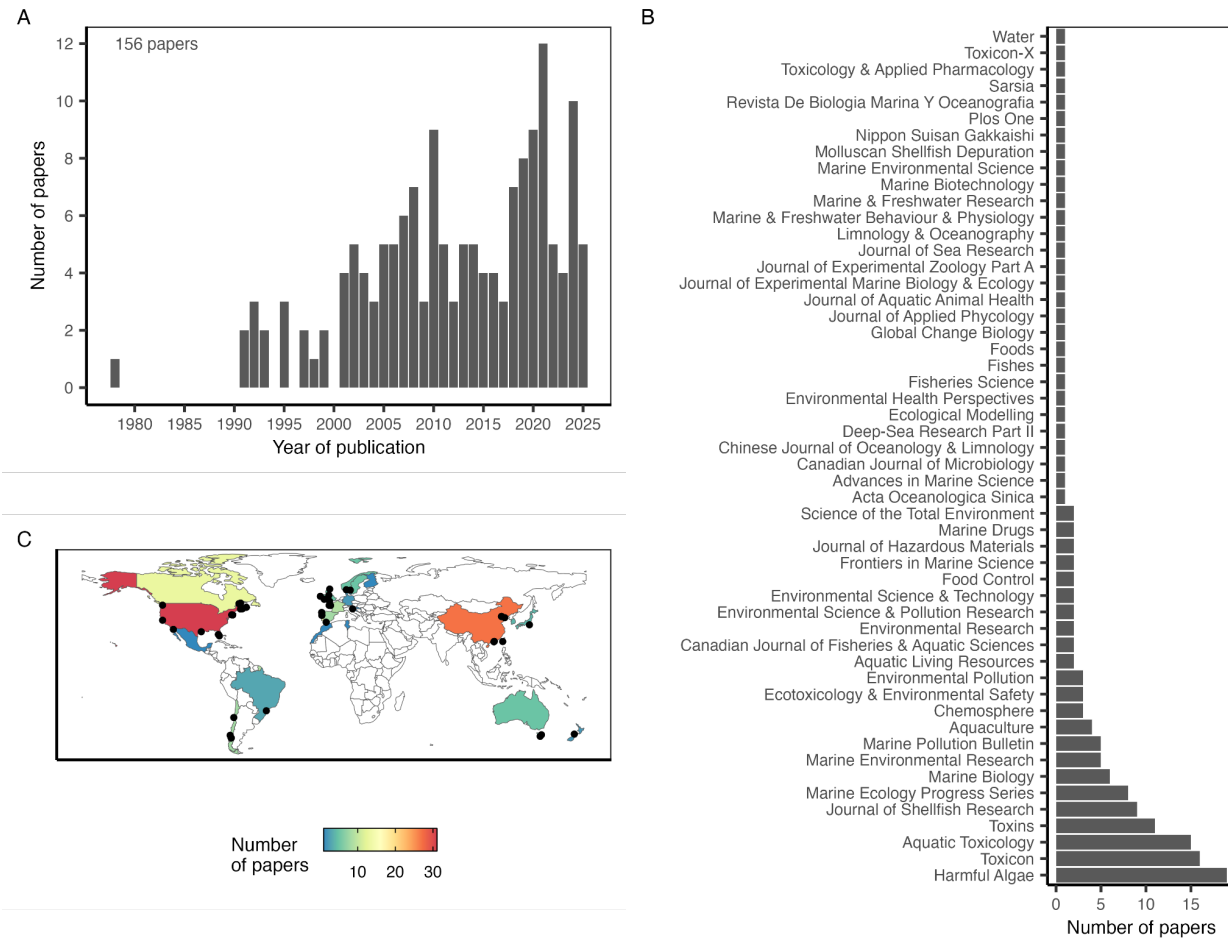
## 1250 Supplemental Figures

1251

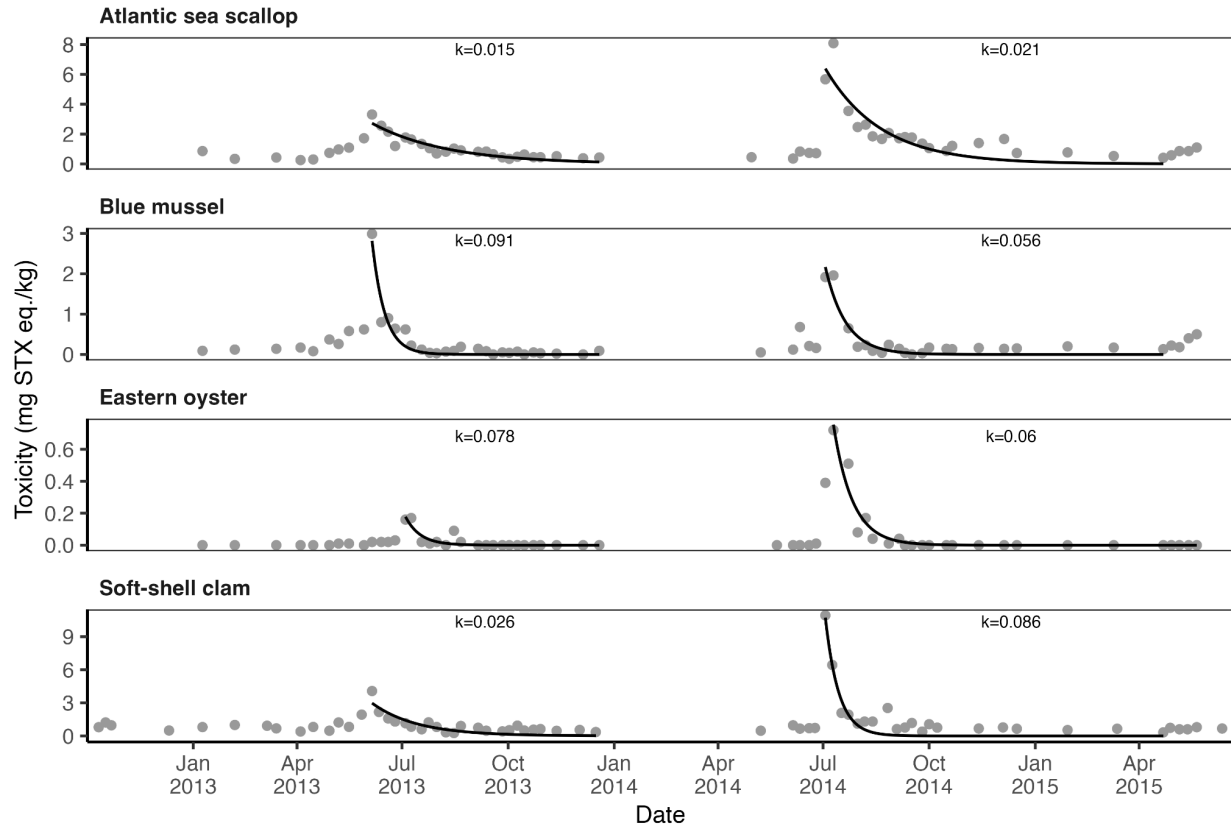


1252

1253 **Figure S1.** PRISMA 2020 flow diagram detailing the literature review inclusion criteria.

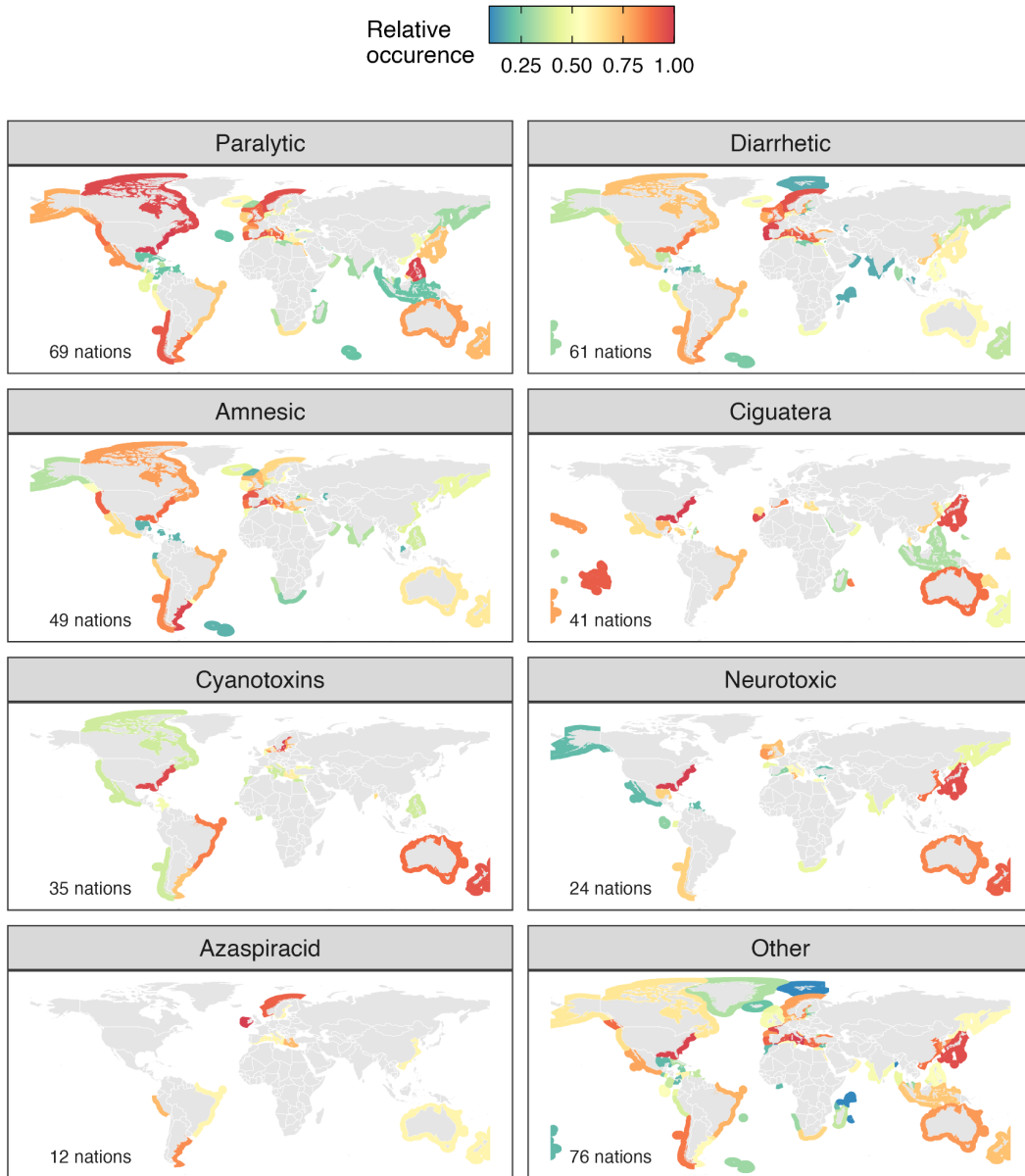


1254  
1255  
1256 **Figure S2.** The number of papers measuring marine biotoxin depuration rates (**A**) over time, (**B**)  
1257 by journal; and (**C**) by country of the lead author's primary affiliation. In (**C**), points mark  
1258 locations where depuration rates have been quantified from field monitoring data.



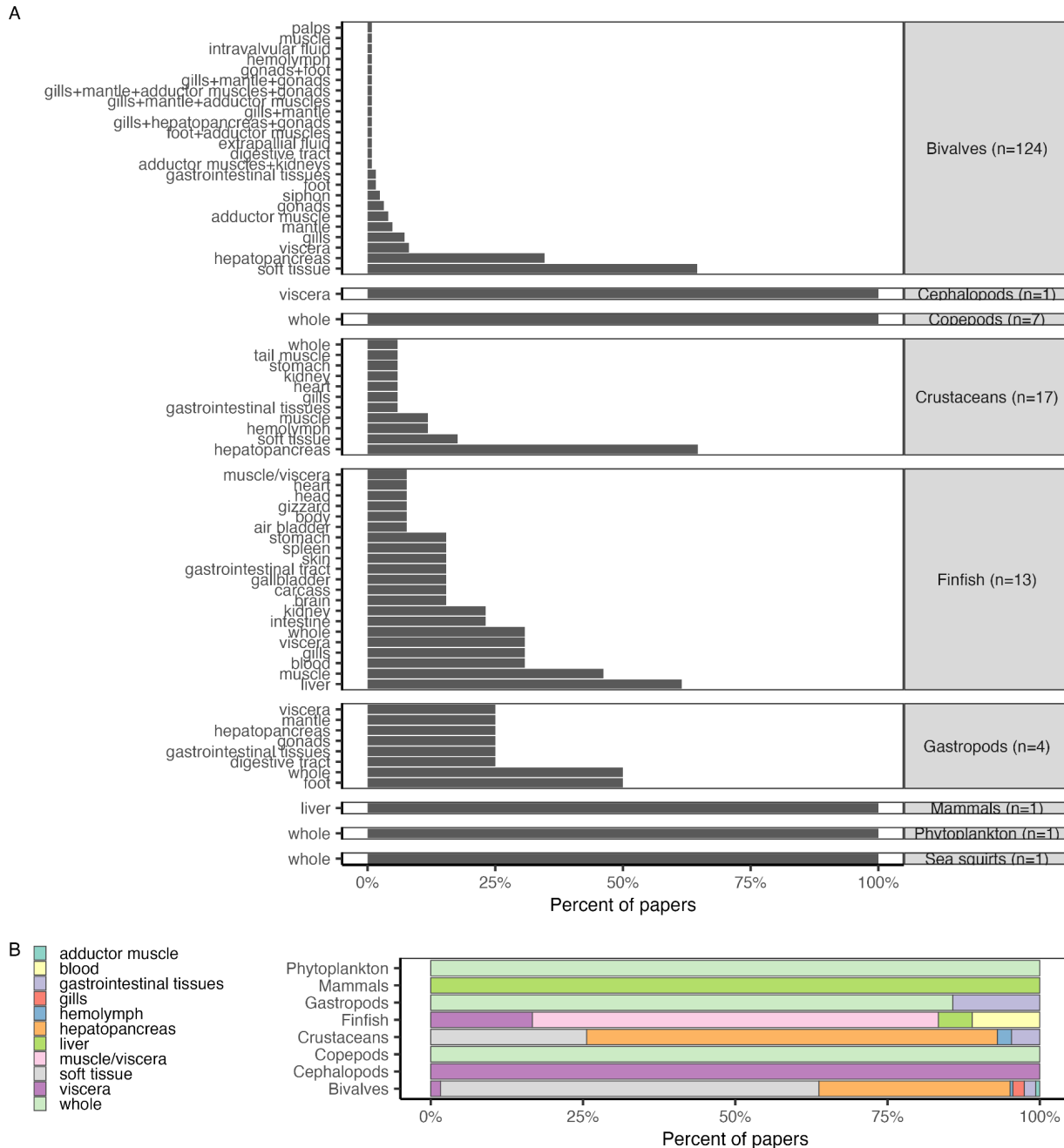
1259  
1260  
1261  
1262  
1263  
1264

**Figure S3.** An illustration of the methods for estimating paralytic shellfish toxin (PST) depuration rates from biotoxin monitoring data on four shellfish species from Deadmans Harbour, New Brunswick, Canada. Data are from (Rourke et al., 2021). The black line shows the fit of a one-compartment depuration model to the depuration phase of annual toxin events; the exponential decay constant ( $k$ ) associated with each curve is printed above the curve.



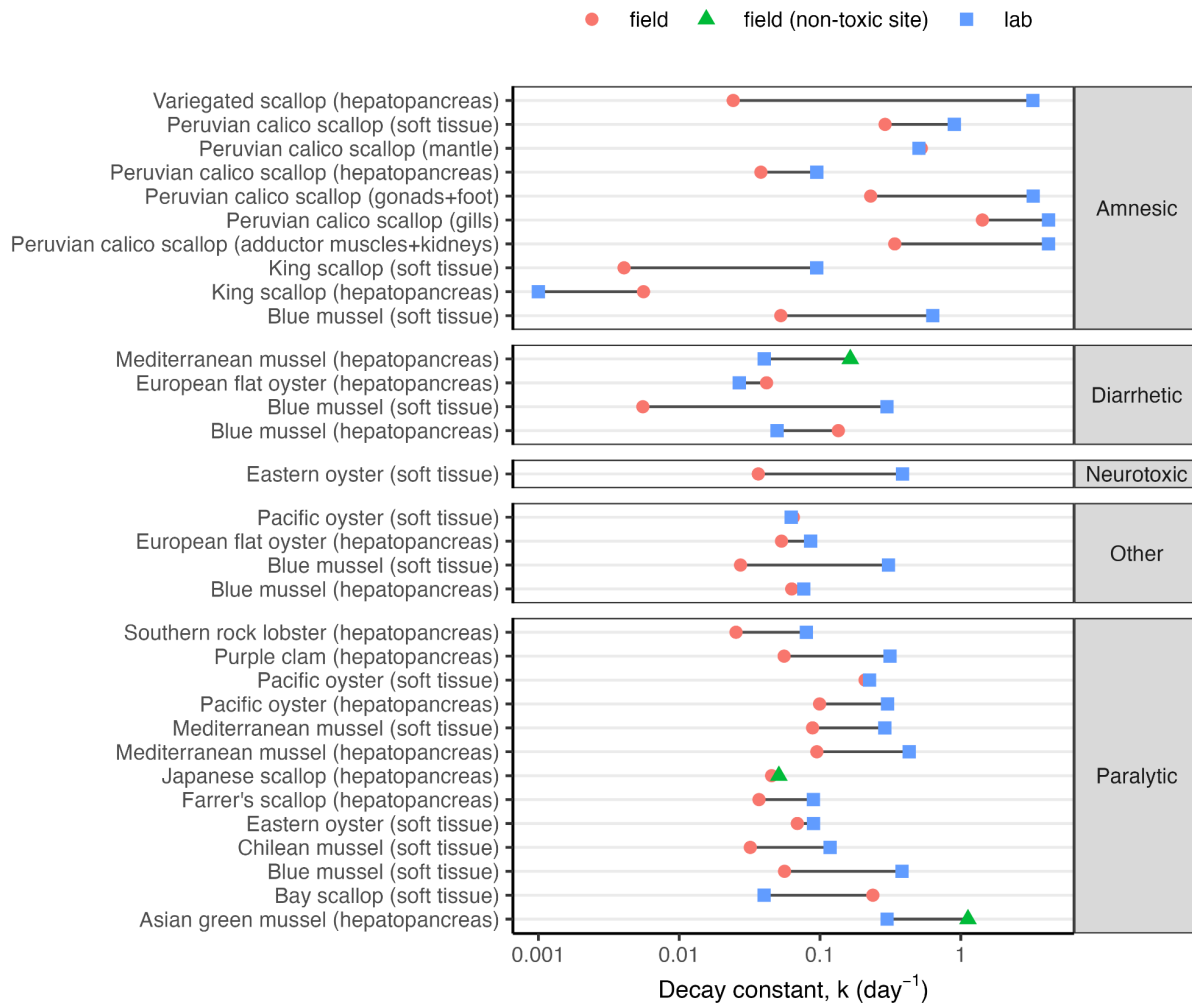
1265  
 1266  
 1267  
 1268  
 1269

**Figure S4.** Exclusive economic zones (EEZs) exposed to harmful algae and their associated public health risks. Shaded EEZs have HAB species present based on OBIS. Syndromes are sorted by the number of EEZs with observations of HAB species; the number of EEZs impacted (out of 257) is printed in the bottom right.



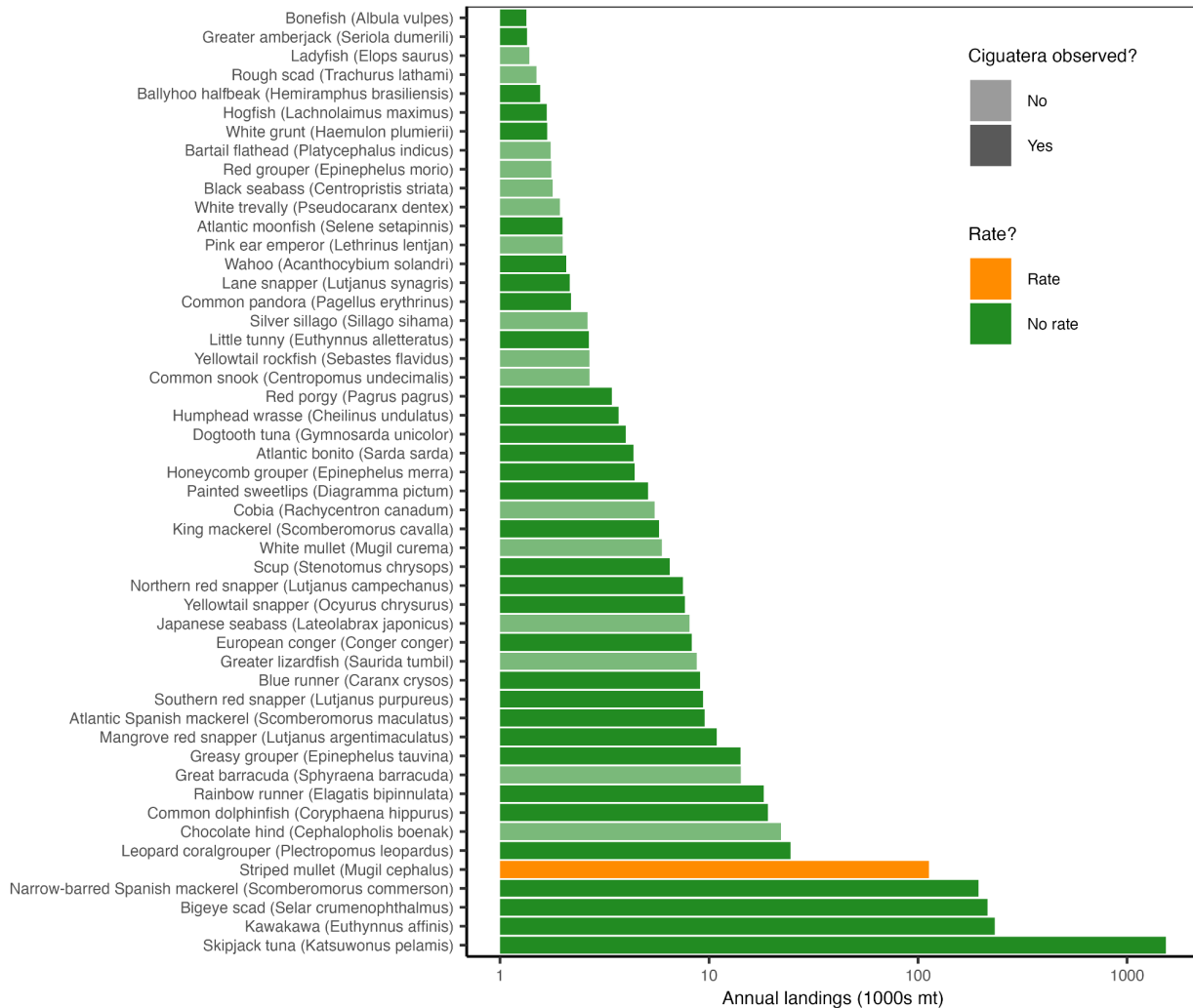
1270

1271 **Figure S5.** Panel A shows the frequency with which different tissues are evaluated for biotoxin  
1272 depuration rates by taxonomic class. The x-axis represents the percent of papers on species  
1273 within each class evaluating depuration rates for each tissue. The number of papers on species  
1274 within each class is printed in the class label. Tissues are ordered in increasing frequency  
1275 (bottom to top). Panel B shows the frequency with which different tissues are evaluated for  
1276 biotoxin depuration rates by taxonomic class in papers in which only a single tissue is  
1277 evaluated.



1278

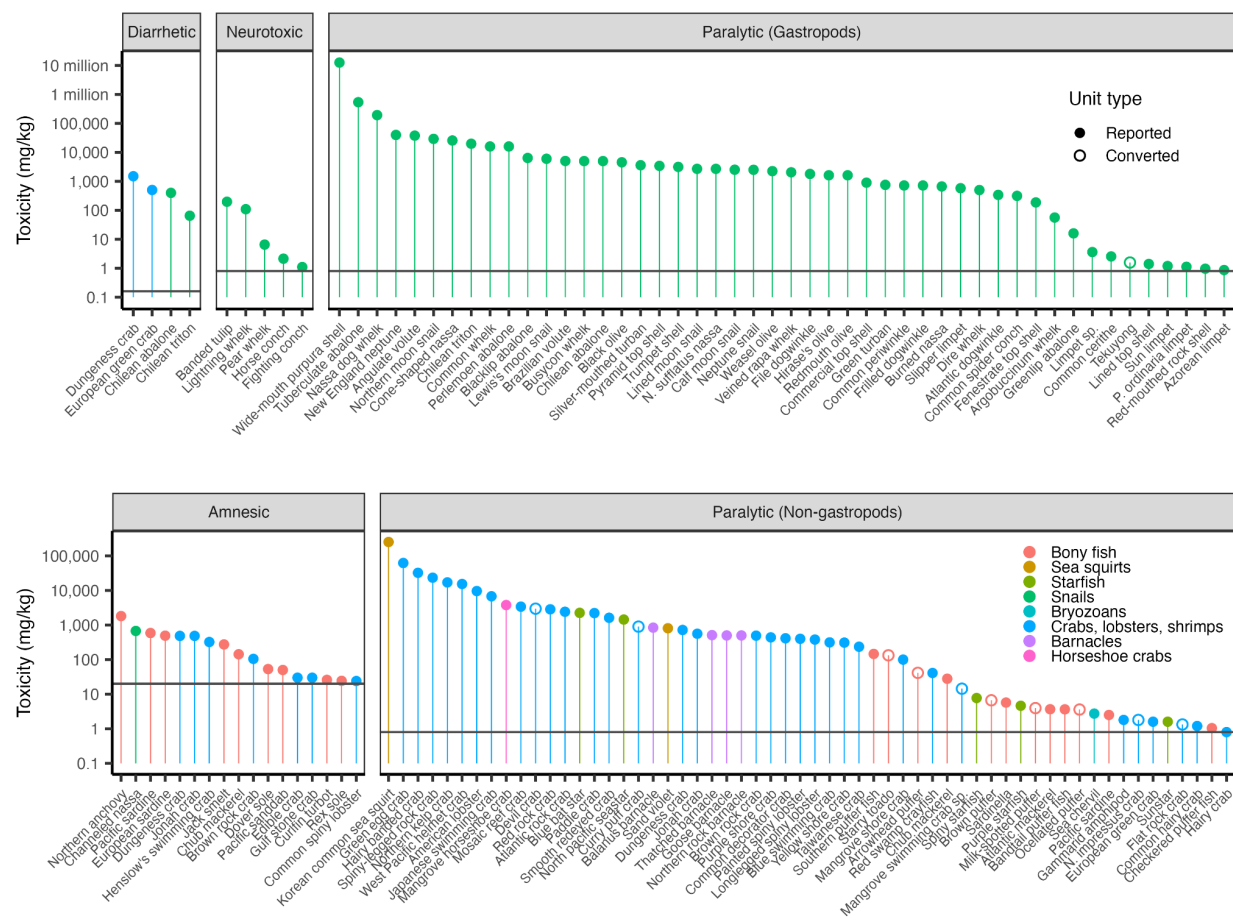
1279 **Figure S6.** A comparison of average depuration rates in the field versus the lab by species,  
 1280 tissue, and toxin. In general, depuration is faster in the lab than in the field.



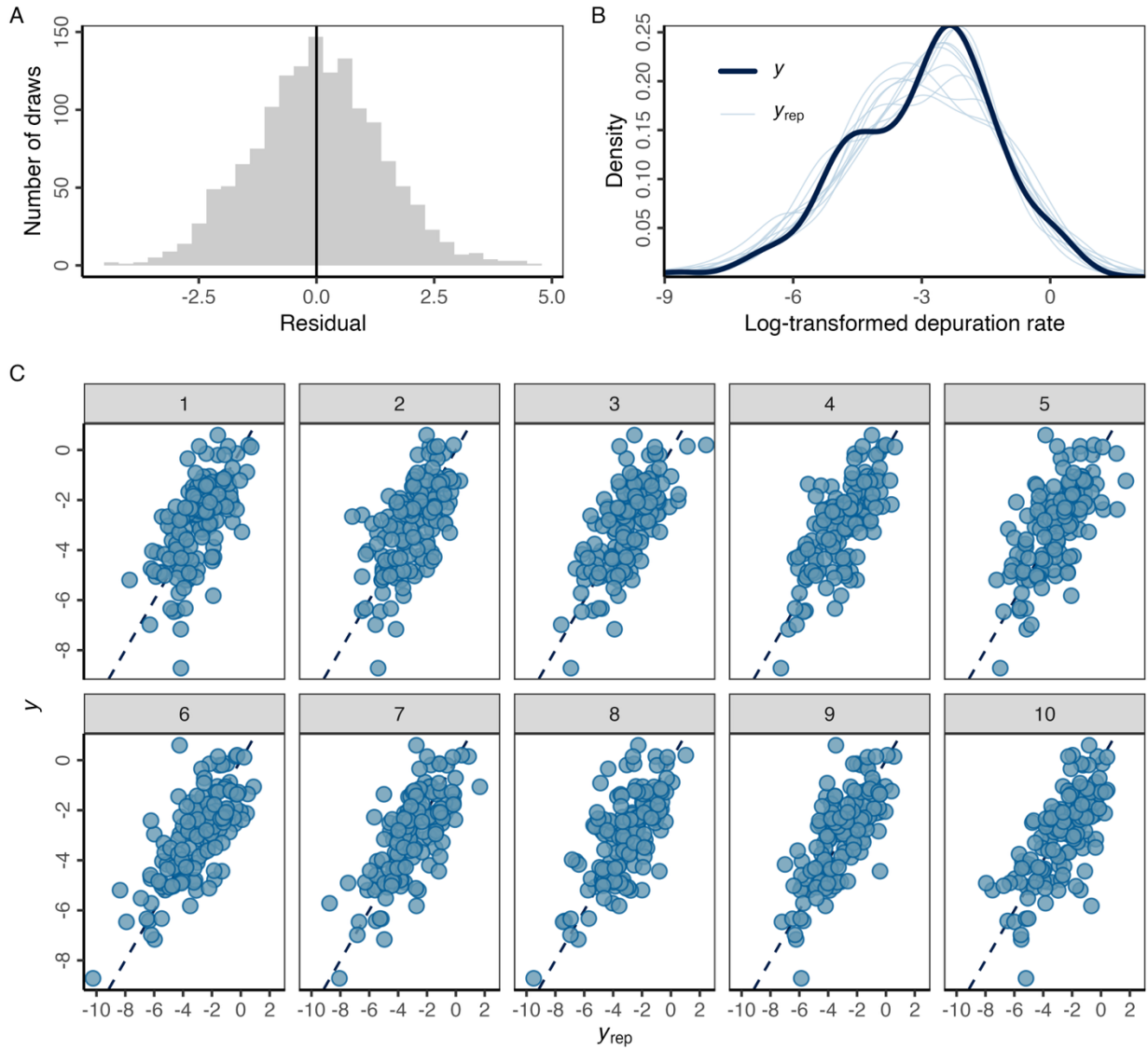
1281

1282

1283 **Figure S7.** The top-50 marine finfish vulnerable to ciguatera most frequently landed by fisheries  
 1284 from 2014-2023 from countries with known ciguatera occurrences. Marine finfish vulnerable to  
 1285 ciguatera were identified as those with reported ciguatera occurrences (known) and large (>25  
 1286 cm max length), reef-associated, non-herbivorous marine finfish speculated to be vulnerable to  
 1287 ciguatera. Ciguatera depuration rates have not been studied for any of these species.

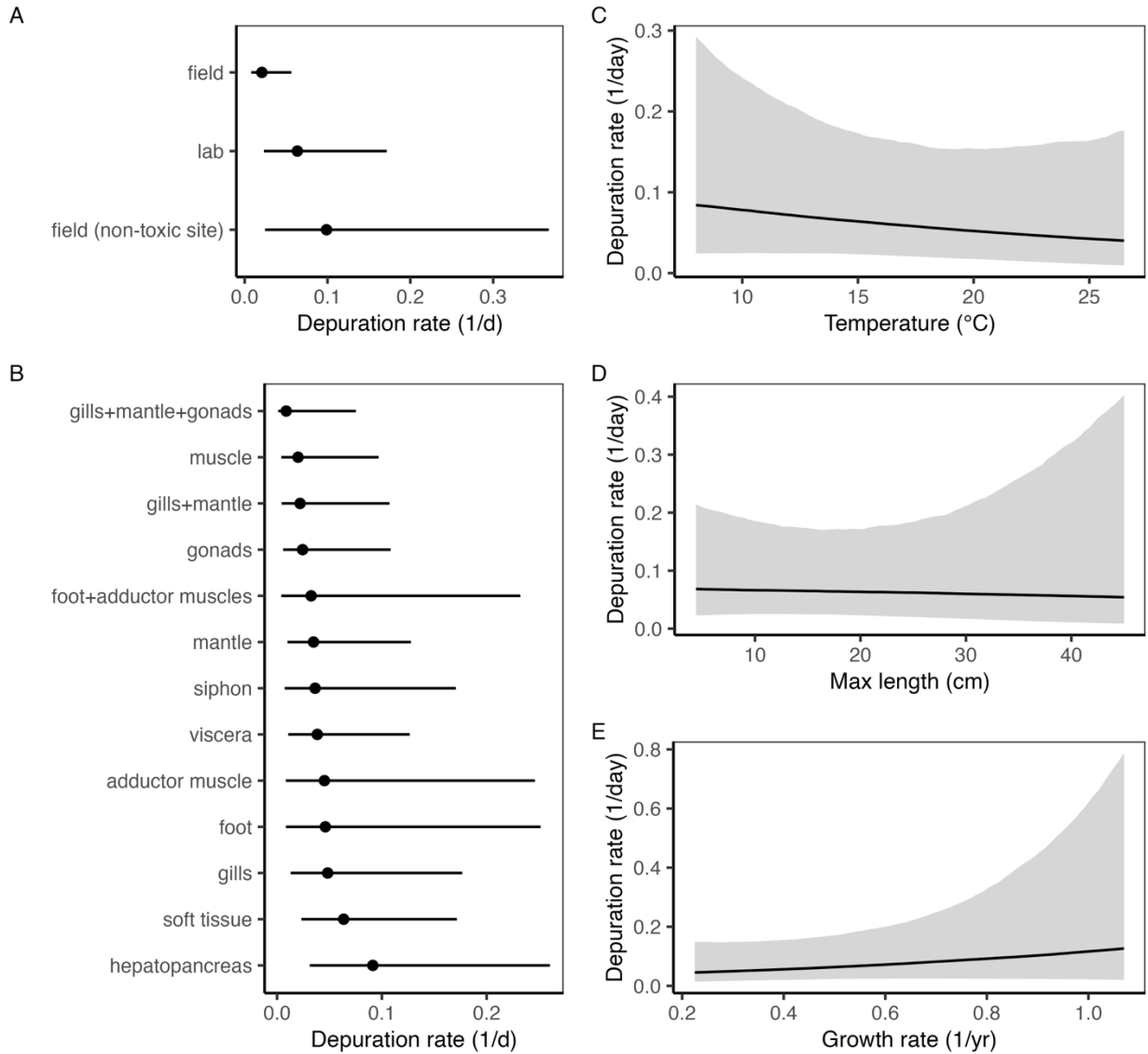


1288  
1289  
1290  
1291  
1292  
1293  
1294  
1295



1296  
1297  
1298  
1299  
1300  
1301

**Figure S9.** Model diagnostic plots for the best performing Bayesian regression model showing (A) the distribution of the residuals in 10 posterior draws; (B) distribution of the response variable in the data ( $y$ ) versus 10 posterior draws ( $y_{rep}$ ); and (C) correlation between the response variable in the data ( $y$ ) versus 10 posterior draws ( $y_{rep}$ ). In (C), the diagonal line represents the one-to-one line and each facet represents a set of posterior draws.



1302  
1303  
1304  
1305  
1306  
1307  
1308

**Figure S10.** The conditional effects of the **(A)** location; **(B)** tissue, **(C)** preferred temperature, **(D)** maximum length, and **(E)** von Bertalanffy growth rate fixed effects variables included in the best performing Bayesian regression model. Conditional effects illustrate the depuration rate expected for each fixed effect value when other fixed and random effects are held at their average. In **(A)** and **(B)**, points represent the median and lines represent the 95% credible interval. In **(C-D)**, lines represent the median and shading indicates the 95% credible interval.